DISSERTATION

INVESTIGATIONS INTO THE MECHANISMS OF TELOMERE STRUCTURE AND FUNCTION

Submitted by

Phuong Nam Le

Graduate Degree Program in Cell and Molecular Biology

In partial fulfillment of the requirements

For the Degree of Doctor of Philosophy

Colorado State University

Fort Collins, Colorado

Spring 2012

Doctoral Committee:

Advisor: Susan M. Bailey

Robert L. Ullrich
Michael M. Weil
Paul J. Laybourn

ABSTRACT

INVESTIGATIONS INTO THE MECHANISMS OF TELOMERE STRUCTURE AND FUNCTION

Telomere dysfunction is most commonly defined as critical shortening; i.e., loss of telomere sequence due to a variety of causes, usually the end-replication problem. However telomeres and their arsenal of associated proteins also provide essential end-capping structure that protects the ends of linear eukaryotic chromosomes. The overall goal of the studies presented here was to provide new insight into underlying mechanisms of telomeric structure and function.

We examined the role of telomere function in Acute Myeloid Leukemia. We observed genomic instability in association with radiation-induced AML, and this association was observed following AML induction with both gamma (ɣ)- ray and 1 Gev ^{56}Fe ion exposure. Furthermore, we observed a clonal fusion event involving telomeres in a human AML cell line. Taken together, our AML studies underline the importance of genome stability and its link to carcinogenesis.

We previously reported a role for the DNA damage repair protein DNA-PKcs in mammalian telomere end-capping function, where inappropriate telomere fusions, as well as telomere fusions to other broken DNA ends, were observed in DNA-PKcs deficient backgrounds. DNA-PKcs has many proposed phosphorylation substrates, one of the most intriguing and relevant being the recently identified heterogeneous nuclear ribonucleoprotein A1 (hnRNP A1), an RNA binding protein that associates with

telomeres. It is also now well accepted that telomeres are transcribed into telomeric repeat-containing RNAs, or TERRA, which are thought to contribute to telomeric chromatin structure. Taken together, *we hypothesized that DNA-PKcs mediated phosphorylation of hnRNA1 plays an important role in tethering TERRA to telomere ends, thereby possibly contributing to telomere chromatin structure and function.*

Our data suggests that TERRA localization at telomeres is independent of hnRNP A1 and DNA-PKcs kinase activity. Rather, we observed decreased TERRA levels following DNA-PKcs kinase inhibition, suggesting DNA-PKcs indirectly regulates TERRA levels. Depletion of hnRNP A1 did not influence TERRA levels, but resulted in elevated frequencies of what have previously been termed "fragile" telomeres and telomere sister chromatid exchange (T-SCE), both indicative of a role for hnRNPA1 in facilitating telomere replication.

ACKNOWLEDGEMENTS

This work would not be possible without the collaboration of many people. I thank Dr. David Maranon and Noeila Altina for their hard work and dedication in this project. I also thank Dr. Susan Bailey, my advisor, for her unending support throughout the years and providing me with the opportunity to pursue my Ph.D. I am grateful for the support and commentary of my committee members, including Dr. Robert Ullrich, Dr. Michael Weil and Dr. Paul Laybourn. I thank Dr. Norman Curthoys and Lynn Taylor for their generous discussions in the ^{32}P experiments.

I would like to thank all my lab members for their scientific support. I thank Abby Williams, Jingyi Nie and Dr. Amanda Ashley for understanding the frustrations of science. I also thank Dr. Ron Carsten for his patient and steadfast support. I am grateful for the scientific discourse and enduring friendship of Dr. Tanner Hagelstrom and Dr. Kristin Fabre. I am eternally grateful to Christine Battaglia for her expertise in the lab, her unwearied support and most importantly a friendship that is greatly valued.

I would like to thank my parents, Hue Le and Tuyet-Mai Nguyen, for all their love and support and for teaching me to approach all I do in life with patience, understanding and integrity. I thank my brothers and sister, Nam, Nhan and Quyhn for their camaraderie and influencing me to see the laughter in all things. Lastly, thank you to my husband, Dr. Stephen Keysar. I am grateful to you as a scientist, my support and the greatest friend I could hope to have.

TABLE OF CONTENTS

Chapter 2

CHROSOMAL INSTABILITY IN IONIZING RADIATION-INDUCED MURINE AML

Chapter 3

DNA-PKcs AND TELOMERE REPEAT-CONTAINING RNA (TERRA) INTERACTIONS IN TELOMERE STRUCTURE AND FUNCTION

CONCLUSIONS AND DISCUSSION

APPENDIX

CHAPTER 1

INTRODUCTION

Background and significance

One in two American men and one in three American women will be diagnosed with cancer in their lifetime according to the American Cancer Society (www.cancer.org). Many factors contribute to cancer risk, including smoking, obesity, alcohol use and age (National Cancer Institute, 2006). At the cellular level, loss of the regulation and function governing cell growth and cell death contributes to tumor growth (Hanahan and Weinberg, 2011). Intimately linked to this life and death balance, is the regulation of chromosome ends, specialized terminal features termed telomeres. In fact, telomere biology has become an integral part of cancer research, the importance of which was recently highlighted by the awarding of the 2009 Nobel Prize in Physiology or Medicine to Drs. Carol Greider, Elizabeth Blackburn and Jack Szostak for the discovery of telomerase, the reverse transcriptase that extends telomere length *de novo*.

Functional telomeres provide end-protection by capping chromosomal termini and preventing inappropriate fusion events, a vital aspect of maintaining genome stability. Our laboratory has been actively investigating telomeric end-capping role(s) of the Non-Homologous End Joining (NHEJ) DNA repair protein DNA Dependent Protein Kinase catalytic subunit (DNA-PKcs). We were intrigued by recent studies demonstrating that heterogeneous nuclear ribonucleoprotein A1 (hnRNP A1), which associates with telomeres, is a phosphorylation substrate of DNA-PKcs (Ting et al., 2009). Additionally, it is now appreciated that telomeres are transcribed into telomere repeat-containing RNA or telomeric RNA, termed TERRA or TelRNA, of very heterogeneous lengths, which are thought to contribute to telomeric chromatin structure (Azzalin et al., 2007; Deng et al., 2009; Schoeftner and Blasco, 2008). TERRA has also been linked to telomerase activity

and cancer, where decreased TERRA expression was observed in high grade tumors (Schoeftner and Blasco, 2008). We hypothesized that hnRNP A1 may act as an "anchor", tethering TERRA to telomere ends, helping to maintain telomere function and structure. Further, we proposed that DNA-PKcs mediated phosphorylation of hnRNP A1 plays a critical role in these processes.

The overall goal of the studies presented here was to provide new insight into the underlying mechanisms of telomere structure and function. We first examined telomere dysfunction and genomic instability associated with ionizing radiation (IR) induced Acute Myeloid Leukemia (AML) in the CBA mouse model following gamma (ɣ)-ray or high-energy ions that have a high charge (Z) and energy (E) (HZE), such as astronauts experience to in space (galactic cosmic rays; GCR).

Next, we tested our model of functional interaction between hnRNP A1 and TERRA at telomeres; i.e., DNA-PKcs mediated phosphorylation of hnRNP A1 regulates the presence of TERRA at telomere ends, thus contributing to telomere chromatin structure/stability. We also investigated whether such an association is altered in human breast cancer by examining human mammary epithelial cell lines, a possibility suggested by decreased DNA-PKcs levels and telomere end-capping failure in the BALB/c mouse model (Williams et al., 2009; Yu et al., 2001).

Telomeres

Introduction

Telomeres are dynamic nucleoprotein structures consisting of conserved tandem repeats of TTAGGG in vertebrates (Meyne et al., 1989). The terminal repeats are directly bound by telomere specific proteins including Telomere Repeat Factor 1 (TRF1), Telomere Repeat Factor 2 (TRF2) and Protection Of Telomeres 1 (POT 1) (de Lange, 2005). Together with a plethora of associated telomeric proteins, a higher order chromatin structure is formed (Palm and de Lange, 2008). Telomeres end in a 3'-single-stranded overhang that folds back upon itself and invades the duplex telomere DNA strand, forming a lariat or loop structure (Griffith et al., 1999). It is believed that this telomere (T-) loop structure helps prevent the telomere from being recognized as a double strand break (DSB) end in need of repair (Figure 1.1).

Due to the semi-conservative nature of DNA replication and the inability of conventional DNA polymerase to synthesize to the very end, telomeres shorten roughly 40-200 base pairs per cell division (Counter et al., 1992; Prowse and Greider, 1995; Vaziri et al., 1993), a phenomenon known as the end-replication problem (Olovnikov, 1973; Watson, 1972). Telomere shortening as a function of increasing age has been observed in many different tissues (Cherif et al., 2003; Harley et al., 1990). With increasing cell division and subsequent telomeric shortening, telomeres eventually reach a critically short length, which serves as a signal to stop dividing and initiate senescence (Bodnar et al., 1998; Harley and Villeponteau, 1995; Lundblad and Szostak, 1989). Cellular senescence involves the activation of p53 and $p16^{INK4a}$, and cells permanently arrest at the G1/S checkpoint (Satyanarayana and Rudolph, 2004)

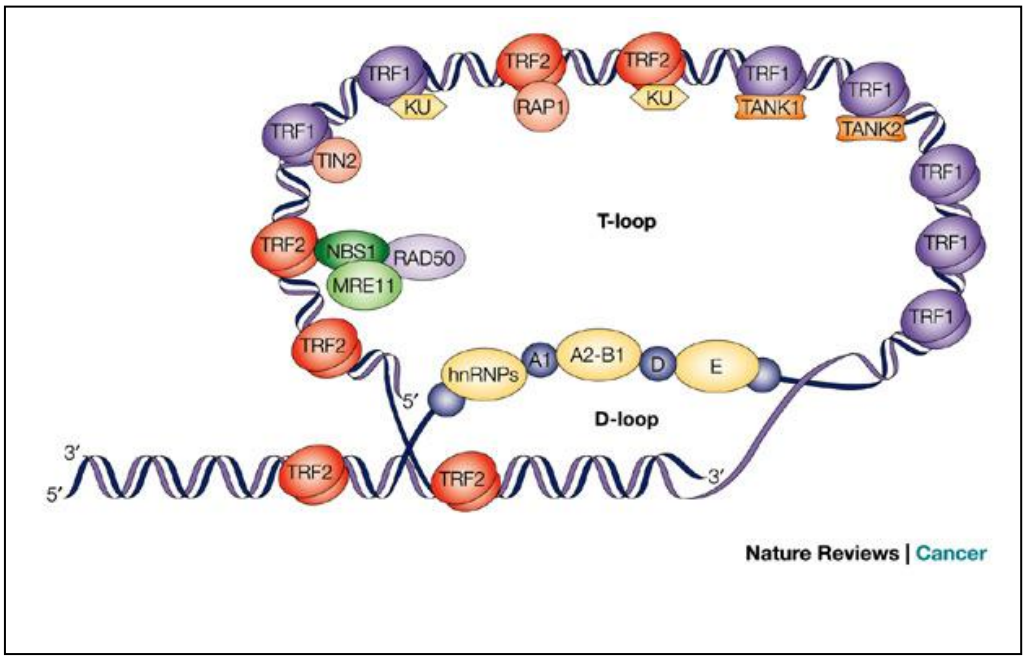

Figure 1.1. A schematic of the T-loop. TRF1, TRF2 and POT1 (not shown) bind directly to the telomere sequence. Many other proteins interact with the telomere end through protein-protein interactions. The 3'single-stranded overhang invades the duplex DNA, forming a t-loop and a displacement (D)-loop. This t-loop structure is believed to cap the chromosome end and protect it from destabilizing fusion events. (Neumann and Reddel, 2002)

and experience an irreversible growth arrest (Collado et al., 2007). Senescence serves as a tumor suppressor in that it prevents unstable, damaged or mutated cells from continuing to divide. Another consequence of critically short telomeres is chromosomal rearrangements such as dicentrics, which are lethal to the cell.

Without senescence or cell death, there would be an accumulation of potentially damaged cells. The human disease Dyskeratosis Congenita (DKC) has been linked to mutations in telomerase, telomere dysfunction (Vulliamy et al., 2001a), defined as short telomeres, and to reduced telomerase activity (Marrone et al., 2004; Vulliamy et al., 2001b). Short telomeres have also been linked to other age-related diseases, such as Werner's syndrome (Crabbe et al., 2007; Tahara et al., 1997). Werner's Syndrome is characterized by pre-mature aging (Gibbs, 1967; Perloff and Phelps, 1958), again implicating telomere function in aging.

In 1985, Carol Greider and Elizabeth Blackburn identified the enzyme that circumvents the telomeric shortening dilemma (Greider and Blackburn, 1985). Telomerase is a reverse transcriptase that adds species-specific telomeric sequences onto the ends of chromosomes *de novo*. Telomerase consists of an RNA component (TERC) and a telomerase reverse transcriptase (TERT) (Greider and Blackburn, 1989; Lingner et al., 1997). TERC serves as a template for the addition of telomeric repeats, while TERT provides the catalytic activity. Although expressed at very low levels in human somatic cells, telomerase is active in stem cell compartments and germ line cells (Chiu et al., 1996; Hiyama et al., 1996b; Mantell and Greider, 1994; Wright et al., 1996). In order for telomerase negative cells to avoid telomere shortening and bypass senescence, telomere length must be maintained and telomerase reactivated. Indeed, this is commonly observed

in human cancers; 85%-90% of human cancers experience telomerase reactivation (de Lange, 1994; Kim et al., 1994), while the remainder maintain telomere length by an alternative mechanism, termed ALT (Bryan et al., 1998; Cech, 2004). Although the mechanism is not well understood, ALT is believed to represent a recombination based mechanism of maintaining telomere length in the absence of telomerase, which is most often found in mesenchymal tumors (Dunham et al., 2000; Stewart, 2005).

Telomere replication

Telomeres are inherently difficult to replicate due to the highly repetitive sequence and propensity to form secondary structures, including G-quadruplex structures. Replication fork stalling has been observed in telomeres and worsens with the depletion of the necessary helicases (Ivessa et al., 2002; Ivessa et al., 2000; Makovets et al., 2004). Recently telomeres were proposed as possible fragile sites, where the conditional deletion of TRF1 led to what is termed "fragile" telomeres (Sfeir et al., 2009). This was defined as an extended telomere or duplicate telomere signal on a single chromatid in metaphase cells using Fluorescence *In Situ Hybridization (FISH).* This phenotype was seen with the treatment of aphidicolin, a DNA polymerase inhibitor, and an increase in replication fork stalling in the telomeres following the deletion of TRF1 was also observed, both implicating that "fragile" telomeres serves an indication of aberrant telomere replication.

Telomeres and radiation

Since functional telomeres are closely correlated with genomic stability, studies investigating radiosensitivity, telomeres and cancer have also been undertaken. A study

noted that short telomeres were predictive of an increase in chromosomal instability following treatment in patients with Hodgkin's lymphoma (M'Kacher et al., 2007). In another study, short telomeres were found to cause increased chromosomal instability and apoptosis in mice following irradiation (Goytisolo et al., 2000). Although decreased telomere length may seem contradictory to the activation of telomerase in cancer, many studies have shown critically short telomeres in cancer. This suggests that even with active telomerase, telomeres in cancer are still shortened (Gisselsson et al., 2001). One study suggests that telomerase may play a role in repair of radiation-induced double strand breaks (DSBs) (Leteurtre et al., 1997). Interestingly in this study, telomerase activity was shown to increase in a dose-dependent manner following gamma-irradiation of hematopoietic cells, a finding with important implications for carcinogenesis. Together, these studies suggest that telomere length and telomerase activity are linked to radiosensitivity.

The role of DNA-PKcs at telomeres

The DNA-dependent protein kinase (DNA-PK) plays a major role in Non-Homologous End-Joining (NHEJ), as DNA-PK deficiency results in hypersensitivity to ionizing radiation (IR) due to reduced DNA DSB repair (Allalunis-Turner et al., 1995; Okayasu et al., 1998). Interestingly, the catalytic subunit of DNA-PK (DNA-PKcs) is also vital in telomere end-capping function, as its loss results in the uncapping of telomeres (Bailey et al., 2004a; Bailey et al., 1999). An increase in telomere-telomere fusions was seen following IC86621 treatment, a specific and potent inhibitor of DNA-PKcs catalytic activity in C57BL/6 mouse fibroblasts, in a transformation related protein

53 (*Trp*53) knock-out background (Bailey et al., 2004a). Telomere-DSB fusion events were observed following IR exposure, in which uncapped telomeres fused to DSBs, which can be distinguished using Chromosome Orientation Fluorescence *In Situ* hybridization (CO-FISH) (Bailey et al., 2004b). Following CO-FISH, increased telomere fusion events were observed specifically involving telomeres produced via leading strand replication (Figure 1.2) (Bailey et al., 2004a). Telomere FISH signals were present at the sites of chromosomal fusion, and therefore critically short telomeres were not the main contributing factor to these aberrations. Increased telomere fusion events were also observed in the BALB/c mouse, which have reduced DNA-PKcs protein levels (Williams et al., 2009; Yu et al., 2001). We have shown that the ability of DNA- PKcs to cap telomere ends is dependent on the threonine- (Thr) 2609 autophosphorylation cluster (Williams et al., 2009). Together, such studies demonstrate that the NHEJ repair protein DNA-PKcs plays a vital role in mammalian telomeric end- capping function. The preferential role of DNA- PKcs in post replicative processing of leading strand telomeres also suggests that regulation of telomere structure may differ between leading and lagging strand telomeres. Although evidence supports the kinase activity of DNA-PKcs as being necessary for telomere end-capping functions, the underlying mechanisms and other possible players involved are unknown. Clearly, more research is needed to elucidate the complex regulation of length maintenance and end-capping structure that occurs at the telomeres.

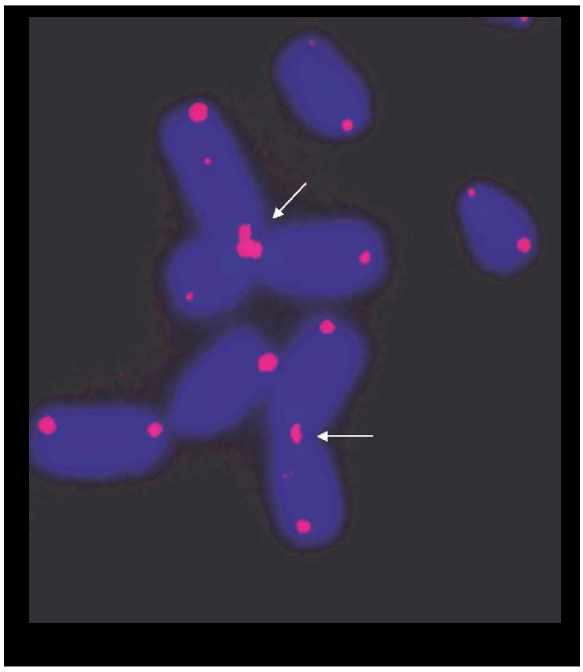

Figure 1.2. Image of CO-FISH with G-rich PNA probe specific for telomere sequence labeled with Cy-3 following inhibition of DNA-PKcs kinase activity in p53-/- mouse fibroblasts. Arrows depict sites of telomere fusion between two chromosomes. CO-FISH enables differentiation between leading- and lagging- strand telomeres. Here the probe for the leading strand was used, providing evidence that inhibition of DNA-PKcs kinase activity leads to failure of end-capping specifically in telomeres produced via leading strand replication (Bailey et al., 2004a).

Heterogeneous Nuclear Ribonucleoprotein A1 and telomeres

Heterogeneous nuclear ribonucleoprotein A1 (hnRNP A1) is an abundant protein that belongs to a large family of proteins known to associate with RNA (He and Smith, 2009). This protein primarily localizes in the nucleus and is involved in mRNA splicing and shuttling mature RNA out of the nucleus and into the cytoplasm. Although knock-down of hnRNP A1 may induce cell death in highly proliferating cells such as cancer cells (Patry et al., 2003; Patry et al., 2004), loss of this protein is not lethal, suggesting other members of the hnRNP family share in this function (Ben-David et al., 1992). Interestingly, hnRNP A1 has been implicated in telomere biology, where it has been shown to physically interact with telomere ends (Zhang et al., 2006), although its role has only begun to be explored. Several groups have shown that hnRNP A1 stimulates telomerase activity and increases telomere length (Ford et al., 2002; LaBranche et al., 1998; Zhang et al., 2006). One group demonstrated that hnRNP A1 stimulation of telomerase activity was concentration dependent, suggesting that it may actually repress telomerase activity when hnRNP A1 is present at greater concentrations (Nagata et al., 2008). Interestingly, hnRNP A1 has also been shown to be phosphorylated by DNA-PKcs *in vitro and in vivo* (Ting et al., 2009; Zhang et al., 2004). However, the function of this phosphorylation event is unknown. The overall goal of the current studies is to investigate a possible role of DNA-PKcs dependent phosphorylation of hnRNP A1 in telomere function in two human mammary epithelial cell lines, MCF7 (tumorigenic) and MCF 10a (non-tumorigenic). Specifically, we analyzed the effects of DNA-PKcs mediated phosphorylation of hnRNP A1 on the possible interaction of hnRNP A1 and telomere repeat-containing RNA (TERRA) at telomeres. We confirm DNA-PKcs

dependent phosphorylation of hnRNP A1 in MCF7 cells, and our data also provide support to the finding that this event is hTR dependent (Ting et al., 2009).

Telomere repeat-containing RNA or Telomeric RNA (TERRA/TelRNA)

Telomeric DNA has been considered a 'buffer zone," protecting internal coding regions of the chromosome from loss of sequence due to the end-replication problem (Olovnikov, 1973; Watson, 1972). Our work has demonstrated that telomeres promote genome stability by preventing chromosome ends from being recognized as DSBs (Bailey et al., 2004a; Bailey et al., 1999). As tracts of repetitive sequences, telomeres have long been presumed transcriptionally silent. Remarkably, recent research provides evidence that telomere ends are actually transcribed into telomeric repeat-containing RNA (TERRA), also termed telomeric RNA (TelRNA) (Azzalin et al., 2007; Schoeftner and Blasco, 2008). To date, TERRA has been identified in humans, yeast, mouse and zebrafish, suggesting it is well conserved (Azzalin et al., 2007; Luke et al., 2008; Schoeftner and Blasco, 2008). TERRA was found to be very heterogeneous in length, ranging from 100 base pairs (bps) to 9 Kbs and predominantly existing as UUAGGG repeats (Azzalin et al., 2007; Schoeftner and Blasco, 2008). In these same studies, TERRA was shown to localize to telomere ends, suggesting a role in telomere function. Decreased TERRA levels have also been associated with cancer progression in human tumor samples derived from the colon, larynx and lymph node (Schoeftner and Blasco, 2008). TERRA is not found at all chromosome ends, suggesting that not all telomere ends are transcribed or not all are transcribed at the same time (Azzalin et al., 2007; Schoeftner and Blasco, 2008). Whether or not this is due to differences in RNA stability is not

known. Furthermore, the question of whether TERRA acts only at the telomere end from which it was transcribed (cis) or at other telomere ends (trans) is largely unexplored. Studies have shown that TERRA may be partly transcribed by RNA polymerase II and degraded by the rap1p 5'-3' exonuclease (Luke et al., 2008). Methylation status in the subtelomeric region has also been shown to influence the transcription of TERRA (Deng et al., 2010; Nergadze et al., 2009; Ng et al., 2009). Telomeric RNA research is in its infancy, so little is known regarding the function(s) of TERRA. One proposed role for TERRA is involvement in the formation of G-quadruplex structures (Xu et al., 2010; Xu et al., 2009). These RNA/DNA hybrid structures may act as regulatory elements at telomere ends by preventing access to nucleases and avoiding degradation or by preventing access to telomerase and facilitating telomere length maintenance. Recent evidence suggests that TERRA may participate in chromatin structure regulation at telomeres, as TERRA was shown to associate with proteins known to be vital in the formation of heterochromatin including heterochromatin protein 1 (HP1) and methylated (trimethyl) histone H3 (H3K4me3; Figure 1.3) (Deng et al., 2009).

Because hnRNPA1 has been shown to: 1) bind to UAGGGA/U sequences with high affinity (Burd and Dreyfuss, 1994), 2) associate with telomere ends (Zhang et al., 2006), and 3) bind DNA and RNA sequences (He and Smith, 2009), we hypothesized that hnRNP A1 may play a role in retaining TERRA at telomere ends. Recently, an interaction between hnRNP A1 and TERRA has been demonstrated *in vivo* via a biotin pull-down assay (de Silanes et al., 2010). Here, we investigated whether hnRNP A1 functions to "tether" TERRA at telomeres. We also examined whether phosphorylation of

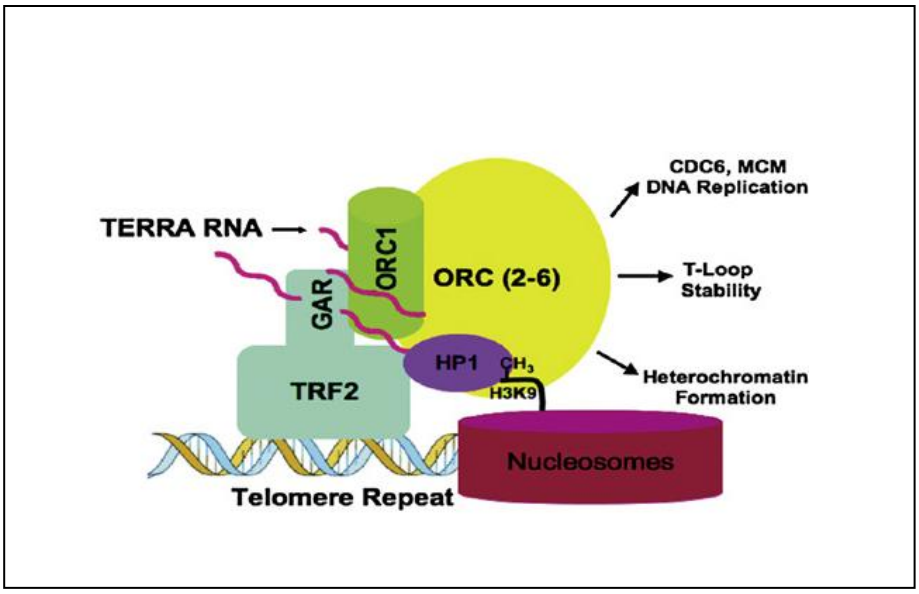

Figure 1.3. Schematic depicting the possible role of TERRA/TelRNA in promoting heterochromatin formation at telomere ends. It has been proposed that TERRA/TelRNA acts to stabilize TRF2 interaction with proteins known to promote heterochromatin formation including origin of recognition complex (ORC) and heterochromatin protein 1 (HP1). (Deng et al., 2009)

hnRNP A1 by DNA-PKcs influenced hnRNP A1 interaction with TERRA. To investigate this possibility, we evaluated TERRA localization at telomere ends visualized as its colocalization with TRF2, a telomere-specific protein, using RNA FISH and immunocytochemistry. We found that TERRA localization at telomere ends was independent of hnRNP A1 and DNA-PKcs kinase activity. However, we observed a decrease in overall TERRA levels with DNA-PKcs kinase activity inhibition in the MCF7 cell line, suggesting that DNA-PKcs kinase activity may indirectly affect TERRA levels.

DNA repair

Introduction

Cells encounter daily insult from DNA damaging agents, both endogenous and exogenous, including ionizing radiation (IR) exposure. Cells possess an arsenal of DNA repair machinery to combat such damage. Cell cycle checkpoints at the G1/S and G2/M cell cycle transitions play essential roles in delaying cell cycle progression, in order to prevent the propagation of damaged cells and provide opportunity for repair (Elledge, 1996). There are many DNA damage repair pathways the cell can engage depending on the type of damage encountered, including base excision repair (BER), nucleotide excision repair (NER) and double strand break (DSB) repair. DSB repair represents the most critical pathway following IR exposure and can proceed by either Homologous Recombination (HR) or Non-Homologous End Joining (NHEJ) (Hall, 2006). HR uses information from a template with sequence homology such as a sister chromatid, while

NHEJ ligates the ends of broken DNA strands with no regard to homology, explaining its mutagenic potential and importance for IR-induced DSB repair (Lieber, 2010).

"Sensing DNA damage"

DNA damage is sensed by Ataxia Telangiectasia Mutated (ATM) and Ataxia Telangiectasia and Rad3 related (ATR), which are rapidly recruited to DSB sites (Andegeko et al., 2001; Bakkenist and Kastan, 2003). In addition to DNA-PKcs, ATM and ATR belong to the phosphoinositide 3-kinase like (PIKK) superfamily of proteins, and ATM is required for the phosphorylation of many proteins involved in DNA repair including p53, MDM2, Chk2, histone H2AX and itself (Burma et al., 2001; Canman et al., 1998; Khosravi et al., 1999; Matsuoka et al., 1998).

Homologous Recombination (HR) Repair

The Mre11, Rad 50 and Nbs1 (MRN) complex is also involved in detection of DNA damage, as it is recruited to the site of the break and plays a role in end resection and the initial recruitment of ATM (Lee and Paull, 2005; Tauchi et al., 2002; Trujillo et al., 1998). Breast cancer 1 (BRCA1) and BRCA 2 are then recruited to the site, and evidence suggests BRCA1 may regulate the MRN complex exonuclease activity (Paull et al., 2001). BRCA2 has been shown to regulate the activity and the availability of RAD51 (Shivji et al., 2009; Wong et al., 1997; Yang et al., 2005). Rad 51 is loaded onto the single stranded overhang and is believed to be involved in strand invasion and exchange (Sung, 1994). With strand invasion and branch migration, a Holliday Junction is formed. Many enzymes have been implicated in the resolution of Holliday Junctions including

Mus81, RecQ helicase and GEN1 resolvase (Chen et al., 2001; Ip et al., 2008; Wu and Hickson, 2003). DNA polymerases fill the gaps and ligase joins the free ends together. This process involves minimal loss of sequence at DNA ends and so is deemed a precise means of DNA repair.

Non-Homologous End Joining (NHEJ)

NHEJ is the predominant mode of DNA DSB repair following exposure of mammalian cells to IR, as it does not require a homologous template strand, and it occurs throughout the cell cycle (Figure 1.4) (Mao et al., 2008; Rothkamm et al., 2003). The Ku70 and Ku80 heterodimer (Ku70/80) responds to and binds the broken DNA ends in a sequence independent manner (Cary et al., 1997; Falzon et al., 1993; Walker et al., 2001). With the recruitment of DNA-PKcs, Ku70/Ku80 translocates inward on the DNA strands and away from the DSB site (Dvir et al., 1992; Gottlieb and Jackson, 1993; Yaneva et al., 1997). Interaction with the DNA-bound Ku70/Ku80 heterodimer significantly increases the kinase activity of DNA-PKcs (Gottlieb and Jackson, 1993). The activated DNA-PK holoenzyme possesses serine/threonine kinase activity. DNA-PKcs has many potential targets and has been shown to phosphorylate and activate the 5'-3' endonuclease activity of Artemis, an important end-processing factor (Ma et al., 2002; Ma et al., 2005). However, Artemis does not appear to be essential to NHEJ, as repair still occurs in its absence (Wang et al., 2005). Rather, the MRN complex appears to play the major role in DNA end processing (Paull and Gellert, 1999; Trujillo et al., 1998). NHEJ does not utilize a homologous template strand, but instead joins DNA ends though sequence microhomology and processes the remaining ends, ultimately leading to sequence loss in

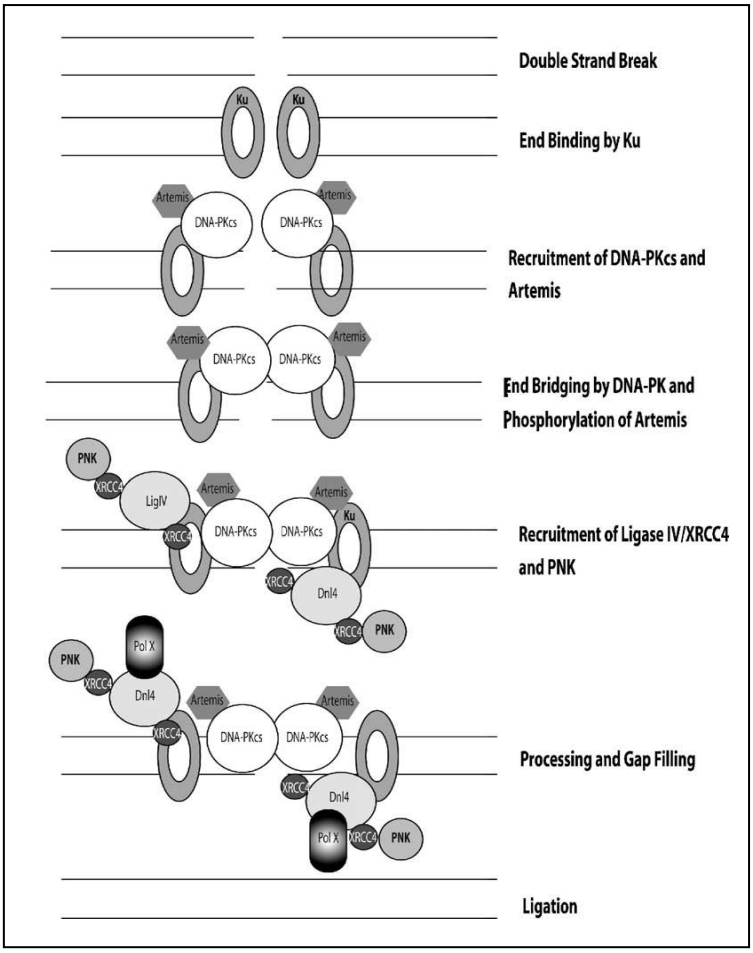

Figure 1.4. Non - Homolgous End Joining (NHEJ). The Ku 70/80 heterodimer is recruited to the site of damage. The binding of DNA-PKcs to Ku70/80 forms the active DNA-PK holoenzyme complex. The DNA ends are processed by the MRN complex and DNA polymerase fills in the gap. Lastly, Ligase IV and XRCC4 are required for ligation and completion of DNA DSB repair. (Hefferin and Tomkinson, 2005)

the area surrounding the breakpoint (Lieber, 1999; Marvo et al., 1983; Roth and Wilson, 1986). Following end processing, DNA polymerase fills in the gaps.

Autophosphorylation of DNA-PKcs is required for its release from the Ku heterodimer and DNA ends (Chan and Lees-Miller, 1996), thus freeing the DNA ends. Lastly, the ends are ligated by Ligase IV and its associative factor XRCC4 (Grawunder et al., 1997; Li et al., 1995).

DNA-repair and Ionizing Radiation (IR)

Increased radiation sensitivity has been associated with impairments in DNA repair factors. For example, severe radiosensitivity was observed in patients deficient in ATM, a disorder termed Ataxia Telangiectasia (Gotoff et al., 1967; Morgan et al., 1968). Exposing patients to "standard" doses of radiation therapy resulted in tissue necrosis, radiation dermatitis and even death. At the cellular level, radiosensitivity can also be associated with the loss of regulation of multiple ATM targets, including p53, CHK2, BRCA1 and NBS1, critical proteins involved in cell-cycle progression and apoptosis (Shiloh, 2001). Artemis defiency has also been found in a Severe Combined Immune Deficiency (SCID) patient, a disease associated with defective V(D)J recombination and reduced functional B and T cells (Moshous et al., 2001). Ku80 deficient mice have also been shown to possess a SCID-like phenotype (Nussenzweig et al., 1996), displaying increased mortality, loss of hair pigmentation and damage to the gastrointestinal tract following ɣ-irradiation; Ku80 deficient embryonic stem (ES) cells showed increased apoptosis and decreased survival (Nussenzweig et al., 1997).

Most relevant to our current studies is the evidence suggesting that the loss of DNA-PKcs greatly increases radiosensitivity. A human malignant glioma cell line, MO59J, was found to be deficient in DNA-PKcs due to a frameshift mutation that produces a truncated protein (Anderson et al., 2001). Decreased clonogenic cell survival and repair of radiation induced damage following ɣ-irradiation was reported in MO59J cells (Allalunis-Turner et al., 1993; Allalunis-Turner et al., 1995). Decreased ability to recover from DNA replication inhibition following x-ray irradiation was also observed in MO59J cells, suggesting that DNA-PKcs also plays a role in replication (Guan et al., 2000). Additional evidence supporting the essential role of DNA-PKcs in repair was provided following treatment of normal human fibroblasts with Wortmannin, a phosphatidylinositol 3-kinase (PI-3-K) inhibitor, as decreased repair of DSBs was observed by pulse-field gel electrophoresis (Okayasu et al., 1998).

The *SCID* mouse possesses a DNA-PKcs gene with an amino acid base transversion resulting in a premature stop codon and a severely decreased amount and activity of protein (Araki et al., 1997; Blunt et al., 1996; Danska et al., 1996). Following x-ray irradiation, SCID cells exhibited slowed DNA repair kinetics and lacked the ability to repair sublethal damage (Nevaldine et al., 1997). Polymorphisms in the coding region of the DNA-PKcs gene, *Prkdc*, have also been reported in the BALB/c mouse strain, resulting in decreased protein levels and reduced activity (Yu et al., 2001). This decreased DNA-PKcs protein expression was associated with increased radiosensitivity due to loss of DSB repair efficiency following irradiation (Okayasu et al., 2000; Yu et al., 2001). Gastrointestinal cells were also observed to be sensitive to radiation in this mouse strain (Hanson et al., 1987). Furthermore, an increased susceptibility to radiation-induced

mammary tumors following irradiation has been observed in the BALB/c mouse strain (Ullrich, 1983). Together, such studies strongly support the critical role of DNA-PKcs in radiation-induced DSB repair, the lack of which contributes to repair deficiency, instability and ultimately carcinogenesis.

DNA Protein Kinase (DNA-PK)

DNA-PKcs is a very large protein, ~460kDa, important for efficient NHEJ and V(D)J recombination (Rathmell and Chu, 1994a, b; Smider et al., 1994; Taccioli et al., 1994). The serine/threonine kinase activity of the DNA-PK holoenzyme has been shown to require the presence of linear DNA ends and the Ku 70/80 heterodimer (Carter et al., 1990; Gottlieb and Jackson, 1993; Lees-Miller et al., 1990). DNA-PK targets a variety of proteins for phosphorylation, including Ku70/Ku80 (Lees-Miller et al., 1990), heat shock protein 90kDs (hsp90) (Carter et al., 1988; Lees-Miller and Anderson, 1989), c-Jun (Bannister et al., 1993), Replication Protein A (RPA) (Boubnov and Weaver, 1995; Brush et al., 1994; Pan et al., 1994), p53 (Lees-Miller et al., 1990; Lees-Miller et al., 1992), and RNA polymerase II (Peterson et al., 1992). Perhaps the most interesting target of DNA-PKcs mediated phosphorylation is itself. The autophosphorylation of DNA-PKcs is necessary for the release of the holoenzyme from DNA ends (Chen et al., 2007; Meek et al., 2007), allowing access to the ends for completion of repair. DNA-PKcs contains two autophosphorylation clusters; six autophosphorylation sites are located in the ABCDE cluster (2609-2647) and another six in the PQR cluster (2023-2056) (Chan et al., 2002; Cui et al., 2005; Ding et al., 2003; Douglas et al., 2002). A protein with five of the six sites in the ABCDE cluster substituted with an alanine renders the mutant protein unable

to salvage NHEJ in DNA-PKcs deficient cells (Ding et al., 2003). One of these phosphorylation sites, Thr-2609, was shown to be targeted in DNA repair, where phosphorylation occurs following irradiation and DNA-PKcs colocalized with damage foci (Chan et al., 2002). Taken together, such evidence suggests that the ability of DNA-PKcs to undergo phophosphorylation is critical to DNA-repair. Interestingly, the role of DNA-PKcs in maintaining telomere end-capping function also requires autophosphorylation at the Thr-2609 site (Williams et al., 2009), thus linking DNA-repair and telomere function in preserving genomic stability and preventing tumorigenesis.

Ionizing Radiation (IR)

Introduction

Radiation is a unique carcinogen in that it produces large numbers of random DSBs. IR exposure presents an interesting contradiction, because it is known to cause cancer, as well as cure cancer. Ionizing radiation, as opposed to excitation radiation (non-ionizing), transfers enough energy to an atom to eject an electron from its orbital. For each ionizing event roughly 33eV is released (Hall, 2006), enough to break chemical bonds and cause DNA double strand breaks (DSBs), giving it great potential to cause damage within the cell.

Linear energy transfer (LET) is the rate of energy transferred per unit length along the radiation track and is expressed in keV/µm. LET is largely dependent on the mass, charge and acceleration of the particle (Hall, 2006). γ-rays produced from a ^{137}Cs source are a low LET radiation, meaning it is sparsely ionizing. 1 GeV ^{56}Fe particles are considered high LET radiation, or densely ionizing radiation. One of our goals was to

evaluate chromosome and telomere aberration frequencies following exposures to different radiation qualities, of relevance to astronaut exposures, in radiation-induced AML mice.

Because LET is an average measure and may not reflect the variation of energy deposition along the track, this qualifying term may be misleading. Another measure of radiation quality is relative biologic effectiveness (RBE). RBE is meant to account for the fact that the same dose of different radiation types does not necessarily lead to the same biological outcome. Generally, RBE is a ratio of the dose of a reference radiation to the dose of the tested radiation required to produce the same effect. RBE is a complex qualifying factor and depends on the radiation quality, radiation dose, the number of dose fractions, dose rate and the end point that is being examined. Radiation involving high-energy ions that have a high charge (Z) and energy (E) (HZE) is further complicated in that an exposure will produce a high energy, heavy ion radiation track, with associated delta rays dispersing from the track. In a previous study examining cytogenetic aberrations following Fe-ion and x-ray irradiation, an RBE of 1.3 was observed in GM10115 cells, a human-hamster hybrid containing a single copy of human chromosome 4 (Limoli et al., 2000). In contrast, another study showed no increase in cytogenetic aberration frequency following x-ray exposure using colony forming unit type A (CFU-A) assay, suggesting a much larger RBE as when compared to the marked increase in aberration frequency following α-particle exposure (Kadhim et al., 1992). Another study suggested that high LET radiation induced more complex aberrations, those involving 3 or more chromosomes, as compared to low LET radiation (Anderson et al., 2000). Contrary to Limoli et al, the latter studies suggested that high LET radiation is much

more efficient at inducing chromosome breaks. With the United States exploring possibilities of extended space travel, it becomes critical to define the effects following HZE radiation exposure, a cancer risk to astronauts (Cucinotta and Durante, 2006).

Ionizing Radiation-induced cancers

Breast cancer introduction

Breast cancer is the one of the most common types of cancer in women; one in eight women will develop invasive breast cancer during their lifetime (American Cancer Society, 2010c). Over the years, the efforts of researchers and doctors have greatly increased the survival rate for breast cancer patients. The discovery of BRCA1 and BRCA2 mutations and their role in familial disposition to breast cancer has greatly facilitated awareness of the genetic factors that influence breast cancer incidence (Hodgson et al., 1999; Peto and Mack, 2000). However, these genes are known to be associated with only 5-10% of the total cases of breast cancer (John et al., 2007; Malone et al., 2006). Therefore, much remains unknown about the mechanisms of breast carcinogenesis.

Many risk factors for breast cancer have been identified. Gender, or more specifically being female, and increasing age are the largest risk factors. Men are about 100 times less likely to develop breast cancer in their lifetime. Family history of breast cancer, exposure to IR, use of post-menopausal hormone therapy, obesity, alcohol consumption and not having children until later in life are all associated risk factors (American Cancer Society, 2010b).

Breast cancer and ionizing radiation

An increased risk of breast cancer following radiation exposure has been well documented. A linear dose-response relationship was observed for relative risk of developing breast cancer following exposure to IR in female Atomic (A)-Bomb survivors (Land et al., 2003; Tokunaga et al., 1987). Radiation exposures experienced from the A-bombs differed greatly from other types of exposure because it was acute and delivered at a high dose-rate. Increased risk of breast cancer has been seen following other radiation exposures as well, e.g. in a pooled analysis of data from eight cohorts including exposure due to fluoroscopy and therapeutic x-rays (Preston et al., 2002). An increased breast cancer risk was also observed following radiation treatment for a primary cancer, including Hodgkin and Non-Hodgkin's Lymphoma (Dores, 2006). Interestingly, all of these studies also reported a correlation between increased breast cancer risk and young ages of exposure, suggesting that risk is associated with an early breast developmental stage in women.

Breast cancer and telomeres

Telomerase activity has been well associated with carcinogenesis (Kim et al., 1994), and telomerase activity has been observed in over 95% of advanced breast cancers (Hiyama et al., 1996a).

Telomere length associated with breast cancer is still debated. Shortened telomere length has been implicated in breast cancer, in spite of increased telomerase activity (Shen et al., 2007). These results imply that telomerase activity acts to maintain critically shortened telomeres. In contrast, others have observed longer telomeres in breast cancer

patients when examining peripheral blood cells (Svenson et al., 2008). This report also observed increased survival in patients with shorter telomeres, suggesting that long telomeres are the better indicator of poor prognosis and advanced disease. Differences in study design may account for some of the conflicting results. Svenson et al. examined node positive samples while the stage of disease in Shen et al. study is unspecified. Variation in telomere lengths between cells and individuals also complicates an accurate assessment. It is clear that more research is required before telomere length can reliably be used as a prognostic indicator.

The loss of telomere sequence may also contribute to breast carcinogenesis, as shown by combined loss of telomerase and p53 in mice, which allowed cells to bypass senescence when telomeres became critically shortened (Artandi et al., 2000). Telomere dysfunction resulting in breakage-fusion-bridge (BFB) and non-reciprocal translocations was observed. Furthermore, mice with severe telomere shortening were at greater increased risk of developing breast adenocarcinoma.

Another goal of our studies was to examine telomere end-capping function in human mammary epithelial cells. We utilized two cell lines, MCF7, a tumorigenic epithelial cell line derived from a metastatic pleural effusion, and MCF 10A, a non-tumorigenic spontaneously immortalized mammary epithelial cell line to evaluate the role of hnRNP A1 in telomere function. We sought to elucidate potential differences in the regulation of telomere function between tumorigenic and non-tumorigenic mammary cell line in relation to hnRNPA1. Although we did observe increased levels of hnRNP A1 in the MCF7 cell line, we found that loss of hnRNP A1 affected both cell lines in a similar manner. Our primary observation was that hnRNP A1 was important in telomere

replication, as indicated by an increase in the "fragile" telomere phenotype with the depletion of hnRNP A1.

Acute Myeloid Leukemia (AML)

Introduction

AML is an aggressive disease of the bone marrow and blood, in which white blood cells are unable to differentiate, leading to an accumulation of myeloblasts (National Cancer Institute, 2011a). AML has been proposed to be a disease that originates in hematopoietic stem cells (Bonnet and Dick, 1997; Lapidot et al., 1994). In these studies, transplantation of $CD34^{+}$ $CD38^{-}$ cells into lethally irradiated SCID mice propagated the disease, suggesting that AML results from a clonal expansion of the stem cell compartment.

Several risk factors are associated with the development of AML including smoking, exposure to Benzene and exposure to IR (American Cancer Society, 2010a). Approximately four in 100,000 men and three in 100,000 women were diagnosed with Acute Myeloid Leukemia (AML) from 2003 to 2007. The five year survival rate for this disease is 22.6%, considerably lower in comparison to other cancers such as the 99.1% five year survival rate of prostate cancer (National Cancer Institute, 2011b).

Diagnosis of AML often depends on the presence of specific chromosomal translocation events, and therefore cytogenetics is a vital diagnostic tool (Vardiman et al., 2009). Chromosome rearrangements often found in patients with AML include t(8;21) (Rowley, 1973), del (16) (Arthur and Bloomfield, 1983) , inv(16) or t(16;16) (Hogge et al., 1984; Le Beau et al., 1983) and t(15;17) (Rowley et al., 1977). These chromosome

translocations often form oncofusion proteins; for example t(15;17) fuses PML and RARA genes (Borrow et al., 1990; de The et al., 1990). In contrast to the common chromosome translocations often observed in *de novo* AML, losses in chromosome 5 and 7 have been noted in therapy-related AML (t-AML) (Liang et al., 1998; Nagarajan, 1995).

AML and ionizing radiation

An association between AML and irradiation was noted in patients following x-ray radiotherapy for the inflammatory disease ankylosing spondylitis (Court-Brown and Doll, 1957). Additional evidence linking AML to radiation exposure was provided by atomic bomb survivors. In 1947, shortly after the bombs fell over Hiroshima and Nagasaki, the U.S. Atomic Bomb Casualty Commision (ABCC) began studying hematological disease as a possible effect of radiation on survivors (NAS, 2010). These initial studies led to a comprehensive larger population-based study termed the Life Span Study (LSS), which continues to this day and investigates the effects of radiation on carcinogenesis. Taken together, such studies provide evidence that AML is the most frequent type of hematological cancer following exposure to radiation from atomic bombs (Preston et al., 1994; Richardson et al., 2009). An association between AML and ionizing radiation is strongly supported, and evidence suggests that dose response is a linear-quadratic function, where the slope increases with doses up to 3-4 Gy and somewhat flattens above these doses (Pierce et al., 1996; Preston et al., 1994; UNSCEAR, 2000).

Although leukemia is a relatively rare cancer, its increased risk following IR exposure is disconcerting, especially to those who may be exposed to it routinely in their occupation. One striking example is astronauts, who are exposed to galactic cosmic rays (GCR) and solar proton events (SPE) during space travel (NASA, 2000). A possible mission to Mars, lasting approximately 3 years, could mean a whole body dose of 1 Sievert (SV) or more (Wilson et al., 1995). During such missions, astronauts may be exposed to protons, high-energy heavy (HZE) ions and secondary radiations such as neutrons and delta rays (Cucinotta and Durante, 2006). While there is considerable data on cancer risk following exposure to gamma rays from atomic bomb survivors, informed cancer risk estimates following exposure to HZE ions are not available in humans.

Sfpi1/PU.1 in AML

Mouse models of AML are in agreement with the observed increases in human AML following radiation exposure. The CBA inbred mouse strain is often used in AML studies due to their low spontaneous incidence of AML and high incidence following irradiation (Rithidech et al., 1999). Similar to the dose response seen following radiation exposure in A-Bomb survivors, AML incidence in CBA mice exposed to x-irradiation peaked between 1.5-3 Gy (Major and Mole, 1978).

Early cytogenetic analysis revealed deletions in chromosome 2 associated with radiation induced AML in the bone marrow of whole body irradiated mice (Bouffler et al., 1996; Hayata et al., 1983). Chromosome 2 hypersensitivity following irradiation was shown via chromosome painting and was two-fold higher as compared to chromosome 1 and 3 (Bouffler et al., 1997). The deleted region of chromosome 2 was more accurately

defined and mapped to a minimal deleted region by examining loss of heterozygosity through microsatellite analysis and mapping (Alexander et al., 1995; Clark et al., 1996; Silver et al., 1999). Within this defined region, possible tumor suppressor genes were identified and narrowed to three of interest, *Ddb2*, *Madd* and *PU.1* (Cook et al., 2004). The remaining allele of these three genes was sequenced; of these only point mutations targeting Arginine 235 (Arg235) and other codons were observed in the E-twenty-six (Ets) domain of *PU.1*, supporting a causative role in leukemogenesis.

PU.1 is a transcription factor encoded by the *Sfpi1* gene that is critical for hematopoiesis and differentiation of bone marrow progenitor cells (Dakic et al., 2005; Iwasaki et al., 2005). Reduced levels of PU.1 have been associated with an expansion of immature myeloid cells (Houston et al., 2007). A conditional knockout of *PU.1* led to the development of AML in C57BL/6 mice (Metcalf et al., 2006). These murine studies provide substantial supporting evidence for an association of AML with loss of PU.1.

Recently, Peng and colleagues quantified the percent PU.1 deletion following radiation exposure of different qualities and dose (Peng et al., 2009). Using Fluorescence *In Situ* Hybridization (FISH), bone marrow cells were examined in CBA/Ca and AML-resistant C57BL/6 mice following 1GeV/nucleon ^{56}Fe, ɣ- and x-irradiation in order to evaluate effects of radiation quality and PU.1 loss. Increased PU.1 loss was observed in ɣ- and ^{56}Fe- irradiated cells one day following irradiation in CBA/Ca and C57BL/6 mice. At one month, PU.1 loss in C57BL/6 decreased to levels similar to that seen without irradiation. Furthermore, at one month following irradiation, the percent of PU.1 loss following 1Gy ^{56}Fe decreased in CBA/Ca mice. The dose response for ^{56}Fe leveled out at 0.2 Gy (Figure 1.5 and 1.6). Peng et al. concluded that although ^{56}Fe initially increased

PU.1 loss, its damaging effects caused the loss of these cells from the bone marrow cell population. However, this frequency increased one year post irradiation. The relative biological effectiveness (RBE) for PU.1 loss was calculated at one day post-irradiation to be ~3-3.5 for ^{56}Fe. However, for AML induction, the RBE was proposed to be ~1 (Weil et al., 2009), illustrating how RBE calculations are confounded by the endpoint and time point evaluated.

AML and telomeres/ radiation

Although increased telomerase activity in both human and murine AML has been reported, the presence of shortened telomeres has also been observed (Hartmann et al., 2005; Rithidech et al., 2001). Critically shortened telomeres may contribute to the formation of chromosomal abnormalities in human AML (Hartmann et al., 2005; Swiggers et al., 2006). Conversely, when telomere length was examined in murine AML, telomere shortening was neglible, and therefore may not play a major role in murine leukemogenesis (Meijne et al., 1996). Finnon et al. provided evidence that although telomeres were long in a mouse AML cell line (7926), telomere dysfunction and not shortening actually sensitized the 7926 cell line to radiation-induced chromosomal aberrations as compared to its AML mouse cell line counterpart (8709), which displayed little telomere dysfunction (Finnon et al., 2001). These findings suggest that although telomere length is maintained in murine AML, telomere dysfunction cannot be ruled out as a possible mechanism. However, whether telomere dysfunction plays a role in the early onset of the disease or is a result of cancer progression has not been determined.

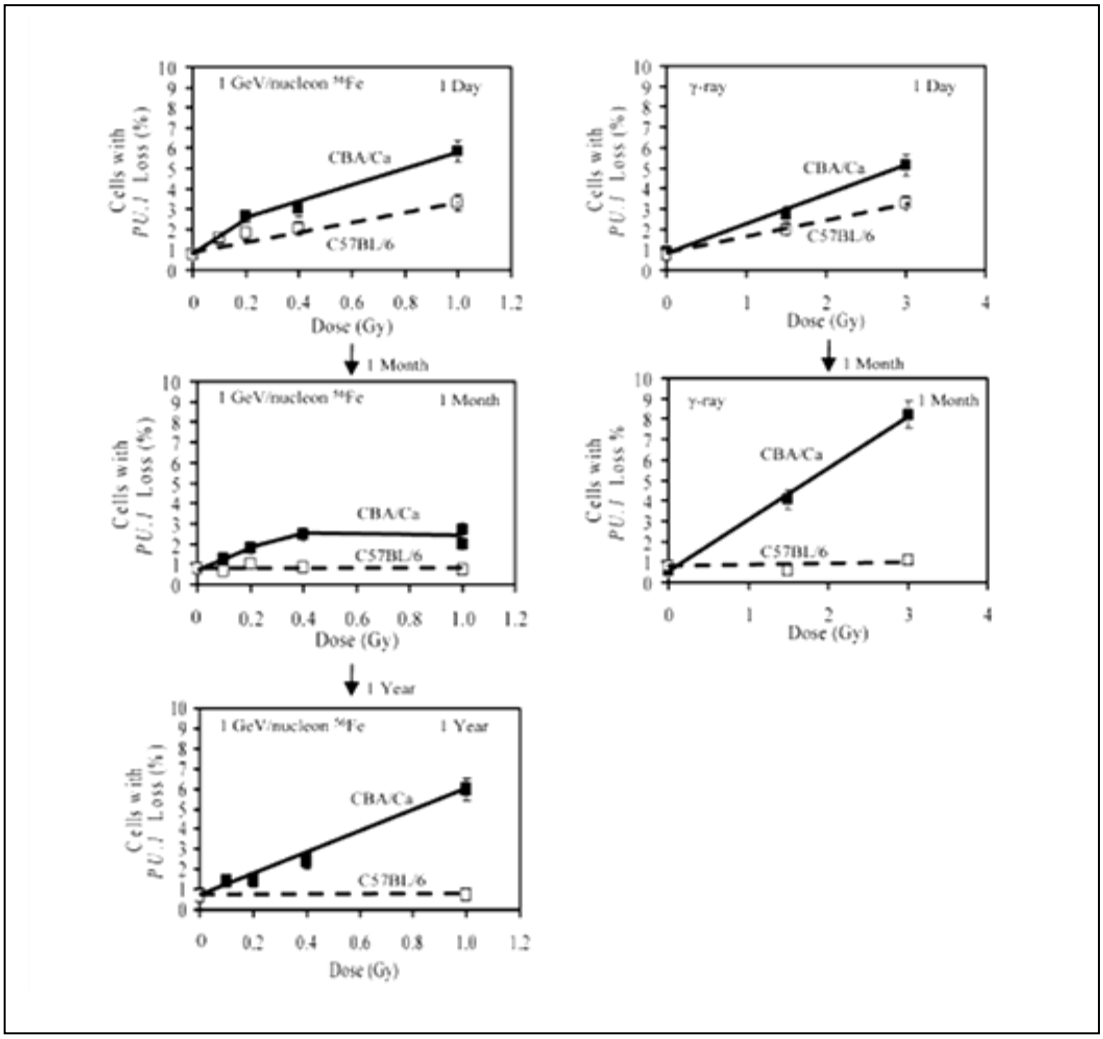

Figure 1.5. Graphs depict dose response for PU.1 loss measured by FISH using a bacterial artificial chromosome (BAC) probe for PU.1. Timepoints examined include 1 day, 1 month and 1 year post irradiation for ^{56}Fe and 1 day and 1 month for ^{137}Cs. Graphs show the sustained loss of PU.1 long after irradiation in the CBA/Ca mouse in comparison to the AML-resistant C57BL/6 mouse. (Peng et al., 2009)

TABLE 1

Dose (Gy)	Mouse strain	Time after irradiation (days)	Number of mitotic cells scored (no. mice)	Number of cells with *PU.1* loss	Percentage with *PU.1* loss ± SD
PU.1 loss after exposure to 1 GeV/nucleon ^{56}Fe ions					
0	CBA/Ca	1	1760 (4)	16	0.91 ± 0.23
		30	2035 (4)	11	0.54 ± 0.16
		365	1816 (4)	15	0.83 ± 0.21
	C57BL/6	1	1578 (3)	12	0.76 ± 0.22
		30	2044 (4)	16	0.78 ± 0.20
		365	1609 (3)	11	0.68 ± 0.21
0.1	CBA/Ca	1	1706 (4)	26	1.52 ± 0.30
		30	2103 (4)	26	1.24 ± 0.24
		365	1801 (4)	26	0.44 ± 0.28
	C57BL/6	1	2101 (4)	33	1.57 ± 0.27
		30	2090 (4)	14	0.67 ± 0.20
		365	—	—	—
0.2	CBA/Ca	1	2092 (4)	55	2.63 ± 0.35
		30	2123 (4)	38	1.79 ± 0.29
		365	1347 (4)	20	1.48 ± 0.33
	C57BL/6	1	2058 (4)	37	1.80 ± 0.30
		30	2162 (4)	22	1.02 ± 0.22
		365	—	—	—
0.4	CBA/Ca	1	2033 (4)	61	3.00 ± 0.38
		30	2119 (4)	52	2.45 ± 0.34
		365	2077 (4)	50	2.41 ± 0.34
	C57BL/6	1	2056 (4)	42	2.04 ± 0.32
		30	2105 (4)	18	0.85 ± 0.20
		365	—	—	—
1.0	CBA/Ca	1	2050 (4)	120	5.85 ± 0.53
		30	2040 (4)	40	1.96 ± 0.31
		30	1328 (4)	36	2.71 ± 0.36[a]
		365	1175 (4)	70	5.96 ± 0.71
	C57BL/6	1	2044 (4)	37	3.28 ± 0.40
		30	2086 (4)	15	0.72 ± 0.19
		365	2204 (4)	16	0.73 ± 0.18
PU.1 loss after exposure to γ rays					
1.5	CBA/Ca	1	1697 (4)	46	2.71 ± 0.39
		30	1660 (4)	67	4.04 ± 0.49
	C57BL/6	1	1863 (4)	37	1.99 ± 0.33
		30	2127 (4)	12	0.56 ± 0.16
3.0	CBA/Ca	1	1967 (4)	101	5.13 ± 0.51
		30	2035 (4)	167	8.21 ± 0.64
	C57BL/6	1	2093 (4)	68	3.25 ± 0.39
		30	2180 (4)	21	0.96 ± 0.21

[a] Independent repeat 6 months later.

Figure 1.6. Table depicting the actual percent of PU.1 loss observed following ^{56}Fe or ^{137}Cs exposure. (Peng et al., 2009)

We examined chromosomal aberrations and telomere end-capping function associated with PU.1 loss following ɣ- and HZE irradiation of CBA and C57BL/6 mice. Our studies evaluated chromosomal instabilities in cells many generations following radiation exposure. To further analyze the instability observed in clonal progeny, cells were injected into radiation ablated recipient mice and subsequent individual spleen colonies were evaluated for chromosomal aberrations. Analysis of spleen colonies provided a means to isolate and examine single clones for telomeric and chromosomal instabilities early in the process of tumorigenesis. Our purpose was to evaluate the generation and role of ongoing instability in the process of leukemogenesis. We also examined potential differences based on radiation quality following ɣ- versus HZE irradiation in an effort to assess related carcinogenetic effects.

Conclusions

Our goal in the present studies was to better elucidate the mechanisms in telomere structure and function. First, we examined a possible correlation between telomeres, genomic instability and the development of IR-induced murine AML. We found an association between increased chromatid-type aberrations, indicative of on-going instability, and IR-induced murine AML. We analyzed spleen colonies using the CFU-S assay and found increased instability at our 5 day time point in CBA/Ca mice, suggesting that this instability may contribute to cancer initiation. We also found evidence of telomere end-capping dysfunction in human AML, using a human AML cell line. Taken together, these data support genomic instability contributing to murine IR-induced AML. Although telomere end-capping dysfunction may not play a large role in murine AML, it

may contribute to chromosomal instability in human AML, as demonstrated in our human AML cell line.

We next analyzed the interaction of DNA-PKcs, hnRNP A1 and TERRA at telomeres. We found evidence that hnRNP A1 plays a role in the correct and efficient replication of telomeres, as evident with the presence of "fragile" telomeres, as previously described in TRF1 deficient mice (Sfeir et al., 2009). Although we did observe a decrease in hnRNP A1 phosphorylation following decreased DNA-PKcs or kinase activity, we did not observe a change in TERRA localization at telomeres following siRNA silencing of hnRNP A1. Interestingly, we found decreased TERRA localization was independent of hnRNP A1 and DNA-PKcs kinase activity. We also observed a decrease in overall TERRA levels following DNA-PKcs kinase inhibition, suggesting the kinase activity of DNA-PKcs may indirectly affect TERRA levels.

Altogether, our studies provide evidence for the vital role of telomere end-capping structure and function. In addition to the proposed roles of hnRNP A1 in telomere length maintenance and telomerase activity, we also provide evidence for its role in telomere replication. We also provide evidence that TERRA localization at telomeres does not require hnRNP A1 or DNA-PKcs kinase activity. Furthermore we present data suggesting a novel role for DNA-PKcs, where DNA-PKcs kinase activity affected the total levels of TERRA although the mechanism of this interaction remains to be explored. The data shown here emphasize the complex regulation of telomere maintenance. Since the initial observation of telomeres and the importance of their role in chromosome end protection by Herman Muller and Barbara McClintock (McClintock, 1939; Muller, 1938), several groups have conducted research in the telomere field in order to elucidate

the mechanisms that protect the telomeres from being recognized as broken DNA ends. However, we still have much to learn about telomeres, as evidenced by the recent observation that telomeres are transcribed into TERRA. TERRA has been implicated in maintaining chromatin structure, and evidence also suggests that DNA-PKcs is important in telomere end-capping. Therefore, one could speculate that the DNA-PKcs regulation of TERRA may aid in facilitating end capping function. We provide evidence that hnRNP A1 is required for efficient telomere replication and suggest a role for DNA-PKcs in the regulation of TERRA levels.

References

Alexander, B.J., Rasko, J.E., Morahan, G., and Cook, W.D. (1995). Gene deletion explains both in vivo and in vitro generated chromosome 2 aberrations associated with murine myeloid leukemia. Leukemia *9*, 2009-2015.

Allalunis-Turner, M.J., Barron, G.M., Day, R.S., 3rd, Dobler, K.D., and Mirzayans, R. (1993). Isolation of two cell lines from a human malignant glioma specimen differing in sensitivity to radiation and chemotherapeutic drugs. Radiat Res *134*, 349-354.

Allalunis-Turner, M.J., Zia, P.K., Barron, G.M., Mirzayans, R., and Day, R.S., 3rd (1995). Radiation-induced DNA damage and repair in cells of a radiosensitive human malignant glioma cell line. Radiat Res *144*, 288-293.

American Cancer Society (2010a). What are the risk factors for Acute Myeloid Leukemia? (American Cancer Society).

American Cancer Society (2010b). What are the risk factors for breast cancer? (American Cancer Society).

American Cancer Society (2010c). What are the statistics about breast cancer? (American Cancer Society).

Andegeko, Y., Moyal, L., Mittelman, L., Tsarfaty, I., Shiloh, Y., and Rotman, G. (2001). Nuclear retention of ATM at sites of DNA double strand breaks. J Biol Chem *276*, 38224-38230.

Anderson, C.W., Dunn, J.J., Freimuth, P.I., Galloway, A.M., and Allalunis-Turner, M.J. (2001). Frameshift mutation in PRKDC, the gene for DNA-PKcs, in the DNA repair-defective, human, glioma-derived cell line M059J. Radiat Res *156*, 2-9.

Anderson, R.M., Marsden, S.J., Wright, E.G., Kadhim, M.A., Goodhead, D.T., and Griffin, C.S. (2000). Complex chromosome aberrations in peripheral blood lymphocytes as a potential biomarker of exposure to high-LET alpha-particles. Int J Radiat Biol *76*, 31-42.

Araki, R., Fujimori, A., Hamatani, K., Mita, K., Saito, T., Mori, M., Fukumura, R., Morimyo, M., Muto, M., Itoh, M., *et al.* (1997). Nonsense mutation at Tyr-4046 in the DNA-dependent protein kinase catalytic subunit of severe combined immune deficiency mice. Proc Natl Acad Sci U S A *94*, 2438-2443.

Artandi, S.E., Chang, S., Lee, S.L., Alson, S., Gottlieb, G.J., Chin, L., and DePinho, R.A. (2000). Telomere dysfunction promotes non-reciprocal translocations and epithelial cancers in mice. Nature *406*, 641-645.

Arthur, D.C., and Bloomfield, C.D. (1983). Partial deletion of the long arm of chromosome 16 and bone marrow eosinophilia in acute nonlymphocytic leukemia: a new association. Blood *61*, 994-998.

Azzalin, C.M., Reichenbach, P., Khoriauli, L., Giulotto, E., and Lingner, J. (2007). Telomeric repeat containing RNA and RNA surveillance factors at mammalian chromosome ends. Science *318*, 798-801.

Bailey, S.M., Brenneman, M.A., Halbrook, J., Nickoloff, J.A., Ullrich, R.L., and Goodwin, E.H. (2004a). The kinase activity of DNA-PK is required to protect mammalian telomeres. DNA Repair (Amst) *3*, 225-233.

Bailey, S.M., Cornforth, M.N., Ullrich, R.L., and Goodwin, E.H. (2004b). Dysfunctional mammalian telomeres join with DNA double-strand breaks. DNA Repair (Amst) *3*, 349-357.

Bailey, S.M., Meyne, J., Chen, D.J., Kurimasa, A., Li, G.C., Lehnert, B.E., and Goodwin, E.H. (1999). DNA double-strand break repair proteins are required to cap the ends of mammalian chromosomes. Proc Natl Acad Sci U S A *96*, 14899-14904.

Bakkenist, C.J., and Kastan, M.B. (2003). DNA damage activates ATM through intermolecular autophosphorylation and dimer dissociation. Nature *421*, 499-506.

Bannister, A.J., Gottlieb, T.M., Kouzarides, T., and Jackson, S.P. (1993). c-Jun is phosphorylated by the DNA-dependent protein kinase in vitro; definition of the minimal kinase recognition motif. Nucleic Acids Res *21*, 1289-1295.

Ben-David, Y., Bani, M.R., Chabot, B., De Koven, A., and Bernstein, A. (1992). Retroviral insertions downstream of the heterogeneous nuclear ribonucleoprotein A1 gene in erythroleukemia cells: evidence that A1 is not essential for cell growth. Mol Cell Biol *12*, 4449-4455.

Blunt, T., Gell, D., Fox, M., Taccioli, G.E., Lehmann, A.R., Jackson, S.P., and Jeggo, P.A. (1996). Identification of a nonsense mutation in the carboxyl-terminal region of DNA-dependent protein kinase catalytic subunit in the scid mouse. Proc Natl Acad Sci U S A *93*, 10285-10290.

Bodnar, A.G., Ouellette, M., Frolkis, M., Holt, S.E., Chiu, C.P., Morin, G.B., Harley, C.B., Shay, J.W., Lichtsteiner, S., and Wright, W.E. (1998). Extension of life-span by introduction of telomerase into normal human cells. Science *279*, 349-352.

Bonnet, D., and Dick, J.E. (1997). Human acute myeloid leukemia is organized as a hierarchy that originates from a primitive hematopoietic cell. Nat Med *3*, 730-737.

Borrow, J., Goddard, A.D., Sheer, D., and Solomon, E. (1990). Molecular analysis of acute promyelocytic leukemia breakpoint cluster region on chromosome 17. Science *249*, 1577-1580.

Boubnov, N.V., and Weaver, D.T. (1995). scid cells are deficient in Ku and replication protein A phosphorylation by the DNA-dependent protein kinase. Mol Cell Biol *15*, 5700-5706.

Bouffler, S.D., Breckon, G., and Cox, R. (1996). Chromosomal mechanisms in murine radiation acute myeloid leukaemogenesis. Carcinogenesis *17*, 655-659.

Bouffler, S.D., Meijne, E.I., Morris, D.J., and Papworth, D. (1997). Chromosome 2 hypersensitivity and clonal development in murine radiation acute myeloid leukaemia. Int J Radiat Biol *72*, 181-189.

Brush, G.S., Anderson, C.W., and Kelly, T.J. (1994). The DNA-activated protein kinase is required for the phosphorylation of replication protein A during simian virus 40 DNA replication. Proc Natl Acad Sci U S A *91*, 12520-12524.

Bryan, T.M., Englezou, A., Dunham, M.A., and Reddel, R.R. (1998). Telomere length dynamics in telomerase-positive immortal human cell populations. Exp Cell Res *239*, 370-378.

Burd, C.G., and Dreyfuss, G. (1994). RNA binding specificity of hnRNP A1: significance of hnRNP A1 high-affinity binding sites in pre-mRNA splicing. Embo J *13*, 1197-1204.

Burma, S., Chen, B.P., Murphy, M., Kurimasa, A., and Chen, D.J. (2001). ATM phosphorylates histone H2AX in response to DNA double-strand breaks. J Biol Chem *276*, 42462-42467.

Canman, C.E., Lim, D.S., Cimprich, K.A., Taya, Y., Tamai, K., Sakaguchi, K., Appella, E., Kastan, M.B., and Siliciano, J.D. (1998). Activation of the ATM kinase by ionizing radiation and phosphorylation of p53. Science *281*, 1677-1679.

Carter, T., Vancurova, I., Sun, I., Lou, W., and DeLeon, S. (1990). A DNA-activated protein kinase from HeLa cell nuclei. Mol Cell Biol *10*, 6460-6471.

Carter, T.H., Kopman, C.R., and James, C.B. (1988). DNA-stimulated protein phosphorylation in HeLa whole cell and nuclear extracts. Biochem Biophys Res Commun *157*, 535-540.

Cary, R.B., Peterson, S.R., Wang, J., Bear, D.G., Bradbury, E.M., and Chen, D.J. (1997). DNA looping by Ku and the DNA-dependent protein kinase. Proc Natl Acad Sci U S A *94*, 4267-4272.

Cech, T.R. (2004). Beginning to understand the end of the chromosome. Cell *116*, 273-279.

Chan, D.W., Chen, B.P., Prithivirajsingh, S., Kurimasa, A., Story, M.D., Qin, J., and Chen, D.J. (2002). Autophosphorylation of the DNA-dependent protein kinase

catalytic subunit is required for rejoining of DNA double-strand breaks. Genes Dev *16*, 2333-2338.

Chan, D.W., and Lees-Miller, S.P. (1996). The DNA-dependent protein kinase is inactivated by autophosphorylation of the catalytic subunit. J Biol Chem *271*, 8936-8941.

Chen, B.P., Uematsu, N., Kobayashi, J., Lerenthal, Y., Krempler, A., Yajima, H., Lobrich, M., Shiloh, Y., and Chen, D.J. (2007). Ataxia telangiectasia mutated (ATM) is essential for DNA-PKcs phosphorylations at the Thr-2609 cluster upon DNA double strand break. J Biol Chem *282*, 6582-6587.

Chen, X.B., Melchionna, R., Denis, C.M., Gaillard, P.H., Blasina, A., Van de Weyer, I., Boddy, M.N., Russell, P., Vialard, J., and McGowan, C.H. (2001). Human Mus81-associated endonuclease cleaves Holliday junctions in vitro. Mol Cell *8*, 1117-1127.

Cherif, H., Tarry, J.L., Ozanne, S.E., and Hales, C.N. (2003). Ageing and telomeres: a study into organ- and gender-specific telomere shortening. Nucleic Acids Res *31*, 1576-1583.

Chiu, C.P., Dragowska, W., Kim, N.W., Vaziri, H., Yui, J., Thomas, T.E., Harley, C.B., and Lansdorp, P.M. (1996). Differential expression of telomerase activity in hematopoietic progenitors from adult human bone marrow. Stem Cells *14*, 239-248.

Clark, D.J., Meijne, E.I., Bouffler, S.D., Huiskamp, R., Skidmore, C.J., Cox, R., and Silver, A.R. (1996). Microsatellite analysis of recurrent chromosome 2 deletions in acute myeloid leukaemia induced by radiation in F1 hybrid mice. Genes Chromosomes Cancer *16*, 238-246.

Collado, M., Blasco, M.A., and Serrano, M. (2007). Cellular senescence in cancer and aging. Cell *130*, 223-233.

Cook, W.D., McCaw, B.J., Herring, C., John, D.L., Foote, S.J., Nutt, S.L., and Adams, J.M. (2004). PU.1 is a suppressor of myeloid leukemia, inactivated in mice by gene deletion and mutation of its DNA binding domain. Blood *104*, 3437-3444.

Counter, C.M., Avilion, A.A., LeFeuvre, C.E., Stewart, N.G., Greider, C.W., Harley, C.B., and Bacchetti, S. (1992). Telomere shortening associated with chromosome instability is arrested in immortal cells which express telomerase activity. Embo J *11*, 1921-1929.

Court-Brown, W.M., and Doll, R. (1957). Leukaemia and aplastic anaemia in patients irradiated for ankylosing spondylitis. Spec Rep Ser Med Res Counc (G B), 1-135.

Crabbe, L., Jauch, A., Naeger, C.M., Holtgreve-Grez, H., and Karlseder, J. (2007). Telomere dysfunction as a cause of genomic instability in Werner syndrome. Proc Natl Acad Sci U S A *104*, 2205-2210.

Cucinotta, F.A., and Durante, M. (2006). Cancer risk from exposure to galactic cosmic rays: implications for space exploration by human beings. Lancet Oncol *7*, 431-435.

Cui, X., Yu, Y., Gupta, S., Cho, Y.M., Lees-Miller, S.P., and Meek, K. (2005). Autophosphorylation of DNA-dependent protein kinase regulates DNA end processing and may also alter double-strand break repair pathway choice. Mol Cell Biol *25*, 10842-10852.

Dakic, A., Metcalf, D., Di Rago, L., Mifsud, S., Wu, L., and Nutt, S.L. (2005). PU.1 regulates the commitment of adult hematopoietic progenitors and restricts granulopoiesis. J Exp Med *201*, 1487-1502.

Danska, J.S., Holland, D.P., Mariathasan, S., Williams, K.M., and Guidos, C.J. (1996). Biochemical and genetic defects in the DNA-dependent protein kinase in murine scid lymphocytes. Mol Cell Biol *16*, 5507-5517.

de Lange, T. (1994). Activation of telomerase in a human tumor. Proc Natl Acad Sci U S A *91*, 2882-2885.

de Lange, T. (2005). Shelterin: the protein complex that shapes and safeguards human telomeres. Genes Dev *19*, 2100-2110.

de Silanes, I.L., d'Alcontres, M.S., and Blasco, M.A. (2010). TERRA transcripts are bound by a complex array of RNA-binding proteins. Nat Commun *1*, 33.

de The, H., Chomienne, C., Lanotte, M., Degos, L., and Dejean, A. (1990). The t(15;17) translocation of acute promyelocytic leukaemia fuses the retinoic acid receptor alpha gene to a novel transcribed locus. Nature *347*, 558-561.

Deng, Z., Campbell, A.E., and Lieberman, P.M. (2010). TERRA, CpG methylation and telomere heterochromatin: lessons from ICF syndrome cells. Cell Cycle *9*, 69-74.

Deng, Z., Norseen, J., Wiedmer, A., Riethman, H., and Lieberman, P.M. (2009). TERRA RNA binding to TRF2 facilitates heterochromatin formation and ORC recruitment at telomeres. Mol Cell *35*, 403-413.

Ding, Q., Reddy, Y.V., Wang, W., Woods, T., Douglas, P., Ramsden, D.A., Lees-Miller, S.P., and Meek, K. (2003). Autophosphorylation of the catalytic subunit of the DNA-dependent protein kinase is required for efficient end processing during DNA double-strand break repair. Mol Cell Biol *23*, 5836-5848.

Dores, G., Cote TR, and Travis LB (2006). New Malignancies Following Hodgkin Lymphoma, Non-Hodgkin Lymphoma, and Myeloma. In New Malignancies

Among Cancer Survivors: SEER Cancer Registries, 1973-2000 (Bethesda, National Cancer Institute, NIH Publ. No. 05-5302), pp. 397-435.

Douglas, P., Sapkota, G.P., Morrice, N., Yu, Y., Goodarzi, A.A., Merkle, D., Meek, K., Alessi, D.R., and Lees-Miller, S.P. (2002). Identification of in vitro and in vivo phosphorylation sites in the catalytic subunit of the DNA-dependent protein kinase. Biochem J *368*, 243-251.

Dunham, M.A., Neumann, A.A., Fasching, C.L., and Reddel, R.R. (2000). Telomere maintenance by recombination in human cells. Nat Genet *26*, 447-450.

Dvir, A., Peterson, S.R., Knuth, M.W., Lu, H., and Dynan, W.S. (1992). Ku autoantigen is the regulatory component of a template-associated protein kinase that phosphorylates RNA polymerase II. Proc Natl Acad Sci U S A *89*, 11920-11924.

Elledge, S.J. (1996). Cell cycle checkpoints: preventing an identity crisis. Science *274*, 1664-1672.

Falzon, M., Fewell, J.W., and Kuff, E.L. (1993). EBP-80, a transcription factor closely resembling the human autoantigen Ku, recognizes single- to double-strand transitions in DNA. J Biol Chem *268*, 10546-10552.

Finnon, P., Wong, H.P., Silver, A.R., Slijepcevic, P., and Bouffler, S.D. (2001). Long but dysfunctional telomeres correlate with chromosomal radiosensitivity in a mouse AML cell line. Int J Radiat Biol *77*, 1151-1162.

Ford, L.P., Wright, W.E., and Shay, J.W. (2002). A model for heterogeneous nuclear ribonucleoproteins in telomere and telomerase regulation. Oncogene *21*, 580-583.

Gibbs, D.D. (1967). Werner's syndrome ('progeria of the adult'). Proc R Soc Med *60*, 135-136.

Gisselsson, D., Jonson, T., Petersen, A., Strombeck, B., Dal Cin, P., Hoglund, M., Mitelman, F., Mertens, F., and Mandahl, N. (2001). Telomere dysfunction triggers extensive DNA fragmentation and evolution of complex chromosome abnormalities in human malignant tumors. Proc Natl Acad Sci U S A *98*, 12683-12688.

Gotoff, S.P., Amirmokri, E., and Liebner, E.J. (1967). Ataxia telangiectasia. Neoplasia, untoward response to x-irradiation, and tuberous sclerosis. Am J Dis Child *114*, 617-625.

Gottlieb, T.M., and Jackson, S.P. (1993). The DNA-dependent protein kinase: requirement for DNA ends and association with Ku antigen. Cell *72*, 131-142.

Goytisolo, F.A., Samper, E., Martin-Caballero, J., Finnon, P., Herrera, E., Flores, J.M., Bouffler, S.D., and Blasco, M.A. (2000). Short telomeres result in organismal hypersensitivity to ionizing radiation in mammals. J Exp Med *192*, 1625-1636.

Grawunder, U., Wilm, M., Wu, X., Kulesza, P., Wilson, T.E., Mann, M., and Lieber, M.R. (1997). Activity of DNA ligase IV stimulated by complex formation with XRCC4 protein in mammalian cells. Nature *388*, 492-495.

Greider, C.W., and Blackburn, E.H. (1985). Identification of a specific telomere terminal transferase activity in Tetrahymena extracts. Cell *43*, 405-413.

Greider, C.W., and Blackburn, E.H. (1989). A telomeric sequence in the RNA of Tetrahymena telomerase required for telomere repeat synthesis. Nature *337*, 331-337.

Griffith, J.D., Comeau, L., Rosenfield, S., Stansel, R.M., Bianchi, A., Moss, H., and de Lange, T. (1999). Mammalian telomeres end in a large duplex loop. Cell *97*, 503-514.

Guan, J., DiBiase, S., and Iliakis, G. (2000). The catalytic subunit DNA-dependent protein kinase (DNA-PKcs) facilitates recovery from radiation-induced inhibition of DNA replication. Nucleic Acids Res *28*, 1183-1192.

Hall, E.J.a.G., Amato (2006). Radiobiology for the radiologist, 6th edn (Philadelphia, Lippincott Williams and Wilkins).

Hanahan, D., and Weinberg, R.A. (2011). Hallmarks of cancer: the next generation. Cell *144*, 646-674.

Hanson, W.R., Fry, R.J., Sallese, A.R., Frischer, H., Ahmad, T., and Ainsworth, E.J. (1987). Comparison of intestine and bone marrow radiosensitivity of the BALB/c and the C57BL/6 mouse strains and their B6CF1 offspring. Radiat Res *110*, 340-352.

Harley, C.B., Futcher, A.B., and Greider, C.W. (1990). Telomeres shorten during ageing of human fibroblasts. Nature *345*, 458-460.

Harley, C.B., and Villeponteau, B. (1995). Telomeres and telomerase in aging and cancer. Curr Opin Genet Dev *5*, 249-255.

Hartmann, U., Brummendorf, T.H., Balabanov, S., Thiede, C., Illme, T., and Schaich, M. (2005). Telomere length and hTERT expression in patients with acute myeloid leukemia correlates with chromosomal abnormalities. Haematologica *90*, 307-316.

Hayata, I., Seki, M., Yoshida, K., Hirashima, K., Sado, T., Yamagiwa, J., and Ishihara, T. (1983). Chromosomal aberrations observed in 52 mouse myeloid leukemias. Cancer Res *43*, 367-373.

He, Y., and Smith, R. (2009). Nuclear functions of heterogeneous nuclear ribonucleoproteins A/B. Cell Mol Life Sci *66*, 1239-1256.

Hefferin, M.L., and Tomkinson, A.E. (2005). Mechanism of DNA double-strand break repair by non-homologous end joining. DNA Repair (Amst) *4*, 639-648.

Hiyama, E., Gollahon, L., Kataoka, T., Kuroi, K., Yokoyama, T., Gazdar, A.F., Hiyama, K., Piatyszek, M.A., and Shay, J.W. (1996a). Telomerase activity in human breast tumors. J Natl Cancer Inst *88*, 116-122.

Hiyama, E., Tatsumoto, N., Kodama, T., Hiyama, K., Shay, J., and Yokoyama, T. (1996b). Telomerase activity in human intestine. Int J Oncol *9*, 453-458.

Hodgson, S.V., Heap, E., Cameron, J., Ellis, D., Mathew, C.G., Eeles, R.A., Solomon, E., and Lewis, C.M. (1999). Risk factors for detecting germline BRCA1 and BRCA2 founder mutations in Ashkenazi Jewish women with breast or ovarian cancer. J Med Genet *36*, 369-373.

Hogge, D.E., Misawa, S., Parsa, N.Z., Pollak, A., and Testa, J.R. (1984). Abnormalities of chromosome 16 in association with acute myelomonocytic leukemia and dysplastic bone marrow eosinophils. J Clin Oncol *2*, 550-557.

Houston, I.B., Kamath, M.B., Schweitzer, B.L., Chlon, T.M., and Dekoter, R.P. (2007). Reduction in PU.1 activity results in a block to B-cell development, abnormal myeloid proliferation, and neonatal lethality. Exp Hematol *35*, 1056-1068.

Ip, S.C., Rass, U., Blanco, M.G., Flynn, H.R., Skehel, J.M., and West, S.C. (2008). Identification of Holliday junction resolvases from humans and yeast. Nature *456*, 357-361.

Ivessa, A.S., Zhou, J.Q., Schulz, V.P., Monson, E.K., and Zakian, V.A. (2002). Saccharomyces Rrm3p, a 5' to 3' DNA helicase that promotes replication fork progression through telomeric and subtelomeric DNA. Genes Dev *16*, 1383-1396.

Ivessa, A.S., Zhou, J.Q., and Zakian, V.A. (2000). The Saccharomyces Pif1p DNA helicase and the highly related Rrm3p have opposite effects on replication fork progression in ribosomal DNA. Cell *100*, 479-489.

Iwasaki, H., Somoza, C., Shigematsu, H., Duprez, E.A., Iwasaki-Arai, J., Mizuno, S., Arinobu, Y., Geary, K., Zhang, P., Dayaram, T., *et al.* (2005). Distinctive and indispensable roles of PU.1 in maintenance of hematopoietic stem cells and their differentiation. Blood *106*, 1590-1600.

John, E.M., Miron, A., Gong, G., Phipps, A.I., Felberg, A., Li, F.P., West, D.W., and Whittemore, A.S. (2007). Prevalence of pathogenic BRCA1 mutation carriers in 5 US racial/ethnic groups. Jama *298*, 2869-2876.

Kadhim, M.A., Macdonald, D.A., Goodhead, D.T., Lorimore, S.A., Marsden, S.J., and Wright, E.G. (1992). Transmission of chromosomal instability after plutonium alpha-particle irradiation. Nature *355*, 738-740.

Khosravi, R., Maya, R., Gottlieb, T., Oren, M., Shiloh, Y., and Shkedy, D. (1999). Rapid ATM-dependent phosphorylation of MDM2 precedes p53 accumulation in response to DNA damage. Proc Natl Acad Sci U S A *96*, 14973-14977.

Kim, N.W., Piatyszek, M.A., Prowse, K.R., Harley, C.B., West, M.D., Ho, P.L., Coviello, G.M., Wright, W.E., Weinrich, S.L., and Shay, J.W. (1994). Specific association of human telomerase activity with immortal cells and cancer. Science *266*, 2011-2015.

LaBranche, H., Dupuis, S., Ben-David, Y., Bani, M.R., Wellinger, R.J., and Chabot, B. (1998). Telomere elongation by hnRNP A1 and a derivative that interacts with telomeric repeats and telomerase. Nat Genet *19*, 199-202.

Land, C.E., Tokunaga, M., Koyama, K., Soda, M., Preston, D.L., Nishimori, I., and Tokuoka, S. (2003). Incidence of female breast cancer among atomic bomb survivors, Hiroshima and Nagasaki, 1950-1990. Radiat Res *160*, 707-717.

Lapidot, T., Sirard, C., Vormoor, J., Murdoch, B., Hoang, T., Caceres-Cortes, J., Minden, M., Paterson, B., Caligiuri, M.A., and Dick, J.E. (1994). A cell initiating human acute myeloid leukaemia after transplantation into SCID mice. Nature *367*, 645-648.

Le Beau, M.M., Larson, R.A., Bitter, M.A., Vardiman, J.W., Golomb, H.M., and Rowley, J.D. (1983). Association of an inversion of chromosome 16 with abnormal marrow eosinophils in acute myelomonocytic leukemia. A unique cytogenetic-clinicopathological association. N Engl J Med *309*, 630-636.

Lee, J.H., and Paull, T.T. (2005). ATM activation by DNA double-strand breaks through the Mre11-Rad50-Nbs1 complex. Science *308*, 551-554.

Lees-Miller, S.P., and Anderson, C.W. (1989). The human double-stranded DNA-activated protein kinase phosphorylates the 90-kDa heat-shock protein, hsp90 alpha at two NH2-terminal threonine residues. J Biol Chem *264*, 17275-17280.

Lees-Miller, S.P., Chen, Y.R., and Anderson, C.W. (1990). Human cells contain a DNA-activated protein kinase that phosphorylates simian virus 40 T antigen, mouse p53, and the human Ku autoantigen. Mol Cell Biol *10*, 6472-6481.

Lees-Miller, S.P., Sakaguchi, K., Ullrich, S.J., Appella, E., and Anderson, C.W. (1992). Human DNA-activated protein kinase phosphorylates serines 15 and 37 in the amino-terminal transactivation domain of human p53. Mol Cell Biol *12*, 5041-5049.

Leteurtre, F., Li, X., Gluckman, E., and Carosella, E.D. (1997). Telomerase activity during the cell cycle and in gamma-irradiated hematopoietic cells. Leukemia *11*, 1681-1689.

Li, Z., Otevrel, T., Gao, Y., Cheng, H.L., Seed, B., Stamato, T.D., Taccioli, G.E., and Alt, F.W. (1995). The XRCC4 gene encodes a novel protein involved in DNA double-strand break repair and V(D)J recombination. Cell *83*, 1079-1089.

Liang, H., Fairman, J., Claxton, D.F., Nowell, P.C., Green, E.D., and Nagarajan, L. (1998). Molecular anatomy of chromosome 7q deletions in myeloid neoplasms: evidence for multiple critical loci. Proc Natl Acad Sci U S A *95*, 3781-3785.

Lieber, M.R. (1999). The biochemistry and biological significance of nonhomologous DNA end joining: an essential repair process in multicellular eukaryotes. Genes Cells *4*, 77-85.

Lieber, M.R. (2010). The mechanism of double-strand DNA break repair by the nonhomologous DNA end-joining pathway. Annu Rev Biochem *79*, 181-211.

Limoli, C.L., Ponnaiya, B., Corcoran, J.J., Giedzinski, E., and Morgan, W.F. (2000). Chromosomal instability induced by heavy ion irradiation. Int J Radiat Biol *76*, 1599-1606.

Lingner, J., Hughes, T.R., Shevchenko, A., Mann, M., Lundblad, V., and Cech, T.R. (1997). Reverse transcriptase motifs in the catalytic subunit of telomerase. Science *276*, 561-567.

Luke, B., Panza, A., Redon, S., Iglesias, N., Li, Z., and Lingner, J. (2008). The Rat1p 5' to 3' exonuclease degrades telomeric repeat-containing RNA and promotes telomere elongation in Saccharomyces cerevisiae. Mol Cell *32*, 465-477.

Lundblad, V., and Szostak, J.W. (1989). A mutant with a defect in telomere elongation leads to senescence in yeast. Cell *57*, 633-643.

M'Kacher, R., Bennaceur-Griscelli, A., Girinsky, T., Koscielny, S., Delhommeau, F., Dossou, J., Violot, D., Leclercq, E., Courtier, M.H., Beron-Gaillard, N., *et al.* (2007). Telomere shortening and associated chromosomal instability in peripheral blood lymphocytes of patients with Hodgkin's lymphoma prior to any treatment are predictive of second cancers. Int J Radiat Oncol Biol Phys *68*, 465-471.

Ma, Y., Pannicke, U., Schwarz, K., and Lieber, M.R. (2002). Hairpin opening and overhang processing by an Artemis/DNA-dependent protein kinase complex in nonhomologous end joining and V(D)J recombination. Cell *108*, 781-794.

Ma, Y., Schwarz, K., and Lieber, M.R. (2005). The Artemis:DNA-PKcs endonuclease cleaves DNA loops, flaps, and gaps. DNA Repair (Amst) *4*, 845-851.

Major, I.R., and Mole, R.H. (1978). Myeloid leukaemia in x-ray irradiated CBA mice. Nature *272*, 455-456.

Makovets, S., Herskowitz, I., and Blackburn, E.H. (2004). Anatomy and dynamics of DNA replication fork movement in yeast telomeric regions. Mol Cell Biol *24*, 4019-4031.

Malone, K.E., Daling, J.R., Doody, D.R., Hsu, L., Bernstein, L., Coates, R.J., Marchbanks, P.A., Simon, M.S., McDonald, J.A., Norman, S.A., *et al.* (2006). Prevalence and predictors of BRCA1 and BRCA2 mutations in a population-based study of breast cancer in white and black American women ages 35 to 64 years. Cancer Res *66*, 8297-8308.

Mantell, L.L., and Greider, C.W. (1994). Telomerase activity in germline and embryonic cells of Xenopus. Embo J *13*, 3211-3217.

Mao, Z., Bozzella, M., Seluanov, A., and Gorbunova, V. (2008). DNA repair by nonhomologous end joining and homologous recombination during cell cycle in human cells. Cell Cycle *7*, 2902-2906.

Marrone, A., Stevens, D., Vulliamy, T., Dokal, I., and Mason, P.J. (2004). Heterozygous telomerase RNA mutations found in dyskeratosis congenita and aplastic anemia reduce telomerase activity via haploinsufficiency. Blood *104*, 3936-3942.

Marvo, S.L., King, S.R., and Jaskunas, S.R. (1983). Role of short regions of homology in intermolecular illegitimate recombination events. Proc Natl Acad Sci U S A *80*, 2452-2456.

Matsuoka, S., Huang, M., and Elledge, S.J. (1998). Linkage of ATM to cell cycle regulation by the Chk2 protein kinase. Science *282*, 1893-1897.

McClintock, B. (1939). The Behavior in Successive Nuclear Divisions of a Chromosome Broken at Meiosis. Proc Natl Acad Sci U S A *25*, 405-416.

Meek, K., Douglas, P., Cui, X., Ding, Q., and Lees-Miller, S.P. (2007). trans Autophosphorylation at DNA-dependent protein kinase's two major autophosphorylation site clusters facilitates end processing but not end joining. Mol Cell Biol *27*, 3881-3890.

Meijne, E.I., Silver, A.R., Bouffler, S.D., Morris, D.J., van Kampen, E.W., Spanjer, S., Huiskamp, R., and Cox, R. (1996). Role of telomeric sequences in murine radiation-induced myeloid leukaemia. Genes Chromosomes Cancer *16*, 230-237.

Metcalf, D., Dakic, A., Mifsud, S., Di Rago, L., Wu, L., and Nutt, S. (2006). Inactivation of PU.1 in adult mice leads to the development of myeloid leukemia. Proc Natl Acad Sci U S A *103*, 1486-1491.

Meyne, J., Ratliff, R.L., and Moyzis, R.K. (1989). Conservation of the human telomere sequence (TTAGGG)n among vertebrates. Proc Natl Acad Sci U S A *86*, 7049-7053.

Morgan, J.L., Holcomb, T.M., and Morrissey, R.W. (1968). Radiation reaction in ataxia telangiectasia. Am J Dis Child *116*, 557-558.

Moshous, D., Callebaut, I., de Chasseval, R., Corneo, B., Cavazzana-Calvo, M., Le Deist, F., Tezcan, I., Sanal, O., Bertrand, Y., Philippe, N., *et al.* (2001). Artemis, a novel DNA double-strand break repair/V(D)J recombination protein, is mutated in human severe combined immune deficiency. Cell *105*, 177-186.

Muller, H.J. (1938). The remaking of chromosomes. Collecting Net *13*, 182-198.

Nagarajan, L. (1995). Molecular analysis of the 5q- chromosome. Leuk Lymphoma *17*, 361-366.

Nagata, T., Takada, Y., Ono, A., Nagata, K., Konishi, Y., Nukina, T., Ono, M., Matsugami, A., Furukawa, A., Fujimoto, N., *et al.* (2008). Elucidation of the mode of interaction in the UP1-telomerase RNA-telomeric DNA ternary complex which serves to recruit telomerase to telomeric DNA and to enhance the telomerase activity. Nucleic Acids Res *36*, 6816-6824.

NAS (2010). Atomic Bomb Casualty Commission, 1945-1982 (The National Academy of Sciences).

NASA (2000). The Natural Space Radiation Hazard (National Aeronautics and Space Administration).

National Cancer Institute (2006). What you need to know about cancer: Risk Factors (National Cancer Institute).

National Cancer Institute (2011a). General Information about Adult Acute Myeloid Leukemia (National Cancer Institute).

National Cancer Institute (2011b). SEER Stat Fact Sheets: Acute Myeloid Leukemia (National Cancer Institute).

Nergadze, S.G., Farnung, B.O., Wischnewski, H., Khoriauli, L., Vitelli, V., Chawla, R., Giulotto, E., and Azzalin, C.M. (2009). CpG-island promoters drive transcription of human telomeres. Rna *15*, 2186-2194.

Neumann, A.A., and Reddel, R.R. (2002). Telomere maintenance and cancer -- look, no telomerase. Nat Rev Cancer *2*, 879-884.

Nevaldine, B., Longo, J.A., and Hahn, P.J. (1997). The scid defect results in much slower repair of DNA double-strand breaks but not high levels of residual breaks. Radiat Res *147*, 535-540.

Ng, L.J., Cropley, J.E., Pickett, H.A., Reddel, R.R., and Suter, C.M. (2009). Telomerase activity is associated with an increase in DNA methylation at the proximal

subtelomere and a reduction in telomeric transcription. Nucleic Acids Res *37*, 1152-1159.

Nussenzweig, A., Chen, C., da Costa Soares, V., Sanchez, M., Sokol, K., Nussenzweig, M.C., and Li, G.C. (1996). Requirement for Ku80 in growth and immunoglobulin V(D)J recombination. Nature *382*, 551-555.

Nussenzweig, A., Sokol, K., Burgman, P., Li, L., and Li, G.C. (1997). Hypersensitivity of Ku80-deficient cell lines and mice to DNA damage: the effects of ionizing radiation on growth, survival, and development. Proc Natl Acad Sci U S A *94*, 13588-13593.

Okayasu, R., Suetomi, K., and Ullrich, R.L. (1998). Wortmannin inhibits repair of DNA double-strand breaks in irradiated normal human cells. Radiat Res *149*, 440-445.

Okayasu, R., Suetomi, K., Yu, Y., Silver, A., Bedford, J.S., Cox, R., and Ullrich, R.L. (2000). A deficiency in DNA repair and DNA-PKcs expression in the radiosensitive BALB/c mouse. Cancer Res *60*, 4342-4345.

Olovnikov, A.M. (1973). A theory of marginotomy. The incomplete copying of template margin in enzymic synthesis of polynucleotides and biological significance of the phenomenon. J Theor Biol *41*, 181-190.

Palm, W., and de Lange, T. (2008). How shelterin protects mammalian telomeres. Annu Rev Genet *42*, 301-334.

Pan, Z.Q., Amin, A.A., Gibbs, E., Niu, H., and Hurwitz, J. (1994). Phosphorylation of the p34 subunit of human single-stranded-DNA-binding protein in cyclin A-activated G1 extracts is catalyzed by cdk-cyclin A complex and DNA-dependent protein kinase. Proc Natl Acad Sci U S A *91*, 8343-8347.

Patry, C., Bouchard, L., Labrecque, P., Gendron, D., Lemieux, B., Toutant, J., Lapointe, E., Wellinger, R., and Chabot, B. (2003). Small interfering RNA-mediated reduction in heterogeneous nuclear ribonucleoparticule A1/A2 proteins induces apoptosis in human cancer cells but not in normal mortal cell lines. Cancer Res *63*, 7679-7688.

Patry, C., Lemieux, B., Wellinger, R.J., and Chabot, B. (2004). Targeting heterogeneous nuclear ribonucleoparticule A1 and A2 proteins by RNA interference promotes cell death in transformed but not in normal mouse cell lines. Mol Cancer Ther *3*, 1193-1199.

Paull, T.T., Cortez, D., Bowers, B., Elledge, S.J., and Gellert, M. (2001). Direct DNA binding by Brca1. Proc Natl Acad Sci U S A *98*, 6086-6091.

Paull, T.T., and Gellert, M. (1999). Nbs1 potentiates ATP-driven DNA unwinding and endonuclease cleavage by the Mre11/Rad50 complex. Genes Dev *13*, 1276-1288.

Peng, Y., Brown, N., Finnon, R., Warner, C.L., Liu, X., Genik, P.C., Callan, M.A., Ray, F.A., Borak, T.B., Badie, C., *et al.* (2009). Radiation leukemogenesis in mice: loss of PU.1 on chromosome 2 in CBA and C57BL/6 mice after irradiation with 1 GeV/nucleon 56Fe ions, X rays or gamma rays. Part I. Experimental observations. Radiat Res *171*, 474-483.

Perloff, J.K., and Phelps, E.T. (1958). A review of Werner's syndrome, with a report of the second autopsied case. Ann Intern Med *48*, 1205-1220.

Peterson, S.R., Dvir, A., Anderson, C.W., and Dynan, W.S. (1992). DNA binding provides a signal for phosphorylation of the RNA polymerase II heptapeptide repeats. Genes Dev *6*, 426-438.

Peto, J., and Mack, T.M. (2000). High constant incidence in twins and other relatives of women with breast cancer. Nat Genet *26*, 411-414.

Pierce, D.A., Shimizu, Y., Preston, D.L., Vaeth, M., and Mabuchi, K. (1996). Studies of the mortality of atomic bomb survivors. Report 12, Part I. Cancer: 1950-1990. Radiat Res *146*, 1-27.

Preston, D.L., Kusumi, S., Tomonaga, M., Izumi, S., Ron, E., Kuramoto, A., Kamada, N., Dohy, H., Matsuo, T., Matsui, T., *et al.* (1994). Cancer incidence in atomic bomb survivors. Part III. Leukemia, lymphoma and multiple myeloma, 1950-1987. Radiat Res *137*, S68-97.

Preston, D.L., Mattsson, A., Holmberg, E., Shore, R., Hildreth, N.G., and Boice, J.D., Jr. (2002). Radiation effects on breast cancer risk: a pooled analysis of eight cohorts. Radiat Res *158*, 220-235.

Prowse, K.R., and Greider, C.W. (1995). Developmental and tissue-specific regulation of mouse telomerase and telomere length. Proc Natl Acad Sci U S A *92*, 4818-4822.

Rathmell, W.K., and Chu, G. (1994a). A DNA end-binding factor involved in double-strand break repair and V(D)J recombination. Mol Cell Biol *14*, 4741-4748.

Rathmell, W.K., and Chu, G. (1994b). Involvement of the Ku autoantigen in the cellular response to DNA double-strand breaks. Proc Natl Acad Sci U S A *91*, 7623-7627.

Richardson, D., Sugiyama, H., Nishi, N., Sakata, R., Shimizu, Y., Grant, E.J., Soda, M., Hsu, W.L., Suyama, A., Kodama, K., *et al.* (2009). Ionizing radiation and leukemia mortality among Japanese Atomic Bomb Survivors, 1950-2000. Radiat Res *172*, 368-382.

Rithidech, K., Gordon, C.R., and Cronkite, E.P. (2001). Telomerase activity in mouse myeloid leukemic cells and in cells from normal hematopoietic systems. Blood Cells Mol Dis *27*, 496-504.

Rithidech, K.N., Cronkite, E.P., and Bond, V.P. (1999). Advantages of the CBA mouse in leukemogenesis research. Blood Cells Mol Dis *25*, 38-45.

Roth, D.B., and Wilson, J.H. (1986). Nonhomologous recombination in mammalian cells: role for short sequence homologies in the joining reaction. Mol Cell Biol *6*, 4295-4304.

Rothkamm, K., Kruger, I., Thompson, L.H., and Lobrich, M. (2003). Pathways of DNA double-strand break repair during the mammalian cell cycle. Mol Cell Biol *23*, 5706-5715.

Rowley, J.D. (1973). Identificaton of a translocation with quinacrine fluorescence in a patient with acute leukemia. Ann Genet *16*, 109-112.

Rowley, J.D., Golomb, H.M., and Dougherty, C. (1977). 15/17 translocation, a consistent chromosomal change in acute promyelocytic leukaemia. Lancet *1*, 549-550.

Satyanarayana, A., and Rudolph, K.L. (2004). p16 and ARF: activation of teenage proteins in old age. J Clin Invest *114*, 1237-1240.

Schoeftner, S., and Blasco, M.A. (2008). Developmentally regulated transcription of mammalian telomeres by DNA-dependent RNA polymerase II. Nat Cell Biol *10*, 228-236.

Sfeir, A., Kosiyatrakul, S.T., Hockemeyer, D., MacRae, S.L., Karlseder, J., Schildkraut, C.L., and de Lange, T. (2009). Mammalian telomeres resemble fragile sites and require TRF1 for efficient replication. Cell *138*, 90-103.

Shen, J., Terry, M.B., Gurvich, I., Liao, Y., Senie, R.T., and Santella, R.M. (2007). Short telomere length and breast cancer risk: a study in sister sets. Cancer Res *67*, 5538-5544.

Shiloh, Y. (2001). ATM and ATR: networking cellular responses to DNA damage. Curr Opin Genet Dev *11*, 71-77.

Shivji, M.K., Mukund, S.R., Rajendra, E., Chen, S., Short, J.M., Savill, J., Klenerman, D., and Venkitaraman, A.R. (2009). The BRC repeats of human BRCA2 differentially regulate RAD51 binding on single- versus double-stranded DNA to stimulate strand exchange. Proc Natl Acad Sci U S A *106*, 13254-13259.

Silver, A., Moody, J., Dunford, R., Clark, D., Ganz, S., Bulman, R., Bouffler, S., Finnon, P., Meijne, E., Huiskamp, R., *et al.* (1999). Molecular mapping of chromosome 2 deletions in murine radiation-induced AML localizes a putative tumor suppressor gene to a 1.0 cM region homologous to human chromosome segment 11p11-12. Genes Chromosomes Cancer *24*, 95-104.

Smider, V., Rathmell, W.K., Lieber, M.R., and Chu, G. (1994). Restoration of X-ray resistance and V(D)J recombination in mutant cells by Ku cDNA. Science *266*, 288-291.

Stewart, S.A. (2005). Telomere maintenance and tumorigenesis: an "ALT"ernative road. Curr Mol Med *5*, 253-257.

Sung, P. (1994). Catalysis of ATP-dependent homologous DNA pairing and strand exchange by yeast RAD51 protein. Science *265*, 1241-1243.

Svenson, U., Nordfjall, K., Stegmayr, B., Manjer, J., Nilsson, P., Tavelin, B., Henriksson, R., Lenner, P., and Roos, G. (2008). Breast cancer survival is associated with telomere length in peripheral blood cells. Cancer Res *68*, 3618-3623.

Swiggers, S.J., Kuijpers, M.A., de Cort, M.J., Beverloo, H.B., and Zijlmans, J.M. (2006). Critically short telomeres in acute myeloid leukemia with loss or gain of parts of chromosomes. Genes Chromosomes Cancer *45*, 247-256.

Taccioli, G.E., Gottlieb, T.M., Blunt, T., Priestley, A., Demengeot, J., Mizuta, R., Lehmann, A.R., Alt, F.W., Jackson, S.P., and Jeggo, P.A. (1994). Ku80: product of the XRCC5 gene and its role in DNA repair and V(D)J recombination. Science *265*, 1442-1445.

Tahara, H., Tokutake, Y., Maeda, S., Kataoka, H., Watanabe, T., Satoh, M., Matsumoto, T., Sugawara, M., Ide, T., Goto, M., *et al.* (1997). Abnormal telomere dynamics of B-lymphoblastoid cell strains from Werner's syndrome patients transformed by Epstein-Barr virus. Oncogene *15*, 1911-1920.

Tauchi, H., Kobayashi, J., Morishima, K., van Gent, D.C., Shiraishi, T., Verkaik, N.S., vanHeems, D., Ito, E., Nakamura, A., Sonoda, E., *et al.* (2002). Nbs1 is essential for DNA repair by homologous recombination in higher vertebrate cells. Nature *420*, 93-98.

Ting, N.S., Pohorelic, B., Yu, Y., Lees-Miller, S.P., and Beattie, T.L. (2009). The human telomerase RNA component, hTR, activates the DNA-dependent protein kinase to phosphorylate heterogeneous nuclear ribonucleoprotein A1. Nucleic Acids Res *37*, 6105-6115.

Tokunaga, M., Land, C.E., Yamamoto, T., Asano, M., Tokuoka, S., Ezaki, H., and Nishimori, I. (1987). Incidence of female breast cancer among atomic bomb survivors, Hiroshima and Nagasaki, 1950-1980. Radiat Res *112*, 243-272.

Trujillo, K.M., Yuan, S.S., Lee, E.Y., and Sung, P. (1998). Nuclease activities in a complex of human recombination and DNA repair factors Rad50, Mre11, and p95. J Biol Chem *273*, 21447-21450.

Ullrich, R.L. (1983). Tumor induction in BALB/c female mice after fission neutron or gamma irradiation. Radiat Res *93*, 506-515.

UNSCEAR (2000). UNSCEAR 2000 Report: "Sources and effects of ionizing radiation", pp. 1-153.

Vardiman, J.W., Thiele, J., Arber, D.A., Brunning, R.D., Borowitz, M.J., Porwit, A., Harris, N.L., Le Beau, M.M., Hellstrom-Lindberg, E., Tefferi, A., *et al.* (2009). The 2008 revision of the World Health Organization (WHO) classification of myeloid neoplasms and acute leukemia: rationale and important changes. Blood *114*, 937-951.

Vaziri, H., Schachter, F., Uchida, I., Wei, L., Zhu, X., Effros, R., Cohen, D., and Harley, C.B. (1993). Loss of telomeric DNA during aging of normal and trisomy 21 human lymphocytes. Am J Hum Genet *52*, 661-667.

Vulliamy, T., Marrone, A., Goldman, F., Dearlove, A., Bessler, M., Mason, P.J., and Dokal, I. (2001a). The RNA component of telomerase is mutated in autosomal dominant dyskeratosis congenita. Nature *413*, 432-435.

Vulliamy, T.J., Knight, S.W., Mason, P.J., and Dokal, I. (2001b). Very short telomeres in the peripheral blood of patients with X-linked and autosomal dyskeratosis congenita. Blood Cells Mol Dis *27*, 353-357.

Walker, J.R., Corpina, R.A., and Goldberg, J. (2001). Structure of the Ku heterodimer bound to DNA and its implications for double-strand break repair. Nature *412*, 607-614.

Wang, J., Pluth, J.M., Cooper, P.K., Cowan, M.J., Chen, D.J., and Yannone, S.M. (2005). Artemis deficiency confers a DNA double-strand break repair defect and Artemis phosphorylation status is altered by DNA damage and cell cycle progression. DNA Repair (Amst) *4*, 556-570.

Watson, J.D. (1972). Origin of concatemeric T7 DNA. Nat New Biol *239*, 197-201.

Weil, M.M., Bedford, J.S., Bielefeldt-Ohmann, H., Ray, F.A., Genik, P.C., Ehrhart, E.J., Fallgren, C.M., Hailu, F., Battaglia, C.L., Charles, B., *et al.* (2009). Incidence of acute myeloid leukemia and hepatocellular carcinoma in mice irradiated with 1 GeV/nucleon (56)Fe ions. Radiat Res *172*, 213-219.

Williams, E.S., Klingler, R., Ponnaiya, B., Hardt, T., Schrock, E., Lees-Miller, S.P., Meek, K., Ullrich, R.L., and Bailey, S.M. (2009). Telomere dysfunction and DNA-PKcs deficiency: characterization and consequence. Cancer Res *69*, 2100-2107.

Wilson, J.W., Thibeault, S.A., Cucinotta, F.A., Shinn, J.L., Kim, M., Kiefer, R., and Badavi, F.F. (1995). Issues in protection from galactic cosmic rays. Radiat Environ Biophys *34*, 217-222.

Wong, A.K., Pero, R., Ormonde, P.A., Tavtigian, S.V., and Bartel, P.L. (1997). RAD51 interacts with the evolutionarily conserved BRC motifs in the human breast cancer susceptibility gene brca2. J Biol Chem *272*, 31941-31944.

Wright, W.E., Piatyszek, M.A., Rainey, W.E., Byrd, W., and Shay, J.W. (1996). Telomerase activity in human germline and embryonic tissues and cells. Dev Genet *18*, 173-179.

Wu, L., and Hickson, I.D. (2003). The Bloom's syndrome helicase suppresses crossing over during homologous recombination. Nature *426*, 870-874.

Xu, Y., Suzuki, Y., Ito, K., and Komiyama, M. (2010). Telomeric repeat-containing RNA structure in living cells. Proc Natl Acad Sci U S A *107*, 14579-14584.

Xu, Y., Suzuki, Y., Kaminaga, K., and Komiyama, M. (2009). Molecular basis of human telomere DNA/RNA structure and its potential application. Nucleic Acids Symp Ser (Oxf), 63-64.

Yaneva, M., Kowalewski, T., and Lieber, M.R. (1997). Interaction of DNA-dependent protein kinase with DNA and with Ku: biochemical and atomic-force microscopy studies. Embo J *16*, 5098-5112.

Yang, H., Li, Q., Fan, J., Holloman, W.K., and Pavletich, N.P. (2005). The BRCA2 homologue Brh2 nucleates RAD51 filament formation at a dsDNA-ssDNA junction. Nature *433*, 653-657.

Yu, Y., Okayasu, R., Weil, M.M., Silver, A., McCarthy, M., Zabriskie, R., Long, S., Cox, R., and Ullrich, R.L. (2001). Elevated breast cancer risk in irradiated BALB/c mice associates with unique functional polymorphism of the Prkdc (DNA-dependent protein kinase catalytic subunit) gene. Cancer Res *61*, 1820-1824.

Zhang, Q.S., Manche, L., Xu, R.M., and Krainer, A.R. (2006). hnRNP A1 associates with telomere ends and stimulates telomerase activity. Rna *12*, 1116-1128.

Zhang, S., Schlott, B., Gorlach, M., and Grosse, F. (2004). DNA-dependent protein kinase (DNA-PK) phosphorylates nuclear DNA helicase II/RNA helicase A and hnRNP proteins in an RNA-dependent manner. Nucleic Acids Res *32*, 1-10.

CHAPTER 2

CHROMOSOMAL INSTABILITY IN IONIZING RADIATION-INDUCED MURINE AML

Chromosomal instability in ionizing radiation-induced murine AML

Phuong N. Le, Yualin Peng, Jessica Goldstrohm, Joel S. Bedford, Michael M. Weil, Robert L. Ullrich, and Susan M. Bailey

Department of Environmental and Radiological Health Sciences, Colorado State University, Fort Collins, CO 80538, USA

Overview

Space exploration poses many hazards, including exposure to Galactic Space Radiation (GSR), which includes, among other species, high energy, high atomic mass, heavy ions (HZE) (Cucinotta and Durante, 2006; Wilson et al., 1995). The cancer risk associated with such densely ionizing exposures is largely unknown. To help better assess such risk, we examined chromosomal instability (CIN) in a murine model (CBA/Ca mice) of radiation-induced acute myeloid leukemia (AML) following HZE particle (1 GeV/n ^{56}Fe ions) or ^{137}Cs gamma (ɣ)-ray exposures. We found no significant difference in the frequencies of chromosome-type or telomere aberrations in the mice that developed AML after exposure as compared to their respective controls. However, an increased frequency of *chromatid*-type aberrations following both types of exposures was observed in leukemic cells from AML mice, providing supporting evidence of on-going instability, which was independent of age. Our results also did not support a direct link between *chromatid*-type aberrations and loss of *Pu.1* (*Sfpi1*), a transcription factor previously shown to be correlated with radiation-induced murine AML (Cook et al., 2004; Peng et al., 2009). Lastly, we examined two human AML cell lines and found elevated frequencies of both chromosome and chromatid-type aberrations. We also identified a clonal telomere aberration associated with a previously identified chromosome translocation. Taken together, our results support chromosomal and telomeric instability in both murine and human AML.

Introduction

Acute Myeloid Leukemia (AML) is characterized by the uncontrolled proliferation of immature myeloblasts in the bone marrow (National Cancer Institute, 2011). The accumulation of these aberrant cells displaces healthy blood cells, resulting in infections and/or anemia. AML is often associated with certain chromosomal aberrations, including t(8;21) (Rowley, 1973), del (16) (Arthur and Bloomfield, 1983), inv(16) or t(16;16) (Hogge et al., 1984; Le Beau et al., 1983) and t(15;17) (Rowley et al., 1977). Chromosome aberrations associated with therapy related AML (t-AML) differ somewhat, in that deletions involving chromosome 5 and 7 are most often observed (Liang et al., 1998; Nagarajan, 1995; Smith et al., 2003). Although, AML is relatively rare, occurring in 3.5 per 100,000 people, it is a devastating disease and its cure rate remains low, 22.6% (National Cancer Institute, www.cancer.gov.statfacts).

Development of some AMLs has been linked to exposure to ionizing radiation (IR). For example, AML has been shown to be the most common and earliest arising type of cancer in the atomic (A-) bomb survivors (Preston et al., 1994; Richardson et al., 2009). This unique cohort of individuals experienced an acute, high dose rate exposure, and so, may not represent the true induction of AML following other less instantaneous, chronic radiation exposures. While, the dose-response relationships have been extensively examined in the A-bomb survivors, these studies also do not aid in the understanding of cancer risk following exposures to different radiation qualities, including highly ionizing, high energy particles (HZE).

HZE radiation exposures to astronauts during space travel represent an unknown cancer risk. A mission to Mars, for example, is estimated to take approximately three years, with astronauts experiencing a possible radiation exposure of 1 Sievert (Wilson et

al., 1995). Although Galactic Space Radiation (GSR) primarily involves exposure to protons and low Linear Energy Transfer (LET) particles, high LET HZE are a primary concern (Cucinotta and Durante, 2006; Durante and Cucinotta, 2008). Because information on human exposure to HZE radiation is not available, animal studies and modeling are especially valuable.

PU.1 (Sfpi1) encodes a transcription factor involved in differentiation of progenitor cells during hematopoeisis, has been strongly correlated with murine AML (Cook et al., 2004). PU.1 regulates the differentiation of multipotent lymphoid and myeloid progenitor cells by interacting with other transcription factors, including AML-1 (Vangala et al., 2003), c-jun (Behre et al., 1999) and GATA-1 (Rekhtman et al., 1999; Zhang et al., 2000). The loss of PU.1 also leads to reduced responsiveness to cytokines responsible for the differentiation of progenitor cells into the myeloid lineage, including granulocyte-macrophage colony-stimulating factor (GM-CSF) and macrophage colony stimulating factor (M-CSF) (Dakic et al., 2005). Peng et al, assessed bone marrow cells for the loss of PU.1 located on chromosome 2 in the CBA/Ca mouse model following gamma (ɣ-), x- or 1 GeV/n ^{56}Fe irradiation (Peng et al., 2009). PU.1 loss was observed one day post irradiation following all three types of radiation, with HZE exposure being the most effective in inducing PU.1 loss. By 30 days, however, levels of PU.1 loss decreased in HZE samples but remained high in CBA/Ca mice exposed to x- or ɣ-irradiation. Interestingly, an increase in the loss of PU.1 reemerges one year post HZE-irradiation in exposed CBA/Ca mice. These studies propose that the assessment of PU.1 loss is a valuable biomarker for evaluating the leukemogenic effects of differing radiation qualities.

Genomic instability has previously been reported following radiation exposure (Kadhim et al., 1994; Watson et al., 2001) and in atomic bomb survivors with Myelodysplastic Syndrome (MDS) or AML (Nakanishi et al., 1999). Genomic instability may facilitate selection of chromosomal changes that allow the cell to bypass cell cycle regulation and/or death and thereby contribute to cellular transformation. Mammary epithelial cells isolated from the IR-induced breast cancer susceptible BALB/c mouse strain showed an increase in delayed cytogenetic instability versus the resistant C57/BL6 strain 16 population doublings post ɣ-irradiation (Ponnaiya et al., 1997b), supporting a link between instability and tumorigenesis. Similar results were observed following neutron irradiation in MCF 10a human mammary epithelial cells (Ponnaiya et al., 1997a).

One possible factor contributing to genomic instability is telomere dysfunction. Telomeres are repetitive features at the ends of chromosomes that protect them from loss of genomic sequence due to the end-replication problem (Olovnikov, 1973; Watson, 1972) and inappropriate chromosome fusion events. We have demonstrated loss of telomere end-capping function in cells deficient in DNA protein kinase catalytic subunit (DNA-PKcs), activity, which results in telomere fusion events (Bailey et al., 2001; Bailey et al., 1999). Although some chromosome aberrations (e.g. dicentrics) are lethal to the cell, others are less deleterious and so are transmissible; some can lead to breakage-fusion-bridge (BFB) cycles that propagate cytogenetic instability (Rudolph et al., 2001; Stewenius et al., 2005). Previous studies have shown that loss of telomere sequence or function also contributes to instability (Finnon et al., 2001; Hartmann et al., 2005; Swiggers et al., 2006).

Here, we demonstrate delayed genomic instability in splenocytes of CBA/Ca mice with AML following both ɣ- and HZE exposure. The CBA mouse provides an informative model system due to its low spontaneous rate of AML and high efficiency of AML induction following irradiation (Rithidech et al., 1999). Using the Colony Forming Unit-Spleen (CFU-S) assay 5 days post HZE exposure, we observed increased instability in some spleen colonies isolated from CBA/Ca mice as compared to those from C57BL/6 controls. Aberration frequencies decreased by 7.5 months, our latest time point. We did not observe significant telomere instability; however, the inherent differences between mouse and human telomere biology may have masked dysfunction. Therefore, we also assessed two human AML cell lines for chromosomal instability and found increased telomere-, chromatid- and chromosome-type aberrations, all indicative of inherent instability. Furthermore, we identified a clonal telomere fusion event involved in a translocation, suggesting that telomere dysfunction may contribute to overall instability observed in human AML.

Materials and methods

Cell culture

Two human AML cell lines, KG-1a and UoC-M1, were generous gifts from Dr. Michelle Le Beau at the University of Chicago. KG-1a cells were maintained in Iscove's Modified Dulbecco's Media (IMDM) supplemented with 10% FBS, 1 % 4-(2-hydroxyethyl)-1-piperazineethanesulfonic acid (HEPES), 1x Pennicilin/streptomycin, and 1x Glutamax. UoC-M1 cells were maintained in RPMI supplemented with 10% FBS, 1x

Pennicilin/streptomycin and 1% HEPES. Cells were passaged 1-2 times per week and media was changed every 3-4 days.

Mononuclear cell isolation

Normal human cord blood was obtained from the University of Colorado Cord Blood Bank in Aurora, CO. Mononuclear Cells (MNCs) were isolated using lymphocyte separation media (LSM, Mediatech), a density gradient media. In brief, cord blood was diluted with Magnetic Sorting Buffer (MACs; 1X PBS, Ca+ and Mg+ free with 0.5% BSA/2mM EDTA) and layered with LSM. Cells were centrifuged, the interphase layer was collected and washed with repeated centrifugations to isolate MNCs.

Radiation and AML induction

CBA/Ca mice were exposed at 8-12 weeks of age to 1.0, 2.0 or 3.0 Gy ɣ-rays (^{137}Cs source, a J.L. Shepherd Model 81-14, located at Colorado State University) or 0.1, 0.2, 0.4 or 1.0 Gy doses of 1 GeV/n ^{56}Fe (NASA Space Radiation Laboratory (NSRL) at the Brookhaven National Laboratory, New York). Mice were monitored for enlarged spleens, which were collected, dissociated and briefly cultured; AML was confirmed by histopathology on part of the collected spleen. Mice that remained in the mouse colony though out the study, which were age matched but not exposed to radiation served as controls.

A total of 14 CBA/Ca mice with AML following ɣ-irradiation were used for this study. Out of these 14 mice, one received 1 Gy, seven 2 Gy and six 3 Gy. Three CBA/Ca mice with AML following HZE (1 GeV/n ^{56}Fe) exposure were also examined, two of

which were exposed to 1 Gy and one to 0.4 Gy. The low number of HZE-induced AMLs reflects the low efficiency of 1 GeV/n Fe particles at inducing AML as compared to ɣ-irradiation (Weil et al., 2009). Irradiated mice that did not develop AML were also included in the study, including six exposed to ɣ-rays and 19 exposed to ^{56}Fe ions. Five control age-matched mice, sham irradiated, were included in the study and were subjected to the same histopathological analysis as irradiated mice. Four young, 8-12 weeks of age, CBA/Ca mice were also included in order to examine age effects on aberration frequencies. A total of 663 metaphases were scored in the ɣ-induced AML group, 84 in the HZE-induced AML group, 139 in the age-matched non-irradiated group and 103 in the young mice. Another 198 metaphases were assessed from mice that did not develop AML following ɣ-ray exposure and 490 metaphases following HZE exposure. A total of 1677 metaphases were scored in total.

Fluorescence In Situ Hybridization (FISH)

Slides for cytogenetic analysis of whole spleen and spleen colonies were prepared using adapted standard protocols (Becker et al., 1963; Henegariu et al., 2001). Spleens were minced and incubated with RPMI 1640 (Gibco) with 20% FBS and 1x Glutamax. Concanavalin A (Sigma) was added to the media at a concentration of 5µg/mL, and cells were incubated overnight at 37ºC with 5% CO_2. Colcemid was added at a final concentration of 0.1µg/mL, and cells were incubated for another 3-4 hours. Cells were collected, centrifuged and incubated in 0.75M KCl and fixed in 3:1 methanol and acetic acid. Cells were dropped directly onto clean, prepared slides. FISH was performed using a telomere specific G-rich peptide nucleic acid (PNA) telomere probe labeled with Cy-3

(DAKO). Following pre-treatment, slides were denatured in 70% formamide, 2XSSC at 75ºC. The probe was hybridized at 37ºC for 2 hours in the dark, and the slide was washed in 70% formamide, 2xSSC for 15-20 minutes at 32ºC in a shaking water bath. Slides were mounted with antifade and counterstained with Vectashield and 4'6-diamidino-2-phenylindole, dihydrochloride (DAPI; Vector Laboratories). Images were obtained using a Zeiss Fluorescence microscope (Axioplan 2ie MOT) and charge-coupled device (CCD) camera (model CV-m4^{+}CL, JAI PULNiX incorporated). ISIS FISH imaging systems software (Metasystems) was used for image capture and analysis.

Colony Forming Unit-Spleen (CFU-S)

The colony forming unit-spleen assay (CFU-S) has been previously described (McCulloch and Till, 1962; Till and Mc, 1961). Donor male CBA/Ca or C57BL/6 mice (8-12 weeks) were exposed to 1 Gy of 1 GeV/n ^{56}Fe ions, at the NSRL located at Brookhaven National Laboratory in New York. Following 5 days or 7.5 months, the mice were euthanized for bone marrow collection. Approximately 10^4 to 10^6 bone marrow cells were injected into lethally irradiated (8.2 – 9.0 Gy of ɣ-irradiation) recipient female CBA/Ca or C57BL/6 mice. Twelve days later, the recipient mice were humanely sacrificed and spleen colonies collected and processed for cytogenetic analysis. For spleen colonies aberration scoring, 11-31 metaphases were assessed per colony, with a mean of 17 and an average of 16.

Aberration scoring criteria

Only metaphases with a near diploid chromosome number (~40) were scored; aneuploidy was not observed in these samples. A chromatid gap was defined as a discontinuity in the DAPI stain that was less than the width of a single chromatid arm. Chromatid breaks were defined as discontinuities in the Dapi stain that were equal to or greater than the width of a chromatid arm. Differences in numbers were accounted for when perfoming statistical analyses. Statistical analysis was done using T-tests accounting for differences of proportions.

Results

Telomere Aberrations

In order to examine telomere function in radiation-induced murine AML, we evaluated telomere aberrations, including telomere associations, internal telomeric signals, telomere fusions and telomere duplication events. We found no significant increase in any individual category of telomere aberration in the AML samples. Telomere associations were observed at a higher frequency throughout all samples, but were not significant when compared between the AML groups and the controls (data not shown). Even when all telomere aberrations were grouped into one category, no significant increase in total telomere aberrations was observed when comparing AML samples and controls.

Chromatid-type aberrations

Chromosomal instability in radiation-induced AML was evaluated in leukemic cells harvested from CBA/Ca mice that developed AML, specifically chromatid and

chromosome-type aberrations. Chromatid-type aberrations included chromatid gaps and breaks, iso-deletions and chromatid type exchanges. A significant increase in chromatid-type aberrations was observed in AML samples induced by both ɣ- and HZE- irradiation (Figure 2.1), consisting primarily of chromatid gaps and breaks. Because chromatid-type aberrations arise in the cell-cycle of collection, they are indicative of on-going instability. This increase in chromatid-type aberration frequency was also significant when comparing leukemic cells from radiation-induced AML mice versus splenocytes from irradiated mice that did not develop AML (Figure 2.2). Controls were age-matched with the mice that developed AML; the control mice were aged due to the latency of AML development, which can be up to two years. Therefore we also examined aberration frequencies in young non-irradiated mice to confirm that the increased instability was not due to increased age (Figure 2.2). No increase in either telomeric or chromatid-type aberrations in the younger mice was observed, suggesting that age was not a contributing factor. A significant increase in chromosome aberrations was seen in the older age group when compared to the young age group, an expected result, as increased chromosome-type aberrations do occur with increased age (Tucker et al., 1999).

Chromosome-type Aberrations

We evaluated chromosome-type aberrations, including terminal deletions, dicentrics and robertsonian translocations. We saw no significant increase of chromosome aberrations in AML samples when compared to the controls (Figure 2.1). As with telomere-type and chromatid-type aberrations, we combined all chromosome aberration types into one category. We did not observe an increase in overall

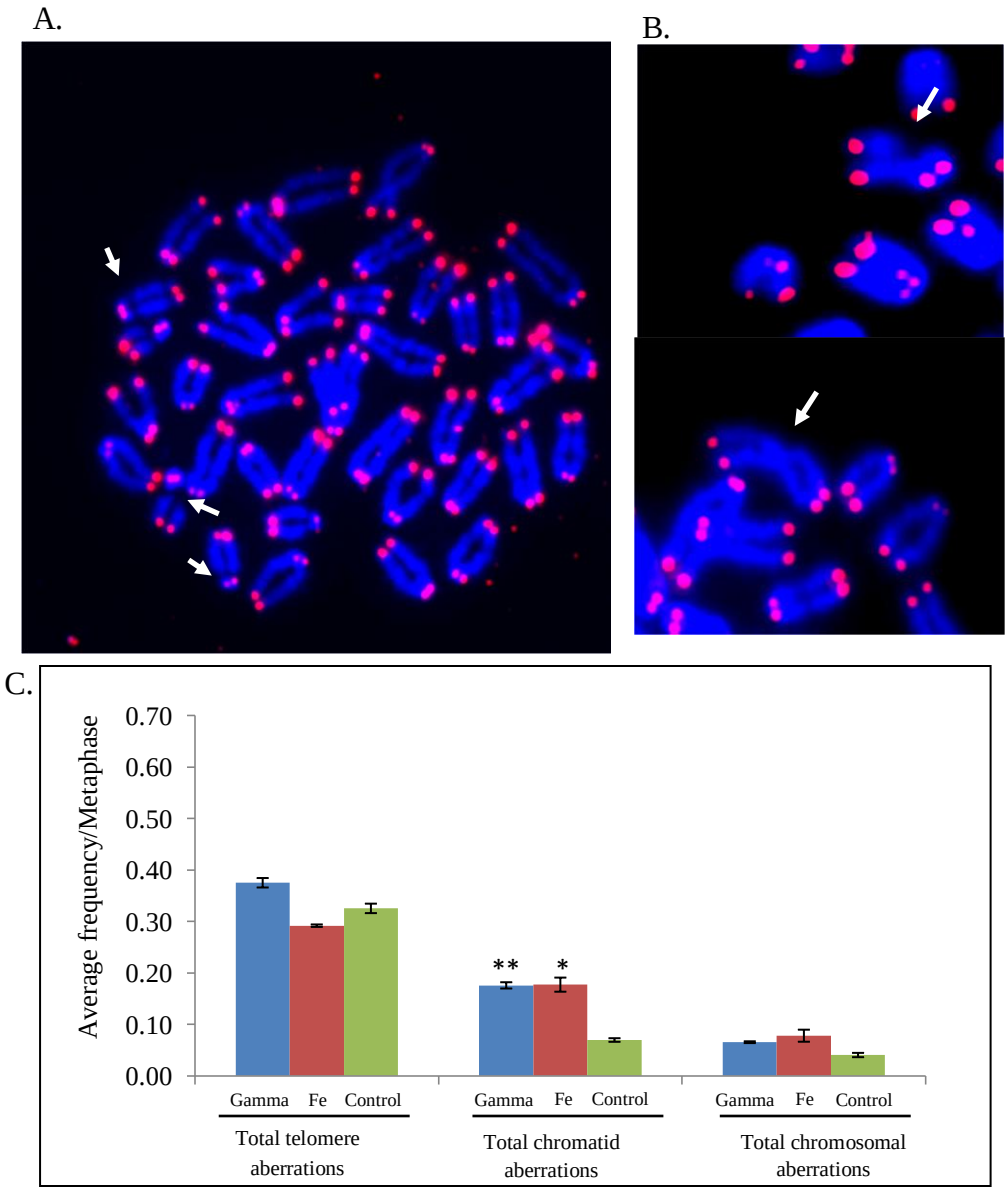

Figure 2.1. Increased chromatid-type aberration frequency in CBA/Ca mice with radiation-induced AML. A) Representative mouse metaphase spread hybridized with PNA G-rich telomere probe labeled with Cy-3. Arrows depict chromosome breaks. B) Arrows depict chromatid break and robertsonian translocation. C) All aberrations in each category were grouped together (e.g. total telomere aberrations). Average total telomere aberration frequencies per metaphase and average total chromosome aberrations were not significantly different between ɣ-induced AML (blue) and ^{56}Fe-induced AML (red) or non-irradiated, splenocytes harvested from age-matched control group (green). A significant increase in chromatid-type aberrations was seen when comparing ɣ-induced AML with non-irradiated controls (**, p=0.01) and when comparing ^{56}Fe-induced AML with controls (*, p=0.05).

chromosomal-type aberration frequency following either ɣ- or HZE exposure as when compared to control samples.

Compared to PU.1 loss

Radiation-induced AML in CBA mice has been correlated with PU.1 loss (Peng et al., 2009). We, therefore, compared aberration frequencies to PU.1 loss, hypothesizing that a high PU.1 loss might be associated with samples that exhibited a greater increase in chromosome aberration frequency. However, no correlation between aberration frequency and PU.1 loss was seen, suggesting the mechanism underlying PU.1 loss was independent of the increase in chromatid-type aberrations we observed (Figure 2.2).

Colony Forming Unit-Spleen (CFU-S)

In order to determine if instability occurs as an early event in leukemogenesis, we assessed chromosome aberrations in spleen colonies utilizing the CFU-S assay. We analyzed colonies at day 5 and 7.5 months post-irradiation using 1 Gy of 1 GeV/n ^{56}Fe. We observed instability at the 5 day time point, which was especially apparent when compared to spleen colonies examined in C57BL/6 mice (Figure 2.3). C57BL/6 mice have been shown to be resistant to radiation-induced AML (Darakhshan et al., 2006). Most metaphases possessing aberrations from C57BL/6 colonies exhibited only one chromatid aberration. An increased frequency of chromatid-type aberrations was observed in CBA/Ca spleen colonies, which decreased at the 7.5 month time point.

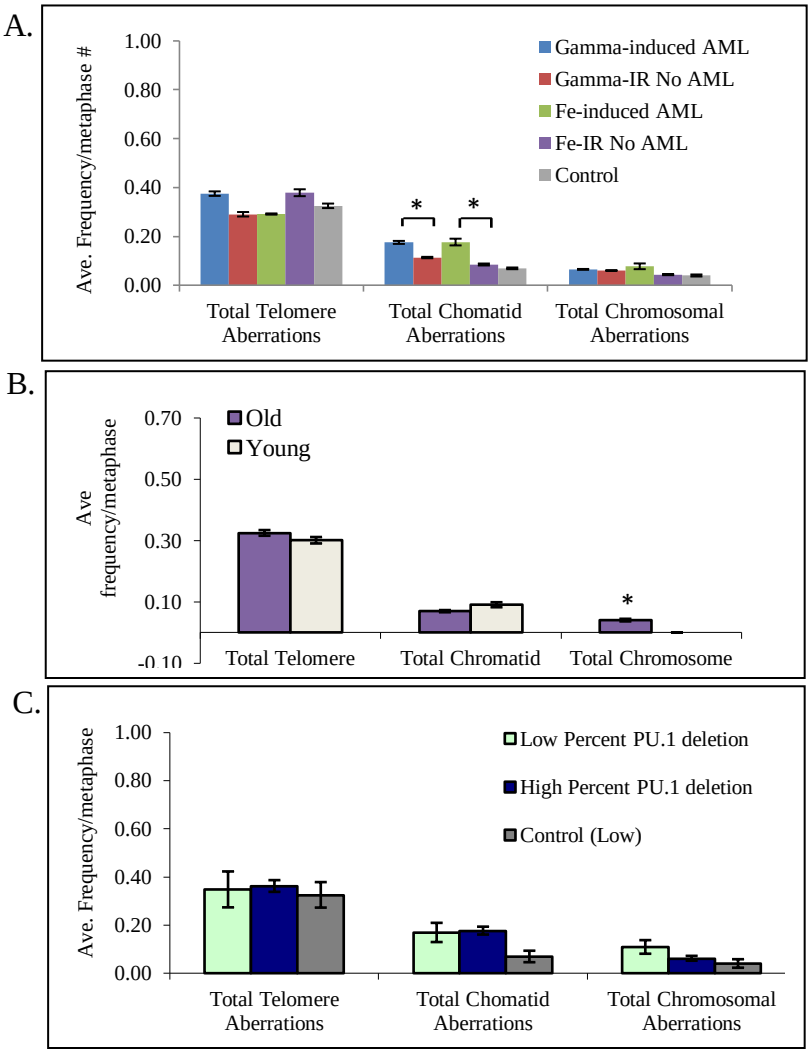

Figure 2.2. Increased chromatid aberration frequency following IR is specific to mice with radiation-induced AML. A) Aberration frequency per metaphase in ^{56}Fe-induced AML (green), ^{56}Fe-irradiated non-AML (purple), ɣ-induced AML (blue), ɣ-irradiated non-AML (red) and non-irradiated controls (gray) in CBA/Ca mice. A significant increase in chromatid-type aberrations was seen when comparing radiation-induced AML ($p=0.05$) versus samples that are irradiated and did not develop AML, as well as non-irradiated controls. B) The average frequency of aberrations per metaphase was examined in old (purple) versus young (light grey) mice. No increase in chromatid-type aberrations was observed, suggesting age is not a major contributing factor for the increase in chromatid-type aberrations seen in radiation-induced AML mice. The frequency of chromosomal-type aberrations was significantly increased when compared to young non-irradiated controls ($p=0.05$) C) Aberration frequency per metaphase was examined for an association with PU.1 loss. There was no significant difference between those AML samples that exhibited low PU.1 percent deletion ($\leq$7%, light blue) and high PU.1 percent deletion ($\geq$85%, dark blue). Grey bars are included here as the non-irradiated controls, chromatid-type aberrations are increased as previously seen.

Mouse Strain	Time Point	Colonies with ≥1 Chromatid Aberration	Metaphase Number with Chromatid Aberrations (%)	Chromatid Aberrations/Metaphase				Total Chromatid Aberrations	Number of chromosome aberrations (Robertsonians)
				1	2	3	>3		
CBA/Ca	5 day	8/17	19/304 (6.25)	15	3	1	0	24	10
	7.5 month	3/17	4/281 (1.4)	3	1	0	0	5	4
C57BL/6	5 day	4/17	5/321 (1.6)	5	0	0	0	5	3
	7.5 month	3/17	3/270 (1.1)	3	0	0	0	3	4

Figure 2.3. Increased chromatid-type aberrations using CFU-S assay suggests instability may be an early event in AML development. An increase in the number of colonies with 1 or more aberrations is seen at the 5 day time point in CBA/Ca mice as when compared to C57BL/6. However at the 7.5 months time point, the number of colonies with aberrations in CBA/Ca mice is similar to that seen in C57BL/6 mice. The complexity, as determined by the number of chromatid aberrations per metaphase, appears to also be slightly greater at the 5 day time point in the CBA/Ca mouse strain.

It would be of interest to examine the frequency of aberrations in spleen colonies post ɣ-irradiation. However, we were unable to evaluate this group, due to limits of mouse colony maintenance.

Instability in human AML cell lines

Due to the fact that mice express telomerase activity in all their tissues (Chadeneau et al., 1995; Prowse and Greider, 1995), aberrations arising from telomere length abnormalities associated with murine AML are confounded. We, therefore, assessed two human AML cell lines for telomere-, chromatid- and chromosome-type aberrations using FISH with a telomere specific G-rich PNA probe labeled with Cy-3. Increases in telomere-type, chromatid-type and chromosome-type aberrations were seen in both AML cell lines versus mononuclear cells (MNCs). Due to the low number of observed aberrations, statistical analysis was not appropriate. However, we did identify a clonal aberration (translocation) involving telomeres in the KG-1a AML cell line (Figure 2.4). This clonal event was not included in the analysis for total aberration frequencies. Because abundant telomere signal is evident at the point of fusion, this event is likely not due to critical telomere shortening. Rather, we conclude that this fusion event is indicative of telomere dysfunction resulting from loss of end-capping structure. This result suggests that DNA repair deficiency may underlie the observed loss of telomeric end-capping function observed in the AML cell line (Bailey et al., 2001; Bailey et al., 1999).

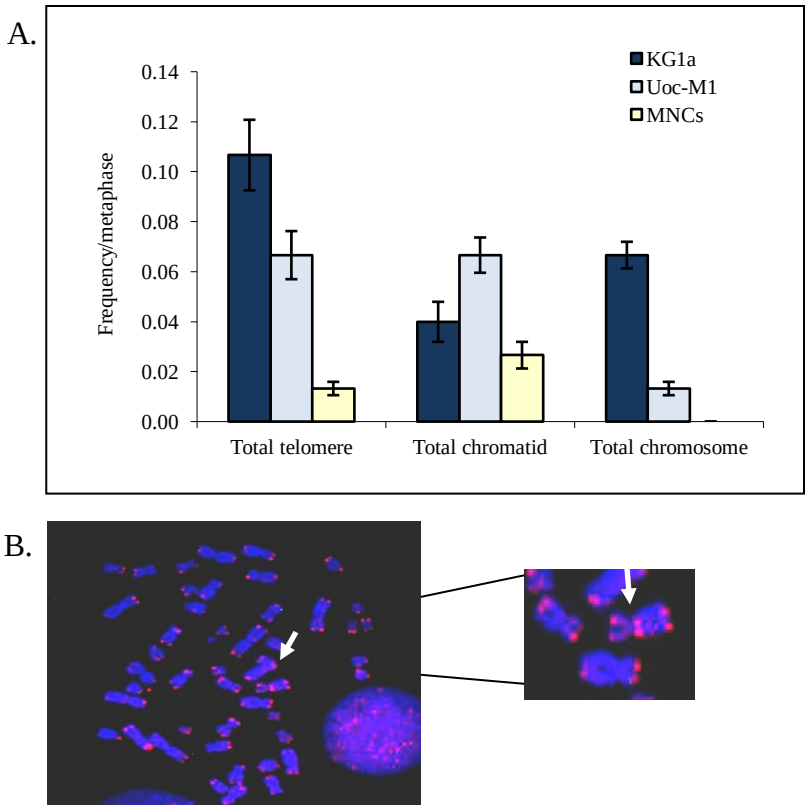

Figure 2.4. Evidence of instability in human AML cell lines. A) An increase in telomere-type, chromatid-type and chromosome-type aberrations in KG-1a cells (dark blue) and UoC-M1 cells (light) when compared to control MNCs (yellow). B) A clonal aberration involving telomere ends was observed in KG-1a cell line, indicative of telomere dysfunction.

Discussion

Chromatid-type aberrations are obliged to occur in the cell cycle in which they are collected, as after replication they present as chromosome-type aberrations. This informative end point is indicative of on-going, delayed instability. In contrast to the data we present here, an increased frequency of chromatid and chromosome-type aberrations has been previously reported in hematopoietic cells following low dose alpha (α)-particle exposure but not following X-ray exposure, suggesting that high LET radiation induces instability, while low LET does not (Kadhim et al., 1994; Kadhim et al., 1992). In this work, a relative biologic effectiveness (RBE) approached infinity when examining chromosomal aberrations as an endpoint. In the Kadhim et al. studies, hematopoietic cells from CBA/H were irradiated in vitro, plated and assayed using the colony-forming unit type A (CFU-A). In contrast to the Kadhim et al. studies, increased instability was observed in cells irradiated with low LET irradiation when examined *in vivo*, suggesting the lack of aberrations presented by Kadhim et al. may partly be due to in vitro artifacts (Watson et al., 2001). This study used the CFU-S assay with bone marrow of CBA/H mice following either α-particle or x-ray exposure to examine the delayed effects of radiation; similar to our studies, most aberrations were of the chromatid-type. Watson et al. also reported cells displaying chromosomal instability in approximately 3-6% of cells following either 3 Gy x-ray or 0.5 Gy of α-particle exposure using the CFU-S assay. In our studies, we observed approximately 1-6% of cells displaying chromatid aberrations, falling relatively close to the percentage Watson et al. reported. Differences may be accounted for when considering the different time points, doses, radiation qualities, as well as individual aberration scoring discrepancies. Temporal effects may also influence

the expression of aberrations and aberration type. Instability following low LET irradiation has been shown to require a greater delay in some cell types (Kadhim et al., 1998; Ponnaiya et al., 1997a). Lastly, Ullrich et al. and Tucker et al. provided further support for increased chromosomal instability following radiation exposure in their studies, where *in* vivo exposure to ^{137}Cs ɣ-irradiation led to increased instability as manifested by chromatid-type aberrations (Turker et al., 2004; Ullrich and Davis, 1999). Ullrich et al. also showed that an increase in chromatid-type aberrations was associated specifically with the BALB/c mouse strain, which has been shown to be susceptible to mammary carcinogenesis, again providing a vital link between instability and carcinogenesis (Ullrich and Davis, 1999).

To the best of our knowledge, this is the first report of chromatid aberrations, an indication of delayed genomic instability, associated with ^{56}Fe ion- and ɣ-induced AML. On-going instability is significantly increased in IR-induced AML samples versus irradiated non-AML samples, suggesting that the instability is specific to AML or cell type and not simply a consequence of radiation exposure. We also showed that the observed increase in chromatid-type aberrations is not due to an increase in age of the mice.

We did not observe a significant difference in aberration frequencies following ^{56}Fe versus ɣ-irradiation in the IR-induced AML samples. This result was unexpected because ^{56}Fe ions have a greater linear energy transfer (LET) than that of ɣ-irradiation from ^{137}Cs. AML induction was not increased in CBA/Ca mice following ^{56}Fe ion radiation exposure; an RBE of approximately one was observed (Weil et al., 2009). However, Weil et al. observed an RBE of 50 when examining hepatocellular carcinoma

as an endpoint (Weil et al., 2009), suggesting that the endpoint may greatly confound the estimated RBE.

Spleen colonies were evaluated for instability at two time points. The CFU-S assay relies on short-term repopulating cells in forming these clonal spleen colonies. The presence of colonies containing aberrations at these time points suggest that instability develops at early times during leukemogenesis. These results also suggest that some genetic changes may occur in these repopulating cells that facilitate propagation of instability in the cell progeny.

Critical telomere shortening, has been shown to be associated with cancer and AML (Finnon et al., 2001; Hartmann et al., 2005; Swiggers et al., 2006). We did not observe an increase in telomere-type aberrations in our AML mouse model. However, because mouse telomeres are maintained by active telomerase (Chadeneau et al., 1995; Prowse et al., 1993), and human telomeres are not, telomere length and function are quite different. To further investigate, we analyzed two human AML cell lines, and observed an increase in telomere-, chromatid- and chromosome-type aberrations. This overall increase in chromosomal instability is suggestive of on-going instability in human AML. Interestingly we identified a clonal aberration in the KG-1a AML cell line that involved telomeres, suggesting that telomere un-capping contributed to the overall ongoing-instability. This telomere fusion event was associated with a previously identified translocation between chromosomes 5 and 17, t(5;17) [(Mrozek et al., 2003) and personal correspondence, Dr. Michelle Le Beau]. Le Beau et al. identified this translocation event by performing FISH using a Bacterial Artificial Chromosome (BAC) clone and suspected

the involvement of the terminus of chromosome 17. Our results confirmed this suspicion and retention of the telomeric ends.

Together, our data provide new evidence that instability contributes to radiation-induced AML in the CBA mouse model following ^{56}Fe ion- and ɣ-irradiation and also in two human AML cell lines. Interestingly, telomere dysfunction may contribute to the instability observed in the KG-1a cell line, a human AML cell line.

The significance of genomic instability and cancer was first suggested by Nowell in 1976 (Nowell, 1976). Instability may manifest itself as sequence mutations, gene amplifications, or chromosomal changes, as we observed here in our studies (Lengauer et al., 1998). The underlying cause of instability has been linked to defective cell cycle checkpoints (Zhou et al., 1996), the mismatch repair (MMR) pathway (Ionov et al., 1993; Thibodeau et al., 1993) and replication fragile sites (Coquelle et al., 1997; Glover et al., 1998; Glover and Stein, 1987; Ozeri-Galai et al.). Delayed genomic instability, or instability observed many generations after irradiation, is more difficult to define. Both reactive oxygen species (ROS) (Limoli et al., 2003) and the inflammatory response (Lorimore et al., 2001) have been proposed as mechanisms to explain how damage is propagated many cell generations later. Although the mechanisms of instability are still largely being explored, the link between instability and tumor progression is undeniable (Lengauer et al., 1998).

Because we observed insignificant differences in the frequencies of instability following ^{56}Fe ion in comparison to ɣ-ray exposure, our results would predict a small if not negligible relative biological effectiveness (RBE) when examining chromosomal

instability as an endpoint. More studies are required in order to fully assess and predict cancer risk to astronauts in future space travel.

Acknowledgements

We would like to thank Dr. Edwin Goodwin for his statistical expertise. Special thanks to Dr. Michelle Le Beau for scientific correspondence and for the human AML cell lines used in this study. We also thank Dr. Paula Genik and Christine Falgren for their care of the mouse colony and mouse work. This work was supported through NASA grant # NAG9 1569, Radiation Leukemogeneis NSCOR.

References

Arthur, D.C., and Bloomfield, C.D. (1983). Partial deletion of the long arm of chromosome 16 and bone marrow eosinophilia in acute nonlymphocytic leukemia: a new association. Blood *61*, 994-998.

Bailey, S.M., Cornforth, M.N., Kurimasa, A., Chen, D.J., and Goodwin, E.H. (2001). Strand-specific postreplicative processing of mammalian telomeres. Science *293*, 2462-2465.

Bailey, S.M., Meyne, J., Chen, D.J., Kurimasa, A., Li, G.C., Lehnert, B.E., and Goodwin, E.H. (1999). DNA double-strand break repair proteins are required to cap the ends of mammalian chromosomes. Proc Natl Acad Sci U S A *96*, 14899-14904.

Becker, A.J., Mc, C.E., and Till, J.E. (1963). Cytological demonstration of the clonal nature of spleen colonies derived from transplanted mouse marrow cells. Nature *197*, 452-454.

Behre, G., Whitmarsh, A.J., Coghlan, M.P., Hoang, T., Carpenter, C.L., Zhang, D.E., Davis, R.J., and Tenen, D.G. (1999). c-Jun is a JNK-independent coactivator of the PU.1 transcription factor. J Biol Chem *274*, 4939-4946.

Chadeneau, C., Siegel, P., Harley, C.B., Muller, W.J., and Bacchetti, S. (1995). Telomerase activity in normal and malignant murine tissues. Oncogene *11*, 893-898.

Cook, W.D., McCaw, B.J., Herring, C., John, D.L., Foote, S.J., Nutt, S.L., and Adams, J.M. (2004). PU.1 is a suppressor of myeloid leukemia, inactivated in mice by gene deletion and mutation of its DNA binding domain. Blood *104*, 3437-3444.

Coquelle, A., Pipiras, E., Toledo, F., Buttin, G., and Debatisse, M. (1997). Expression of fragile sites triggers intrachromosomal mammalian gene amplification and sets boundaries to early amplicons. Cell *89*, 215-225.

Cucinotta, F.A., and Durante, M. (2006). Cancer risk from exposure to galactic cosmic rays: implications for space exploration by human beings. Lancet Oncol *7*, 431-435.

Dakic, A., Metcalf, D., Di Rago, L., Mifsud, S., Wu, L., and Nutt, S.L. (2005). PU.1 regulates the commitment of adult hematopoietic progenitors and restricts granulopoiesis. J Exp Med *201*, 1487-1502.

Darakhshan, F., Badie, C., Moody, J., Coster, M., Finnon, R., Finnon, P., Edwards, A.A., Szluinska, M., Skidmore, C.J., Yoshida, K., *et al.* (2006). Evidence for complex multigenic inheritance of radiation AML susceptibility in mice revealed using a surrogate phenotypic assay. Carcinogenesis *27*, 311-318.

Durante, M., and Cucinotta, F.A. (2008). Heavy ion carcinogenesis and human space exploration. Nat Rev Cancer *8*, 465-472.

Finnon, P., Wong, H.P., Silver, A.R., Slijepcevic, P., and Bouffler, S.D. (2001). Long but dysfunctional telomeres correlate with chromosomal radiosensitivity in a mouse AML cell line. Int J Radiat Biol *77*, 1151-1162.

Glover, T.W., Hoge, A.W., Miller, D.E., Ascara-Wilke, J.E., Adam, A.N., Dagenais, S.L., Wilke, C.M., Dierick, H.A., and Beer, D.G. (1998). The murine Fhit gene is highly similar to its human orthologue and maps to a common fragile site region. Cancer Res *58*, 3409-3414.

Glover, T.W., and Stein, C.K. (1987). Induction of sister chromatid exchanges at common fragile sites. Am J Hum Genet *41*, 882-890.

Hartmann, U., Brummendorf, T.H., Balabanov, S., Thiede, C., Illme, T., and Schaich, M. (2005). Telomere length and hTERT expression in patients with acute myeloid leukemia correlates with chromosomal abnormalities. Haematologica *90*, 307-316.

Henegariu, O., Heerema, N.A., Lowe Wright, L., Bray-Ward, P., Ward, D.C., and Vance, G.H. (2001). Improvements in cytogenetic slide preparation: controlled chromosome spreading, chemical aging and gradual denaturing. Cytometry *43*, 101-109.

Hogge, D.E., Misawa, S., Parsa, N.Z., Pollak, A., and Testa, J.R. (1984). Abnormalities of chromosome 16 in association with acute myelomonocytic leukemia and dysplastic bone marrow eosinophils. J Clin Oncol *2*, 550-557.

Ionov, Y., Peinado, M.A., Malkhosyan, S., Shibata, D., and Perucho, M. (1993). Ubiquitous somatic mutations in simple repeated sequences reveal a new mechanism for colonic carcinogenesis. Nature *363*, 558-561.

Kadhim, M.A., Lorimore, S.A., Hepburn, M.D., Goodhead, D.T., Buckle, V.J., and Wright, E.G. (1994). Alpha-particle-induced chromosomal instability in human bone marrow cells. Lancet *344*, 987-988.

Kadhim, M.A., Macdonald, D.A., Goodhead, D.T., Lorimore, S.A., Marsden, S.J., and Wright, E.G. (1992). Transmission of chromosomal instability after plutonium alpha-particle irradiation. Nature *355*, 738-740.

Kadhim, M.A., Marsden, S.J., and Wright, E.G. (1998). Radiation-induced chromosomal instability in human fibroblasts: temporal effects and the influence of radiation quality. Int J Radiat Biol *73*, 143-148.

Le Beau, M.M., Larson, R.A., Bitter, M.A., Vardiman, J.W., Golomb, H.M., and Rowley, J.D. (1983). Association of an inversion of chromosome 16 with abnormal

marrow eosinophils in acute myelomonocytic leukemia. A unique cytogenetic-clinicopathological association. N Engl J Med *309*, 630-636.

Lengauer, C., Kinzler, K.W., and Vogelstein, B. (1998). Genetic instabilities in human cancers. Nature *396*, 643-649.

Liang, H., Fairman, J., Claxton, D.F., Nowell, P.C., Green, E.D., and Nagarajan, L. (1998). Molecular anatomy of chromosome 7q deletions in myeloid neoplasms: evidence for multiple critical loci. Proc Natl Acad Sci U S A *95*, 3781-3785.

Limoli, C.L., Giedzinski, E., Morgan, W.F., Swarts, S.G., Jones, G.D., and Hyun, W. (2003). Persistent oxidative stress in chromosomally unstable cells. Cancer Res *63*, 3107-3111.

Lorimore, S.A., Coates, P.J., Scobie, G.E., Milne, G., and Wright, E.G. (2001). Inflammatory-type responses after exposure to ionizing radiation in vivo: a mechanism for radiation-induced bystander effects? Oncogene *20*, 7085-7095.

McCulloch, E.A., and Till, J.E. (1962). The sensitivity of cells from normal mouse bone marrow to gamma radiation in vitro and in vivo. Radiat Res *16*, 822-832.

Mrozek, K., Tanner, S.M., Heinonen, K., and Bloomfield, C.D. (2003). Molecular cytogenetic characterization of the KG-1 and KG-1a acute myeloid leukemia cell lines by use of spectral karyotyping and fluorescence in situ hybridization. Genes Chromosomes Cancer *38*, 249-252.

Nagarajan, L. (1995). Molecular analysis of the 5q- chromosome. Leuk Lymphoma *17*, 361-366.

Nakanishi, M., Tanaka, K., Shintani, T., Takahashi, T., and Kamada, N. (1999). Chromosomal instability in acute myelocytic leukemia and myelodysplastic syndrome patients among atomic bomb survivors. J Radiat Res (Tokyo) *40*, 159-167.

National Cancer Institute (2011). General Information about Adult Acute Myeloid Leukemia (National Cancer Institute).

Nowell, P.C. (1976). The clonal evolution of tumor cell populations. Science *194*, 23-28.

Olovnikov, A.M. (1973). A theory of marginotomy. The incomplete copying of template margin in enzymic synthesis of polynucleotides and biological significance of the phenomenon. J Theor Biol *41*, 181-190.

Ozeri-Galai, E., Lebofsky, R., Rahat, A., Bester, A.C., Bensimon, A., and Kerem, B. Failure of origin activation in response to fork stalling leads to chromosomal instability at fragile sites. Mol Cell *43*, 122-131.

Peng, Y., Brown, N., Finnon, R., Warner, C.L., Liu, X., Genik, P.C., Callan, M.A., Ray, F.A., Borak, T.B., Badie, C., *et al.* (2009). Radiation leukemogenesis in mice: loss of PU.1 on chromosome 2 in CBA and C57BL/6 mice after irradiation with 1 GeV/nucleon 56Fe ions, X rays or gamma rays. Part I. Experimental observations. Radiat Res *171*, 474-483.

Ponnaiya, B., Cornforth, M.N., and Ullrich, R.L. (1997a). Induction of chromosomal instability in human mammary cells by neutrons and gamma rays. Radiat Res *147*, 288-294.

Ponnaiya, B., Cornforth, M.N., and Ullrich, R.L. (1997b). Radiation-induced chromosomal instability in BALB/c and C57BL/6 mice: the difference is as clear as black and white. Radiat Res *147*, 121-125.

Preston, D.L., Kusumi, S., Tomonaga, M., Izumi, S., Ron, E., Kuramoto, A., Kamada, N., Dohy, H., Matsuo, T., Matsui, T., *et al.* (1994). Cancer incidence in atomic bomb survivors. Part III. Leukemia, lymphoma and multiple myeloma, 1950-1987. Radiat Res *137*, S68-97.

Prowse, K.R., Avilion, A.A., and Greider, C.W. (1993). Identification of a nonprocessive telomerase activity from mouse cells. Proc Natl Acad Sci U S A *90*, 1493-1497.

Prowse, K.R., and Greider, C.W. (1995). Developmental and tissue-specific regulation of mouse telomerase and telomere length. Proc Natl Acad Sci U S A *92*, 4818-4822.

Rekhtman, N., Radparvar, F., Evans, T., and Skoultchi, A.I. (1999). Direct interaction of hematopoietic transcription factors PU.1 and GATA-1: functional antagonism in erythroid cells. Genes Dev *13*, 1398-1411.

Richardson, D., Sugiyama, H., Nishi, N., Sakata, R., Shimizu, Y., Grant, E.J., Soda, M., Hsu, W.L., Suyama, A., Kodama, K., *et al.* (2009). Ionizing radiation and leukemia mortality among Japanese Atomic Bomb Survivors, 1950-2000. Radiat Res *172*, 368-382.

Rithidech, K.N., Cronkite, E.P., and Bond, V.P. (1999). Advantages of the CBA mouse in leukemogenesis research. Blood Cells Mol Dis *25*, 38-45.

Rowley, J.D. (1973). Identificaton of a translocation with quinacrine fluorescence in a patient with acute leukemia. Ann Genet *16*, 109-112.

Rowley, J.D., Golomb, H.M., and Dougherty, C. (1977). 15/17 translocation, a consistent chromosomal change in acute promyelocytic leukaemia. Lancet *1*, 549-550.

Rudolph, K.L., Millard, M., Bosenberg, M.W., and DePinho, R.A. (2001). Telomere dysfunction and evolution of intestinal carcinoma in mice and humans. Nat Genet *28*, 155-159.

Smith, S.M., Le Beau, M.M., Huo, D., Karrison, T., Sobecks, R.M., Anastasi, J., Vardiman, J.W., Rowley, J.D., and Larson, R.A. (2003). Clinical-cytogenetic associations in 306 patients with therapy-related myelodysplasia and myeloid leukemia: the University of Chicago series. Blood *102*, 43-52.

Stewenius, Y., Gorunova, L., Jonson, T., Larsson, N., Hoglund, M., Mandahl, N., Mertens, F., Mitelman, F., and Gisselsson, D. (2005). Structural and numerical chromosome changes in colon cancer develop through telomere-mediated anaphase bridges, not through mitotic multipolarity. Proc Natl Acad Sci U S A *102*, 5541-5546.

Swiggers, S.J., Kuijpers, M.A., de Cort, M.J., Beverloo, H.B., and Zijlmans, J.M. (2006). Critically short telomeres in acute myeloid leukemia with loss or gain of parts of chromosomes. Genes Chromosomes Cancer *45*, 247-256.

Thibodeau, S.N., Bren, G., and Schaid, D. (1993). Microsatellite instability in cancer of the proximal colon. Science *260*, 816-819.

Till, J.E., and Mc, C.E. (1961). A direct measurement of the radiation sensitivity of normal mouse bone marrow cells. Radiat Res *14*, 213-222.

Tucker, J.D., Spruill, M.D., Ramsey, M.J., Director, A.D., and Nath, J. (1999). Frequency of spontaneous chromosome aberrations in mice: effects of age. Mutat Res *425*, 135-141.

Turker, M.S., Schwartz, J.L., Jordan, R., Ponomareva, O.N., Connolly, L., Kasameyer, E., Lasarev, M., and Clepper, L. (2004). Persistence of chromatid aberrations in the cells of solid mouse tissues exposed to 137Cs gamma radiation. Radiat Res *162*, 357-364.

Ullrich, R.L., and Davis, C.M. (1999). Radiation-induced cytogenetic instability in vivo. Radiat Res *152*, 170-173.

Vangala, R.K., Heiss-Neumann, M.S., Rangatia, J.S., Singh, S.M., Schoch, C., Tenen, D.G., Hiddemann, W., and Behre, G. (2003). The myeloid master regulator transcription factor PU.1 is inactivated by AML1-ETO in t(8;21) myeloid leukemia. Blood *101*, 270-277.

Watson, G.E., Pocock, D.A., Papworth, D., Lorimore, S.A., and Wright, E.G. (2001). In vivo chromosomal instability and transmissible aberrations in the progeny of haemopoietic stem cells induced by high- and low-LET radiations. Int J Radiat Biol *77*, 409-417.

Watson, J.D. (1972). Origin of concatemeric T7 DNA. Nat New Biol *239*, 197-201.

Weil, M.M., Bedford, J.S., Bielefeldt-Ohmann, H., Ray, F.A., Genik, P.C., Ehrhart, E.J., Fallgren, C.M., Hailu, F., Battaglia, C.L., Charles, B., *et al.* (2009). Incidence of

acute myeloid leukemia and hepatocellular carcinoma in mice irradiated with 1 GeV/nucleon (56)Fe ions. Radiat Res *172*, 213-219.

Wilson, J.W., Thibeault, S.A., Cucinotta, F.A., Shinn, J.L., Kim, M., Kiefer, R., and Badavi, F.F. (1995). Issues in protection from galactic cosmic rays. Radiat Environ Biophys *34*, 217-222.

Zhang, P., Zhang, X., Iwama, A., Yu, C., Smith, K.A., Mueller, B.U., Narravula, S., Torbett, B.E., Orkin, S.H., and Tenen, D.G. (2000). PU.1 inhibits GATA-1 function and erythroid differentiation by blocking GATA-1 DNA binding. Blood *96*, 2641-2648.

Zhou, P., Jiang, W., Weghorst, C.M., and Weinstein, I.B. (1996). Overexpression of cyclin D1 enhances gene amplification. Cancer Res *56*, 36-39.

CHAPTER 3

DNA-PKcs AND TELOMERE REPEAT-CONTAINING RNA (TERRA) INTERACTIONS IN TELOMERE STRUCTURE AND FUNCTION

DNA-PKcs and telomere repeat-containing RNA (TERRA) interaction in telomere structure and function

Phuong N. Le, David G. Maranon, Noeila H. Altina and Susan M. Bailey

Department of Environmental and Radiological Health Sciences, Colorado State University, Fort Collins, CO 80538, USA

Overview

The DNA dependent Protein Kinase catalytic subunit (DNA-PKcs) has been shown to be essential for effective mammalian telomeric end-capping function, specifically of leading-strand telomeres (Bailey et al., 2001; Bailey et al., 1999). Interestingly, DNA-PKcs was recently shown to phosphorylate the heterogeneous nuclear ribonucleoprotein A1 (hnRNP A1) (Ting et al., 2009; Zhang et al., 2004), an RNA binding protein shown to play a role in telomere length and telomerase activity (Zhang et al., 2006). hnRNP A1 has also been shown to bind telomere repeat-containing RNA (TERRA) (de Silanes et al., 2010), and TERRA has been proposed to help maintain the heterochromatic state of telomeres (Deng et al., 2009). Taken together, we hypothesized that DNA-PKcs kinase activity mediated phosphorylation of hnRNP A1 contributes to localization of TERRA to telomeres, a sequence of events critical to maintenance of the heterochromatic "capped" state of telomeres. We confirmed that both siRNA depletion of DNA-PKcs protein levels and specific inhibition of DNA-PKcs kinase activity decreased phosphorylation of hnRNP A1. However, we did not see a decrease in TERRA localization at telomeres following inhibition of DNA-PKcs kinase activity, indicating that DNA-PKcs kinase activity is not necessary for maintaining TERRA at telomeres. We did observe a decrease in overall TERRA levels, suggesting an indirect role for DNA-PKcs and TERRA level regulation.

Introduction

Telomeres are protective features at the ends of chromosomes that in vertebrates are composed of tandem TTAGGG repeats (Blackburn, 1991; Moyzis et al., 1988). Telomeres also serve to "cap" the end of chromosomes, primarily through a complex of proteins, termed Shelterin (de Lange, 2005). With each round of replication, telomeres shorten due to the inherent failure of replication machinery to add sequences at the 5' end in lagging strand synthesis (Watson, 1972). Telomere length is maintained by telomerase, a specialized reverse transciptase, in germ line cells, stem cells and a large proportion of tumor cells and is important in bypassing cellular senescence (Chiu et al., 1996; Harley and Villeponteau, 1995; Hiyama et al., 1996; Kim et al., 1994; Mantell and Greider, 1994).

DNA protein kinase catalytic subunit (DNA-PKcs) together with the Ku70 and Ku80 heterodimer form the DNA-PK holoenzyme, an important player in the Non-Homologous End Joining (NHEJ) repair pathway (Gottlieb and Jackson, 1993). Loss or deficiency of DNA-PKcs results in inefficient repair following double strand break (DSB) induction (Okayasu et al., 1998; Okayasu et al., 2000). We have previously shown that DNA-PKcs kinase activity is also vital for maintaining telomere end-capping function and preventing end-to-end fusion events (Bailey et al., 2001; Bailey et al., 1999). We have also found that DNA-PKcs autophosphorylation, specifically at the Thr-2609 cluster, is important for its role in telomere function (Williams et al., 2009). However, the mechanism by which DNA-PKcs contributes to telomere end-capping function remains largely unexplored.

Due to the repetitive nature and heterochromatic structure of telomeres, they have long been regarded as transcriptionally silent. However, it has been demonstrated that

telomeres are in fact transcribed into telomere repeat-containing RNA or telomeric RNA (TERRA/TelRNA), and this sequence has been shown to be predominantly UUAGGG (Azzalin et al., 2007; Schoeftner and Blasco, 2008). TERRA has been proposed to inhibit telomerase activity (Schoeftner and Blasco, 2008), help maintain telomeric heterochromatin structure (Deng et al., 2009) and form G-quadruplex structures with telomeric DNA (Xu et al., 2010; Xu et al., 2009).

Interestingly, DNA-PKcs has been shown to phosphorylate the RNA binding protein, hnRNP A1, *in vitro* and *in vivo* (Ting et al., 2009; Zhang et al., 2004). Heterogenous nuclear ribonucleoprotein A1 (hnRNP A1) is an abundant RNA binding protein important in mRNA shuttling (He and Smith, 2009) and alternative splicing (Martinez-Contreras et al., 2007; Mayeda and Krainer, 1992). hnRNP A1 has also been shown to play a role in telomere biology; hnRNP A1 binds telomere sequences and increases telomerase activity (Zhang et al., 2006). Therefore, we explored the possible role of DNA-PKcs mediated phosphorylation of hnRNP A1 on TERRA localization to telomeres. We confirmed that siRNA knockdown of DNA-PKcs or kinase inhibition decreased phosphorylation of hnRNP A1 in MCF7 cells, a tumorigenic mammary epithelial cell line. Decreased phosphorylation was also observed in MCF 10a cells, a non-tumorigenic mammary epithelial cell line following siRNA treatment. Because hnRNP A1 preferentially binds to UAGGGA/U sequences (Burd and Dreyfuss, 1994; Hamilton et al., 1997), a sequence similar to TERRA, we hypothesized that hnRNP A1 plays a role in the localization of TERRA at telomeres. However, no change in localization of TERRA to telomeres was seen following DNA-PKcs kinase activity inhibition.

To monitor overall TERRA levels, we performed RNA dot blot experiments following DNA-PKcs kinase inhibition. We observed a significant decrease in TERRA levels following DNA-PKcs kinase inhibition in the MCF 7 cell line, suggesting DNA-PKcs kinase activity may have an indirect effect on TERRA levels.

Materials and methods

Cell culture

The MCF7 cell line, a gift from Laura Chubb at Colorado State University Veterinary Teaching Hospital, was originally derived from a metastatic mammary carcinoma and was grown in Minimum Essential Media/Earle's Balanced Salt Solution (MEM/EBSS; Hyclone) media supplemented with 10% fetal bovine serum (FBS; Sigma). The epithelial mammary non-tumorigenic cell line, MCF 10A, was purchased from ATCC and cultured in 1:1 Dulbecco's Modified Eagle's Medium (DMEM) / Ham's F12 growth media (Hyclone) supplemented with 5% FBS , 20ng/ml Epidermal Growth Factor (EGF; Sigma), 0.5ug/ml hydrocortisone (Sigma), 0.1ug/ml cholera toxin (Sigma), 10ug/ml insulin (Sigma), 1% Glutamax (Gibco) and 1% penicillin/streptomycin (Hyclone). Cell media was changed every 3-4 days, and cells were passaged 1-2 times per week.

RNA Fluorescence In Situ Hybridization (FISH) and Immunocytochemistry (ICC)

Cells were grown on chamber slides, washed at room temperature with cytoskeleton (CSK) buffer for 30 seconds, permeabilized with 0.5% Triton X-100 in CSK/vanadyl for 5 minutes and subsequently fixed in 3% paraformaldehyde for 10

minutes at room temperature. Following fixation, slides were blocked in 3% Bovine Serum Albumin (BSA) for 1 hour at room temperature. Slides were then incubated for 1 hour with mouse anti-Telomere Repeat Factor 2 (TRF2) primary antibody at room temperature followed by incubation with anti-mouse Alexa 594 secondary antibody for 45 minutes. Slides were washed once with 1X Phosphate Buffer Saline (PBS), incubated overnight with a FITC labeled Peptide Nucleic Acid (PNA) telomere probe $(CCCTAA)_7$ specific to TERRA and sequentially washed in 50% formamide/2X Saline Sodium Citrate (SSC), 2X SSC, 2X SSC/NP-40 for 2.3 min each at 39^0C. Lastly, the slides were mounted with ProLong Gold Antifade with 4',6-diamidino-2-phenylindole, dihydrochloride (DAPI) (Invitrogen).

Microscopy and imaging

Stacked images were acquired using a Nikon Eclipse E600 epifluorescent microscope, and Metamorph software was used for 3-D deconvolution and reconstruction. Colocalization of TERRA and TRF2 signals was established using different statistical parameters to measure 3-D images and generate the colocalization profile for each particular cell. Metamorph and Image J software were used to measure the colocalization signals from the acquired 3-D images in both channels, green (TERRA) and red (TRF2), using colocalization coefficients, including Pearson's Coefficient and Mander's Coefficient.

Small interfering (si) RNA of DNA-PKcs

The reverse transfection method was performed as recommended by the Lipofectamine RNAimax manufacter (Invitrogen). Cells were seeded at 50% confluency simultaneously treated with lipofectamine alone (mock) or with siRNA oligonucleotide and lipofectamine. An untreated control was included to assess effects from lipofectamine treatment. Cells were treated with siRNA sense sequence: GAUCGCACCUUACUCUGUUdTdT and antisense sequence: AACAGAGUAAGGUGCGAUCdTdT (Dharmacon), as previously described (Peng et al., 2002), at a final concentration of 25nM. Cells were collected at various time points following transfection, and knock down efficiency was evaluated by real-time Polymerase Chain Reaction (PCR) and immunoblot analysis. Optimal knockdown of DNA-PKcs was achieved at 72 hours, which was subsequently used for all experiments.

DNA-PKcs kinase activity inhibition (NU7026)

Cells were treated with the specific DNA-PKcs kinase activity inhibitor **2**-(Morpholin-4-yl)-benzo[h]chromen-4-one (NU7026; Sigma), resuspended in Dimethyl Sulfoxide **(**DMSO), at a final concentration of 10nM and incubated for 24 hours. Alternatively, cells were treated with an equal volume of DMSO as a control.

Phosphorus-32 (^{32}P) uptake assay for phosphorylation status

Cells were rinsed once and incubated with phosphate-free media Dulbecco's Minimum Essential Media (DMEM; Invitrogen) for 24 hours to deplete adenosine triphosphate (ATP) pools. 400µCi of ^{32}P [orthophosphate; Perkin Elmer] was added for

every 2 mL of media and incubated at 37ºC with 95% O_2 and 5% CO_2 for 4 hours to allow for labeling of ATP pools, as previously described (Ting et al., 2009). Cells were subsequently lysed, and total protein amount was quantified via Bradford assay. This was followed by immunoprecipitation of hnRNP A1 and Sodium Dodecyl Sulfate Solution Polyacrylamide Gel Electrophoresis (SDS-PAGE).

Cell lysis and protein quantification

Cells were harvested by trypsinization and pellets were washed with 1X PBS. Pellets were subsequently incubated in lysis buffer for 10 minutes over ice with periodic mixing. Lysis buffer includes 50mM Tris-HCL, 150mM NaCL, 2 mM Ethylenediaminetetraacetic Acid (EDTA), 2mM Ethylene Glycol Tetraacetic Acid (EGTA), 25mM NaF, 25mM β-glycerophosphate, 0.2% triton x-100, 0.3% NP-40, and 0.1mM sodium ortho-vanadate in water. Protease inhibitors were added directly before use, including 0.1mM Phenylmethylsulfonyl Fluoride (PMSF), 5μg/mL leupeptin and 5μg/mL aprotinin. For phosphorylation experiments, cells were rinsed and lysed in the tissue culture flask over ice for 10 minutes with lysis buffer and Halt Phosphatase inhibitors (Pierce). The Bradford Assay was used to quantify total protein amounts in whole cell lysates using Bradford Dye (Bio-Rad).

Immunoprecipitation of hnRNP A1 and SDS-PAGE

Immunoprecipitations were performed using the Direct IP kit (Pierce), as recommended by the manufacturer. Whole cell lysates were precleared by incubating with control resin for 30 minutes with rocking. Immunoprecipitation was performed by

first incubating antibody with resin on a column. Approximately, 1000µg of protein was incubated with 50µg of antibody against hnRNP A1 (Abcam ab5832 clone 9H10) or IgG control (R & D Systems MAB004) for 1 hour with rotation at room temperature. Samples were acetone precipitated, subsequently examined by SDS-PAGE and transferred to a Polyvinylidene Fluoride (PVDF) membrane using a semi-dry transfer method. Transfer was performed at 15V for 1 hour and 15 minutes. The membrane was marked with diluted ^{32}P and coomassie dye in order to orient the images and then exposed to a phosphor imaging screen (Kodak) for 48 hours. The screen was imaged on a Storm 860 (GE Healthcare) and quantified using Image Quant (GE Healthcare) software. The same membrane was rewetted and probed for total amounts of hnRNP A1 via immunoblotting.

Immunoblotting

Protein samples were separated via SDS-PAGE and transferred to a methanol activated polyvinylidene fluoride (PVDF) membrane. The membrane was blocked for 1 hour with 4% powdered milk in Tris-buffered saline with 0.1% Tween (TBST) at room temperature with shaking and rinsed once in TBST before incubating with primary antibody in 1% milk in TBST for 1 hour at room temperature or overnight at 4ºC with shaking. Primary antibody dilutions included hnRNP A1 (Abcam ab5832 clone 9H10) at a 1:1000 concentration, β-tubulin (Abcam ab6046) at a 1:1000 concentration, DNA-PKcs (NeoMarkers MS-423-P) at a 1:40 concentration and Actin (Abcam Ab3280) at 1:1000. The membrane was subsequently washed 4 times in 1X TBST for 5 minutes each at room temperature with shaking, incubated with secondary antibody in Licor Blocking Buffer (Odyssey) for 2 hours at room temperature with shaking and then washed in TBST

washes as above. Alexa Fluor 680 (Invitrogen A21058) and goat anti-rabbit IgG 800 (Thermo Scientific 35571) secondary antibodies were added at a 1:10,000 and 1:40,000 dilution respectively. Lastly, the membrane was imaged on the Odyssey Imaging System (Licor). Relative protein expression was measured as a ratio of the intensity of the bands using Odyssey imaging software, while accounting for background.

Real-time Polymerase Chain Reaction (PCR)

Total RNA was harvested from untreated, mock treated and siRNA treated samples using the Qiagen RNeasy kit (Qiagen). RNA was quantified using a Nanodrop Spectrophotometer and reverse transcribed using the Verso cDNA kit (Thermo Scientific). Real-time PCR was performed using SYBR green (Thermo Scientific) according to manufacter's protocol and performed using a Bio-Rad iCycler IQ. The real time cycle was as follows: Cycle 1 at 95ºC for 15 minutes, cycle 2 (40X) step 1 at 95ºC for 15 seconds, step 2 at 59ºC for 30 seconds and step 3 at 72ºC for 30 seconds. A melt curve was included to assess primer dimers and non-specific amplication as follows: cycle 3 at 95ºC for 30 seconds, cycle 4 at 55ºc for 30 seconds and cycle 5 (80X) at 55ºC for 10 seconds. Primer for amplification of human DNA-PKcs (Sigma) was added at a final concentration of 300nM including a forward sequence: AGCAATGCACCGTTGTGGT and reverse sequence: TCCTTCTTCAGGAGCTTCCA. Primers for amplification of transferrin receptor (TFRC) at a final concentration of 300nM were included as a housekeeping gene with the forward sequence: CGCTGGTCAGTTCGTGATTA and the reverse sequence:

GCATTCCCGAAATCTGTTGT. Relative DNA-PKcs mRNA expression was analyzed using the $2^{-\Delta\Delta CT}$ method.

RNA dot blot

RNA dot blots were performed as previously described with some modifications (Kafatos et al., 1979). Total RNA extraction was accomplished using a Qiagen RNeasy kit (Qiagen), and RNA quality was assessed by gel electrophoresis. Pre-wet GeneScreen Plus Nylon (Perkin Elmer) and Bio-Dot SF filter paper (Biorad) in 20X SSC was assembled into a Bio-rad biodot apparatus that could be attached to a vacuum source. The membrane was rinsed twice in 10X SSC. 7.5ug of RNA was diluted in ddH_20 with 30µL of RNA denaturing solution (66% formamide, 21% Formaldehyde [37%], 13% 10X MOPs pH 7). RNA was denatured for 5 minutes at 75ºC, and then an equal volume of 20X SSC was added. Samples were subsequently applied to the slots, drawn onto the membrane by vacuum and washed twice with 10X SSC. Vacuum was applied for 5 minutes to dry the membrane. The membrane was then removed and UV irradiated in the UV Stratalinker 2400 (Stratagene) for 25-50 seconds. The membrane was stained in 0.02% Methylene blue, 0.5M Sodium Acetate, pH 5.2 in order to visualize and mark RNA dots. Hybridization solution (2mM vanadyl, 50% formamide, 30% 20xSSC, 1% 50X Denhardt's solution, 0.25% SDS [20%], 0.1 % or 250ug/mL of salmon sperm DNA, brought up to volume with ddH_20) was incubated with the membrane for 2 hours at 42ºC. Fresh hybridization buffer was added containing denatured PNA FITC labeled TERRA probe $(CCCTAA)_7$ and denatured FITC labeled-GAPDH PNA probe (DAKO) and then incubated overnight at 42ºC. The membrane was washed with shaking: 1) 4 times in 2X

SSC at room temperature for 10 minutes each; 2) 2 times in 0.1X SSC 2, 0.1% SDS at 50ºC for 30 minutes each; and 3) 2 times in 0.1X SSC, 0.5% SDS at 68ºC for 30 minutes each. Imaging was performed on a Storm 860 (GE Healthcare) and image analysis was done using Image J (National Institute of Health; NIH).

Results

siRNA silencing of DNA-PKcs

In order to confirm DNA-PKcs dependent phosphorylation of hnRNP A1 in our cell lines, we used two approaches, siRNA DNA-PKcs protein depletion and kinase activity inhibition. For the first approach, we decreased DNA-PKcs protein expression by siRNA transfection, and then assessed efficiency of knockdown of both mRNA and protein via real-time PCR analysis and immunoblotting (Figure 3.1). DNA-PKcs mRNA expression was compared to the housekeeping gene, Transferrin Receptor (TFRC), and DNA-PKcs protein expression was compared to actin. Relative protein expression of DNA-PKcs was comparable between MCF 10a and MCF7 cells at 1.66 $\pm$ 0.66 and 2.20 $\pm$ 0.58 respectively, determined from four independent protein isolations and two immunoblots per isolation (data not shown). Decreased mRNA levels were seen as early as 24 hours after siRNA addition, and optimal protein knockdown was achieved at 72 hours (Figure 3.1 and Figure 3.2).

DNA-PKcs phosphorylation of hnRNP A1

DNA-PKcs dependent *in vivo* phosphorylation of hnRNP A1 has previously been demonstrated (Ting et al., 2009). In order to confirm hnRNP A1 phosphorylation by

A. DNA-PKcs relative mRNA expression in MCF 10a

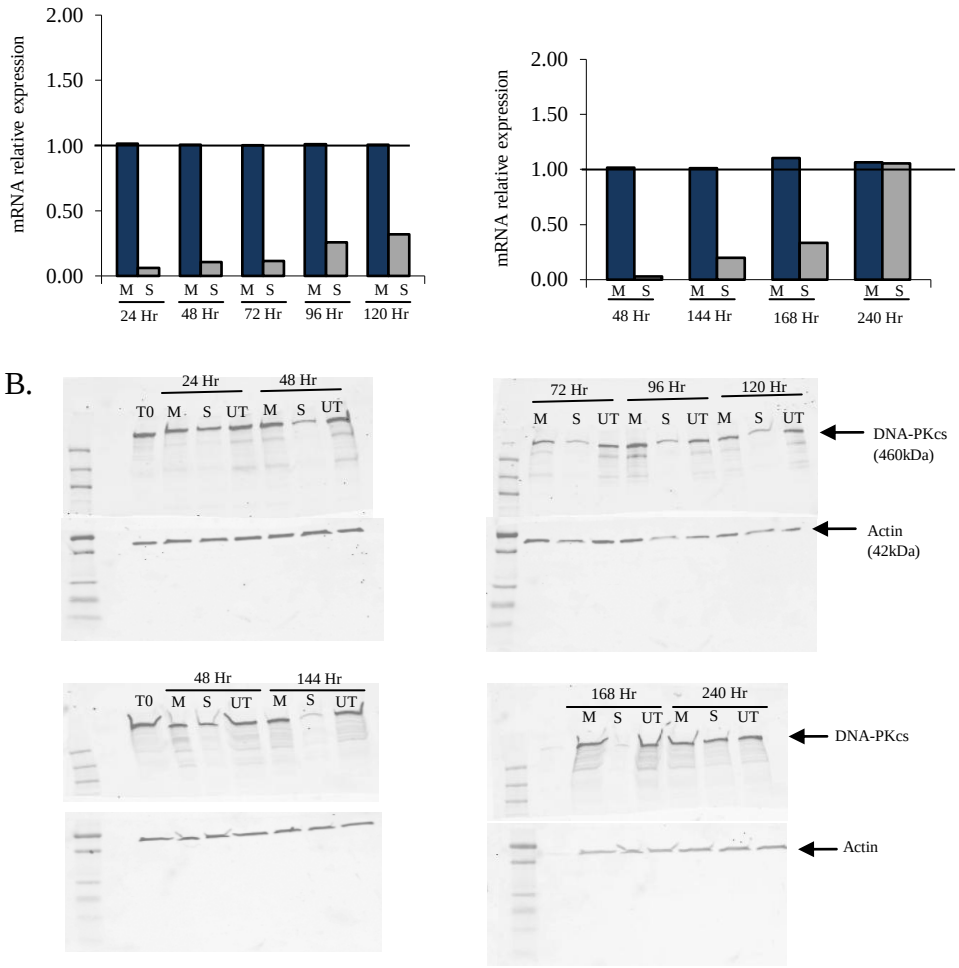

Figure 3.1. Time course and efficiency of siRNA depletion of DNA-PKcs in MCF 10a cell line. A) Relative mRNA expression of DNA-PKcs in mock (M) and siRNA treated (S) as compared to the housekeeping gene (TFRC) over time using real-time PCR analysis and the $2^{-\Delta\Delta CT}$ method. DNA-PKcs mRNA expression was decreased as early as 24 hours following siRNA treatment (gray) when compared to mock treated (blue). DNA-PKcs mRNA levels fully recovered by 240 hours post siRNA treatment. B) Immunoblot analysis shows decreased DNA-PKcs (460kDa) protein levels as early as 48 hours post siRNA treatment (S) when compared to mock (M) or untreated (U) samples. Actin (42kDa) was used as a loading control. Time zero (T0) was included in each immunoblot. Optimal protein knockdown was observed at 72 hours post transfection, and protein levels almost fully recovered by 240 hours.

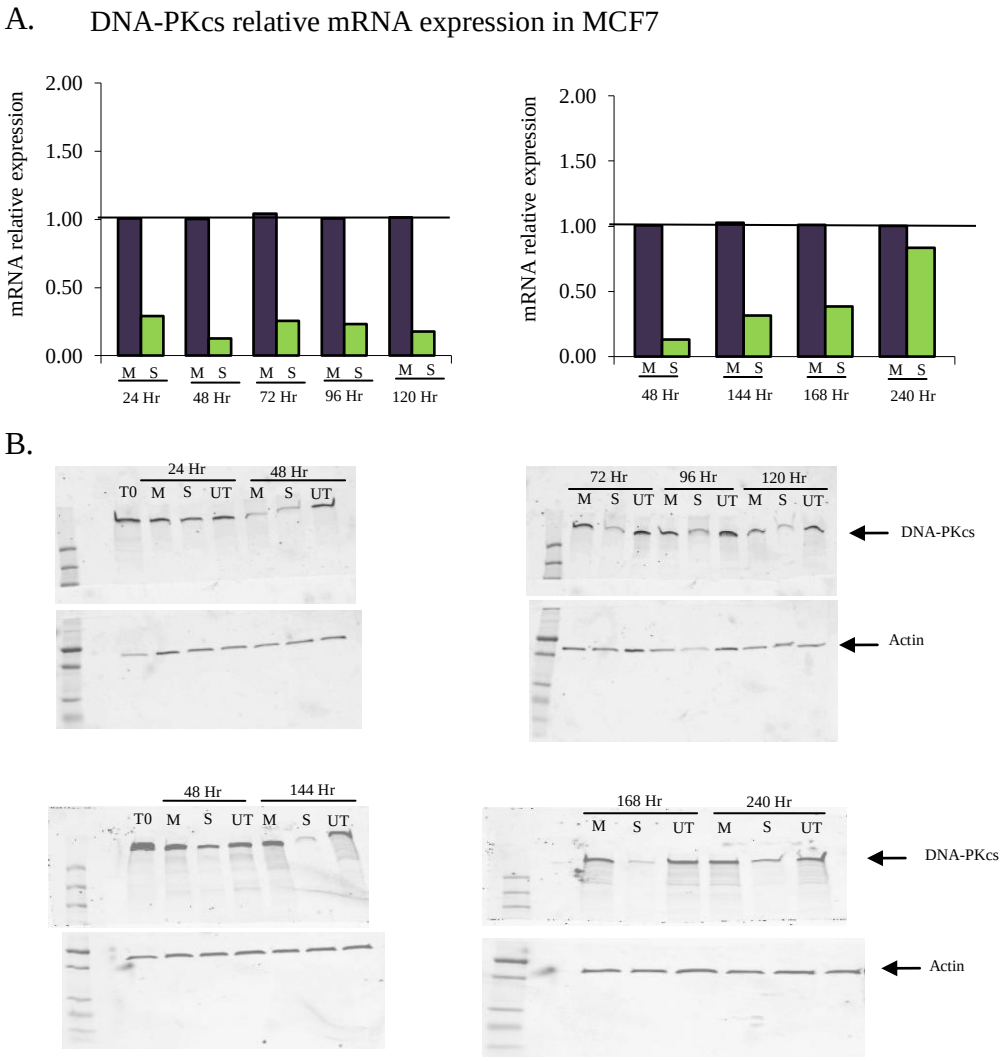

Figure 3.2. Time course and efficiency of silencing of DNA-PKcs in the MCF7 cell line. A) Relative mRNA expression of DNA-PKcs in mock (M) and siRNA treated (S) in comparison to the housekeeping gene (TFRC) using real-time PCR and the $2^{-\Delta\Delta CT}$ method. Decreased DNA-PKcs mRNA expression was seen as early as 24 hours post siRNA treatment (green) as compared to mock treatment (purple). DNA-PKcs mRNA levels were almost fully recovered by 240 hours post siRNA transfection. B) DNA-PKcs (460kDa) protein levels were monitored via immunoblotting, protein was decreased by 48 hours and optimally decreased by 72 hours post siRNA treatment. Time zero (T0) was included, and actin (42kDa) was used as a loading control.

DNA- PKcs in our human mammary epithelial cells, we assessed ^{32}P uptake following either siRNA silencing of DNA-PKcs protein or the specific inhibition of DNA-PKcs kinase activity with NU7026 (Hollick et al., 2003). Protein was harvested at 72 hours post siRNA transfection or 24 hours post kinase activity inhibition (NU7026), and hnRNP A1 was immunoprecipitated (IP). Following IP, SDS-PAGE was performed, protein was transferred to a PVDF membrane, which was then exposed to a phosphor screen for 48 hours before scanning on a Storm imager. Decreased ^{32}P uptake following siRNA depletion of DNA-PKcs was observed in both MCF 10a and MCF7 cell lines (Figure 3.3). A decrease in ^{32}P uptake was also seen following DNA-PKcs kinase inhibition in MCF7 cells. However, a decrease in ^{32}P uptake following inhibitor treatment in MCF 10a cells was not seen. These results may be partly explained by the different levels of human telomerase RNA component (hTR) in the two cell lines, as hTR influences the specific phosphorylation of hnRNP A1 by DNA-PKcs (Ting et al., 2009). hTR levels, as well as telomerase activity, have been shown to be decreased in MCF 10a in comparison to MCF7 (Ramachandran et al., 2002). Furthermore, decreased ^{32}P uptake following siRNA knockdown of DNA-PKcs may be due to indirect effects on other kinases, as the depletion or defiency in DNA-PKcs has been shown to also affect the levels of ATM (Peng et al., 2005). ATM and DNA-PKcs have been shown to share many phosphorylation targets, including ɣH2AX (Wang et al., 2005) and Replication Protein A (RPA) (Boubnov and Weaver, 1995; Brush et al., 1994; Brush et al., 1996; Gately et al., 1998).

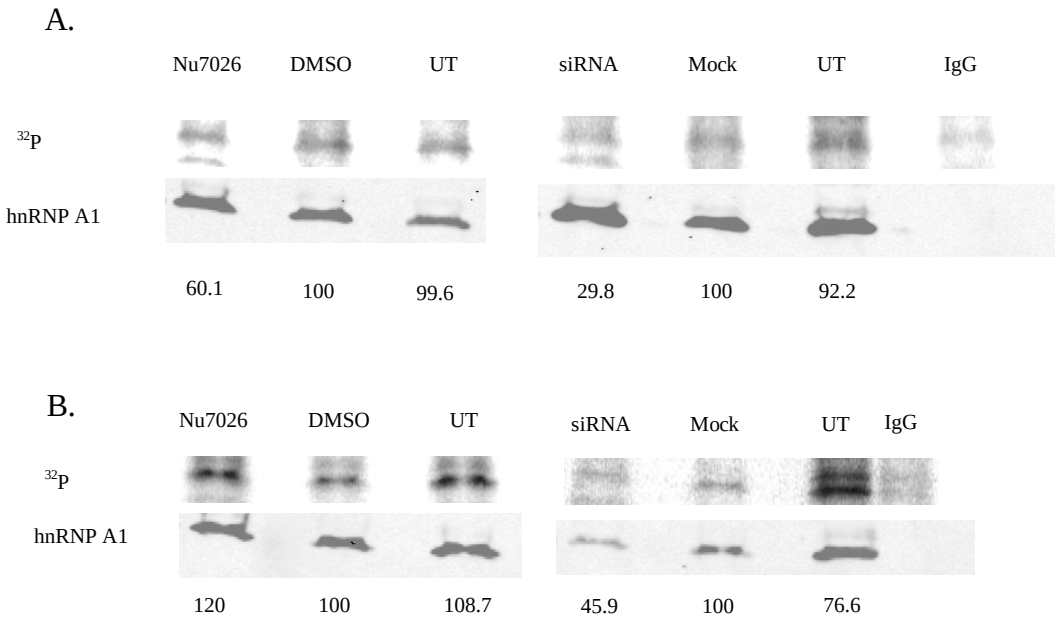

Figure 3.3. DNA-PKcs dependent phosphorylation of hnRNP A1. A) ^{32}P uptake in MCF7 cell line, relative to total intensity of protein by immunoblotting and Odyssey imaging. Decreased uptake was seen following both siRNA silencing of DNA-PKcs (~40%) and kinase activity inhibition (~70%). Untreated samples were comparable to that of mock and DMSO treated cells. B) ^{32}P uptake in MCF 10a cell lines. A decrease was observed following siRNA. We observed a difference between untreated and mock sample versus previous runs, suggesting slightly more variation in this sample. No decrease in hnRNP A1 phosphorylation was observed following DNA-PKcs kinase activity inhibition, suggesting that DNA-PKcs does not play a large role in phosphorylating hnRNP A1 in the MCF 10a cell line.

TERRA localization at telomeres following inhibition of DNA-PKcs kinase activity

Because deficient levels of DNA-PKcs, as well as siRNA knockdown of DNA-PKcs, has been shown to also reduce the levels of ATM (Peng et al., 2005), we treated cells with a specific DNA-PKcs kinase activity inhibitor (NU7026) to evaluate TERRA localization at telomeres. Having confirmed that NU7026 treatment decreased phosphorylation of hnRNP A1 in the MCF7 cell line, we repeated the treatment and analyzed the effects of DNA-PKcs kinase activity inhibition on TERRA localization at telomeres. We performed RNA FISH using a probe specific to TERRA in conjunction with immunocytochemistry using an antibody against TRF2, a telomere specific protein. We analyzed 38 cells per treatment type. Using a novel 3-D imaging and reconstruction technique, significant changes in TERRA colocalization with TRF2 following NU7026 treatment in MCF7 cells were not observed, suggesting that loss of DNA-PKcs kinase activity does not affect TERRA localization at telomeres (Figure 3.4 and Figure 3.5). This was seen both visually when examining the images and also analyzed by applying statistical methods. Here, Pearson's Correlation Coefficient was used to assess the correlation of the two molecules, where a coefficient of 0.69 represents the colocalization of the two molecules (Bolte and Cordelieres, 2006). Similar to previous studies, we observed that not all cells expressed TERRA (Azzalin et al., 2007; Schoeftner and Blasco, 2008). Furthermore, not all telomere ends had TERRA; i.e., red (TRF2) foci were often seen alone, while all green (TERRA) foci were seen colocalized with red. In essence, all TERRA molecules were observed to be at telomere ends. Interestingly, we noted a small percent of colocalized foci where TERRA and TRF2

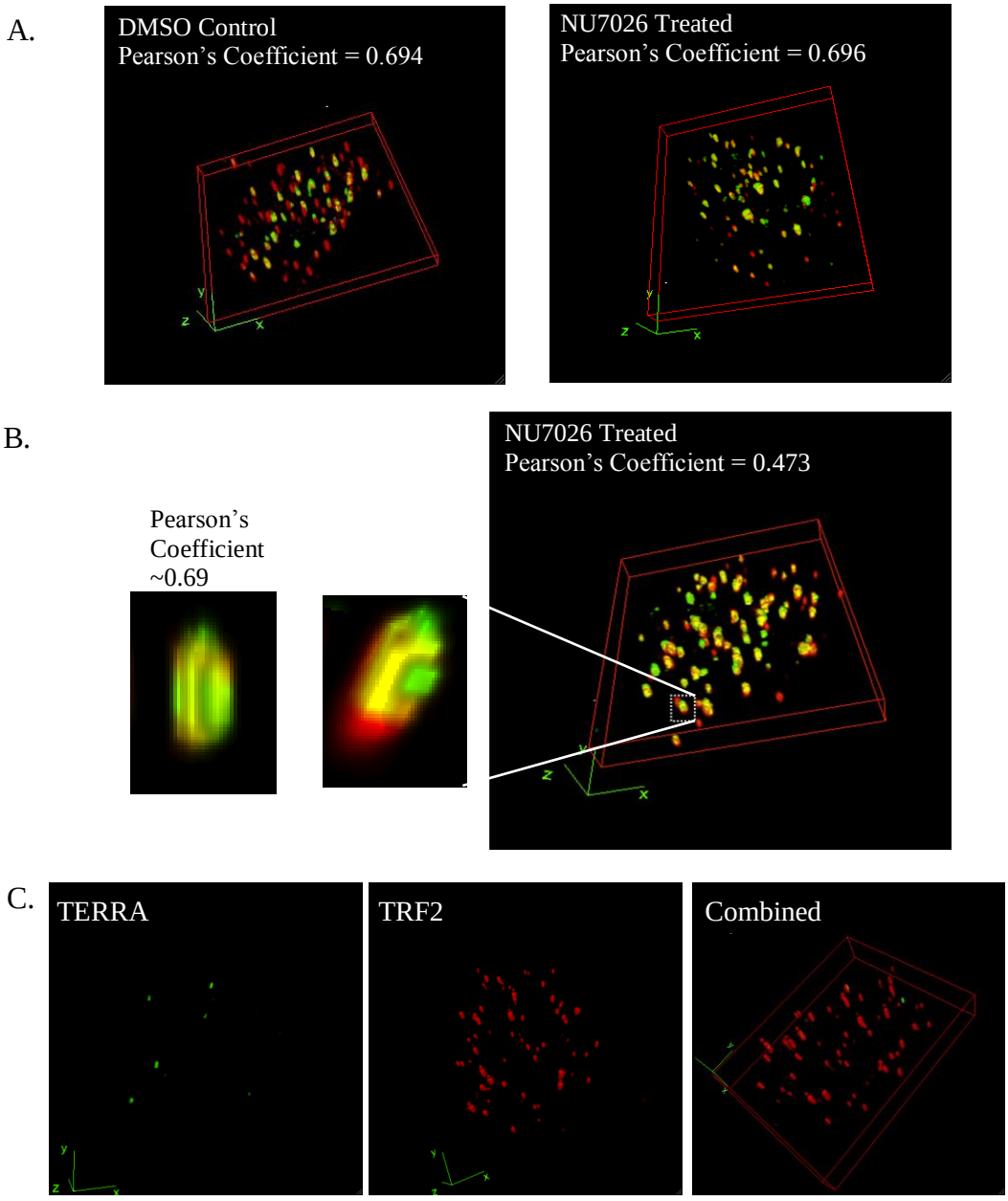

Figure 3.4. TERRA localization following DNA-PKcs kinase inhibition in MCF7. A) 3-D images of TERRA (green) and TRF2 (red) colocalization. Every TERRA molecule colocalized (yellow) with a TRF2 molecule. No significant decrease in TERRA colocalization with TRF2 was observed following NU7026 treatment. B) A shift in colocalization of TRF2 and TERRA was seen in a small subset of cells treated with NU7026 resulting in decreased overlap of the two molecules. The image on the left depicts what is generally seen with a Pearson's Coefficient of ~0.69. C) RNase treatment was done as a control to confirm that the probe was specific to TERRA.

A.

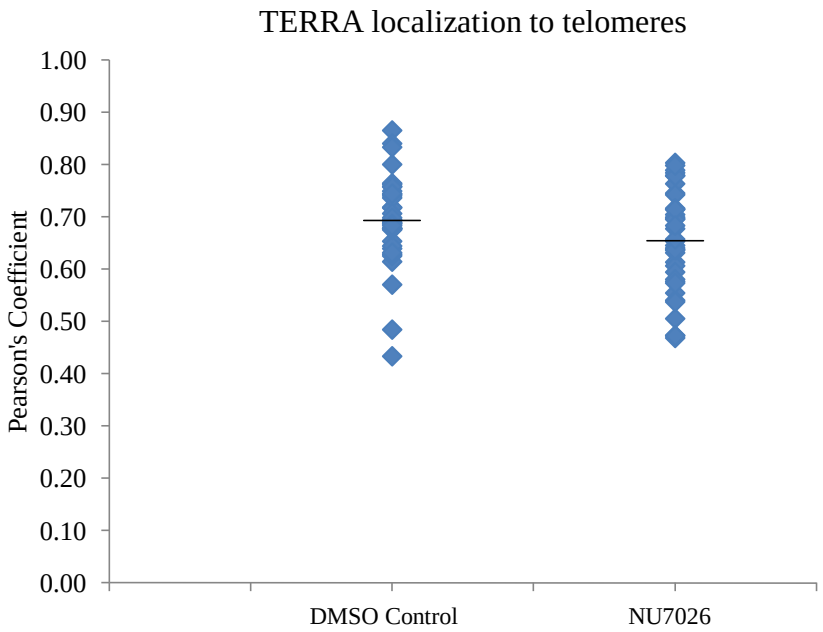

Figure 3.5. A) Scatter plot depicting average Pearson's Correlation Coefficient per cell in DMSO control in comparison to NU7026 treated. The bars depict the mean value of total data, where the mean is slightly decreased in NU7026 treated samples (DMSO=0.694, NU7026=0.654), and this correlates with a decrease in TERRA and TRF2 foci overlap in a small subset of the colocalized foci.

appeared differentially spaced, and this was slightly increased following DNA-PKcs kinase inhibition. Specifically, TERRA and TRF2 were colocalized but appeared to overlap to a lesser degree following NU7026 treatment, suggesting a shift in their interaction following DNA-PKcs kinase inhibition (Figure 3.4). This was visually observed when Pearson's Correlation Coefficient was ~0.4. We, therefore, grouped the data into two categories, with one including Pearson's Correlation Coefficient that fell at or above 0.5 and the other with those that fell below. For DMSO control, 5.3 % of cells scored had an average Pearson's Correlation Coefficient that fell below 0.5, while 7.9 % or NU7026 treated cells had an average Pearson's Correlation Coefficient that fell below this number. Furthermore, this shift is also reflected by a lower overall mean for Pearson's Coefficient when all data was combined (Figure 3.4 and Figure 3.5).

DNA-PKcs influences TERRA levels

In order to assess the contribution of DNA-PKcs kinase activity on TERRA levels, we performed RNA dot blots on total RNA following 24 hour NU7026 inhibitor treatment in both MCF7 and MCF 10a cells. Three independent experiments were performed. TERRA levels in the MCF 10a cell line were sensitive to Dimethyl Sulfoxide (DMSO) treatment, as a decrease in TERRA was observed with both DMSO alone or with NU7026, resuspended in DMSO (Figure 3.6). This result could be due to changes in cell growth or cell cycle, as TERRA levels have been shown to vary with cell cycle phases (Flynn et al., 2011; Porro et al.). However, no significant change in TERRA level was observed between the DMSO control and NU7026 treated samples, suggesting DNA-PKcs kinase activity did not affect TERRA levels in the MCF

A.

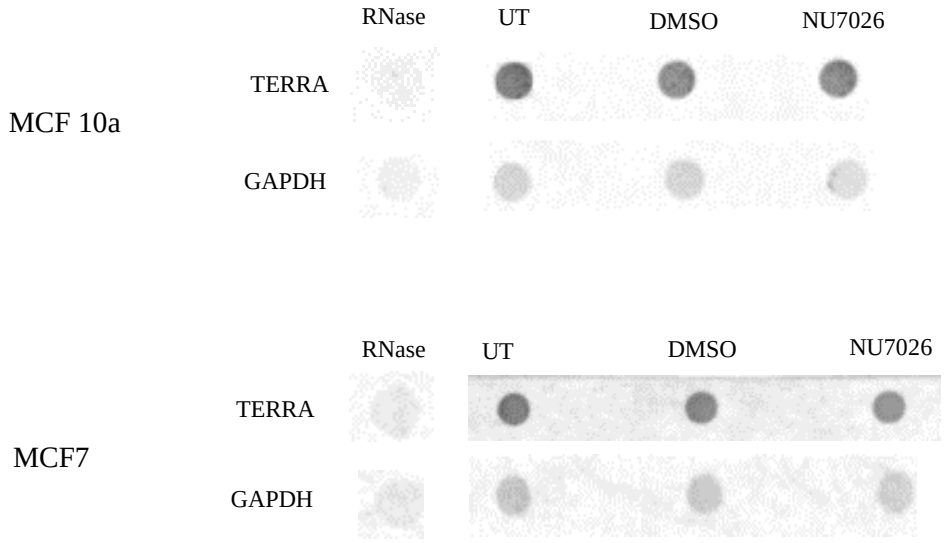

B.

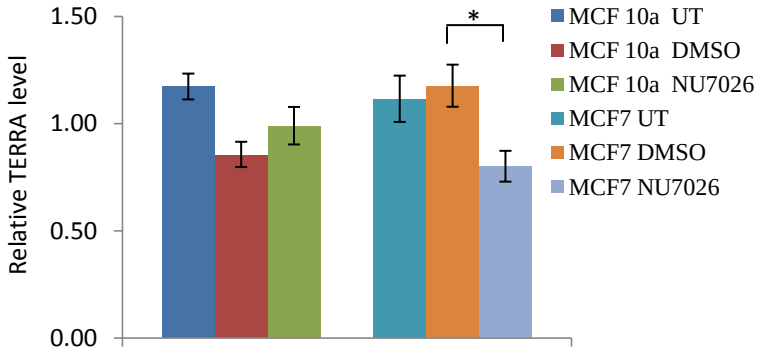

Figure 3.6. TERRA RNA levels evaluated via RNA dot blot following DNA-PKcs kinase inhibition (NU7026). A) RNA dot blots were used to evaluate TERRA levels relative to a housekeeping gene (GAPDH). TERRA levels were analyzed in untreated (UT), DMSO control or following the treatment with the DNA-PKcs kinase inhibitor, NU7026. RNase treatment confirms that probe is specific to RNA. B) TERRA levels in MCF 10a cells appear to be sensitive to DMSO treatment. No significant change in TERRA levels relative to GAPDH was seen following NU7026 treatment in comparison to DMSO control. A significant ($p=0.037$) decrease in TERRA level was observed following NU7026 treatment in the MCF7 cell line.

10a cell line. However, a significant decrease ($p=0.037$) in TERRA levels was observed following NU7026 treatment in the MCF7 cell line when compared to the DMSO control. This suggests that DNA-PKcs kinase inhibition indirectly affected TERRA levels.

Discussion

We have shown that DNA-PKcs kinase activity plays an important role in mammalian telomere end-capping function (Bailey et al., 2001; Bailey et al., 1999). However, the mechanism by which DNA-PKcs operates to cap telomeres is largely unknown. Here, we explored a possible interaction between DNA-PKcs and TERRA.

We hypothesized that DNA-PKcs dependent changes in TERRA localization at telomeres may be mediated through hnRNP A1, as hnRNP A1 has been shown to be a phosphorylation target of DNA-PKcs (Ting et al., 2009; Zhang et al., 2004) and to play a role in telomere biology (Zhang et al., 2006). We confirmed that DNA-PKcs targets hnRNP A1 for phosphorylation by analyzing ^{32}P uptake following siRNA depletion of DNA-PKcs or kinase inhibition. We found decreased hnRNP A1 phosphorylation following siRNA depletion of DNA-PKcs in both MCF7 and MCF 10a cell lines. However, decreased hnRNP A1 phosphorylation was not observed in the MCF 10a cell line following NU7026 treatment, suggesting hnRNP A1 phosphorylation in MCF 10a cells was not DNA-PKcs dependent. This may be due to the reduced hTR status of MCF 10a cells (Ting et al., 2009); a previous study demonstrated decreased hTR levels in MCF 10a cells (Ramachandran et al., 2002). The observed decrease in ^{32}P uptake following siRNA depletion of DNA-PKcs in the MCF 10a cell line may reflect the indirect effects of siRNA transfection, such as concomitant decreases in ATM kinase protein (Peng et al., 2005). Our results and those of others suggest that DNA-PKcs dependent

phosphorylation of hnRNP A1 is dependent on hTR expression (Ting et al., 2009). Furthermore, other kinases are likely involved in hnRNP A1 phosphorylation, as ^{32}P uptake was still observed in hnRNP A1 immunoprecipitates with inhibition of DNA-PKcs kinase activity. Other candidate kinases include p38 MAP kinase (Shimada et al., 2009), protein kinase A (Cobianchi et al., 1993), casein kinase (Gao et al., 2000) and protein kinase C (Municio et al., 1995).

Inhibition of DNA-PKcs kinase activity did not significantly influence TERRA localization at telomeres, implying that DNA-PKcs does not participate in keeping TERRA at telomere ends. However, 3-D imaging revealed a shift in TRF2 and TERRA distribution within colocalized foci, suggesting changes may be occurring at individual telomeres, where loss of DNA-PKcs influences the interaction between TRF2 and TERRA. Alternatively, DNA-PKcs kinase inhibition may affect the telomeric heterochromatin structure. Such instances might occur during repair, for example repair of oxidative damage or during replication, where individual telomeres respond independently. TERRA has been shown to inhibit telomerase activity by binding the telomerase RNA template itself (Schoeftner and Blasco, 2008) or by hindering access to telomerase by forming a G-quadruplex structures on telomere ends (Xu et al., 2010; Xu et al., 2009). Interestingly, TERRA has also been implicated in heterochromatin maintenance at telomere ends (Deng et al., 2009). It is tempting to postulate that one of the mechanisms by which DNA-PKcs functions to cap telomeres is through an interaction TERRA, where TERRA acts by regulating heterochromatin status. However, this change was minor and preliminary; more research is required in order to speculate on this. Furthermore, cell cycle status must be taken into account before any conclusions may be

drawn. For example, cells in early S-phase naturally experience changes in heterochromatin status.

We observed a significant decrease in TERRA levels following inhibition of DNA-PKcs kinase activity in the MCF7 mammary epithelial cell line, suggesting that DNA-PKcs may indirectly affect TERRA levels. Just how DNA-PKcs functions to affect TERRA levels needs further exploration. DNA-PKcs has been linked to transcription (Chibazakura et al., 1997; Peterson et al., 1992; Peterson et al., 1995; Sheppard and Liu, 2000) and has also been shown to phosphorylate RNA polymerase II (Dvir et al., 1992). Previous studies have found that RNA polymerase II is partly responsible for transcription of TERRA (Azzalin et al., 2007; Schoeftner and Blasco, 2008), providing one possible explanation for the decrease in TERRA levels following DNA-PKcs kinase inhibition. However, decreased TERRA levels were not observed in the MCF 10a cell line. This finding may be attributed to the differing characteristics between the non-tumorigenic MCF 10a and tumorigenic MCF 7 cell lines, including increased cell growth and thus transcription rate in the MCF 7 cell line.

Other transcription factors have also been shown to be phosphorylated by DNA-PKcs, including the TATA-binding protein and transcription factor IIB (Chibazakura et al., 1997), c-jun (Bannister et al., 1993), c-myc (Iijima et al., 1992) and FOS (Abate et al., 1993). Although the function of this phosphorylation is still largely unknown, such observations do support a role for DNA-PKcs kinase activity in the regulation of transcription.

Another possible explanation for decreased TERRA levels in the MCF7 cell line following DNA-PKcs kinase inhibition may be linked to hnRNP A1. We provide

evidence for the DNA-PKcs dependent phosphorylation of hnRNP A1 in the MCF 7 cell line; a similar effect was not seen in the MCF 10a cell line. Previously, de Silanes observed increased TERRA levels following the inhibition of various hnRNPs, specifically hnRNP F (de Silanes et al., 2010). This study suggested that this may be due to the role of hnRNP F in pre-mRNA cleavage, where loss of hnRNP F leads to an accumulation of TERRA. Similarly, we suggest that the decreased TERRA levels following DNA-PKcs kinase inhibition may partly be due to the role of hnRNP A1 in pre-mRNA processing. Increased hnRNP A1 phosphorylation has been reported when cells undergo stress, and this phosphorylation has been shown to lead to the accumulation of hnRNP A1 in the cytoplasm (Allemand et al., 2005; Guil et al., 2006; van der Houven van Oordt et al., 2000). Therefore, phosphorylation of hnRNP A1 may act as a switch in the cellular distribution of hnRNP A1, such that in a hypophosphorylated state, hnRNP A1 remains in the nucleus, where it is most often observed. Assuming there is a basal level of hnRNP A1 phosphorylation when cells are not stressed, as our ^{32}P data suggests, inhibition of DNA-PKcs kinase activity potentially results in increasesd hnRNP A1 accumulation in the nucleus thus increasing the opportunity for hnRNP A1 and TERRA interaction. This would then lead to a decrease in TERRA levels due to the role of hnRNP A1 in pre-mRNA cleavage. Because existing studies suggest a specific phosphorylation site for the cytoplasmic accumulation of hnRNP A1, termed the F-peptide, and this site does not correlate with the proposed hnRNP A1 phosphorylation site by DNA-PKcs, we favor an alternative explanation (Allemand et al., 2005; Ting et al., 2009). An independent study found decreased hnRNP A1 interaction with Tumor Necrosis Factor F alpha (TNF α) mRNA with the hyperphosphorylation of hnRNP A1 by

map kinase signaling (Buxade et al., 2005). This suggests that phosphorylation may affect the ability of hnRNP A1 to interact with its target RNA. Furthermore, Serine 192 (Ser192) was identified as one of the phosphorylation sites by map kinase signaling-integrating kinases (MNK), a site shared by DNA-PKcs (Buxade et al., 2005; Ting et al., 2009). Taken together, decreased TERRA levels following DNA-PKcs kinase inhibition, specifically in the MCF7 cell line, may reflect a combination of decreased RNA polymerase II transcription and decreased TERRA/hnRNP A1 interaction.

Taken together, we demonstrate that DNA-PKcs kinase activity does not influence TERRA localization to telomeres. We provide evidence that DNA-PKcs kinase activity affects TERRA levels, and this may be partly due to the involvement of DNA-PKcs in transcription regulation as well as the DNA-PKcs dependent phosphorylation of hnRNP A1. Determining the exact mechanism of DNA-PKcs kinase activity on TERRA requires further investigation.

Acknowledgements

We would like to thank Christine Battaglia for her work and assistance in the metabolic ^{32}P uptake experiment. We would also like to thank Dr. Andrew Ray for overseeing the work in dispersible radioisotopes, as well as the Radiation Control Office (RCO) at Colorado State University for managing the safe use and disposal of ^{32}P.

References

Abate, C., Baker, S.J., Lees-Miller, S.P., Anderson, C.W., Marshak, D.R., and Curran, T. (1993). Dimerization and DNA binding alter phosphorylation of Fos and Jun. Proc Natl Acad Sci U S A *90*, 6766-6770.

Allemand, E., Guil, S., Myers, M., Moscat, J., Caceres, J.F., and Krainer, A.R. (2005). Regulation of heterogenous nuclear ribonucleoprotein A1 transport by phosphorylation in cells stressed by osmotic shock. Proc Natl Acad Sci U S A *102*, 3605-3610.

Azzalin, C.M., Reichenbach, P., Khoriauli, L., Giulotto, E., and Lingner, J. (2007). Telomeric repeat containing RNA and RNA surveillance factors at mammalian chromosome ends. Science *318*, 798-801.

Bailey, S.M., Cornforth, M.N., Kurimasa, A., Chen, D.J., and Goodwin, E.H. (2001). Strand-specific postreplicative processing of mammalian telomeres. Science *293*, 2462-2465.

Bailey, S.M., Meyne, J., Chen, D.J., Kurimasa, A., Li, G.C., Lehnert, B.E., and Goodwin, E.H. (1999). DNA double-strand break repair proteins are required to cap the ends of mammalian chromosomes. Proc Natl Acad Sci U S A *96*, 14899-14904.

Bannister, A.J., Gottlieb, T.M., Kouzarides, T., and Jackson, S.P. (1993). c-Jun is phosphorylated by the DNA-dependent protein kinase in vitro; definition of the minimal kinase recognition motif. Nucleic Acids Res *21*, 1289-1295.

Blackburn, E.H. (1991). Structure and function of telomeres. Nature *350*, 569-573.

Bolte, S., and Cordelieres, F.P. (2006). A guided tour into subcellular colocalization analysis in light microscopy. J Microsc *224*, 213-232.

Boubnov, N.V., and Weaver, D.T. (1995). scid cells are deficient in Ku and replication protein A phosphorylation by the DNA-dependent protein kinase. Mol Cell Biol *15*, 5700-5706.

Brush, G.S., Anderson, C.W., and Kelly, T.J. (1994). The DNA-activated protein kinase is required for the phosphorylation of replication protein A during simian virus 40 DNA replication. Proc Natl Acad Sci U S A *91*, 12520-12524.

Brush, G.S., Morrow, D.M., Hieter, P., and Kelly, T.J. (1996). The ATM homologue MEC1 is required for phosphorylation of replication protein A in yeast. Proc Natl Acad Sci U S A *93*, 15075-15080.

Burd, C.G., and Dreyfuss, G. (1994). RNA binding specificity of hnRNP A1: significance of hnRNP A1 high-affinity binding sites in pre-mRNA splicing. Embo J *13*, 1197-1204.

Buxade, M., Parra, J.L., Rousseau, S., Shpiro, N., Marquez, R., Morrice, N., Bain, J., Espel, E., and Proud, C.G. (2005). The Mnks are novel components in the control of TNF alpha biosynthesis and phosphorylate and regulate hnRNP A1. Immunity *23*, 177-189.

Chibazakura, T., Watanabe, F., Kitajima, S., Tsukada, K., Yasukochi, Y., and Teraoka, H. (1997). Phosphorylation of human general transcription factors TATA-binding protein and transcription factor IIB by DNA-dependent protein kinase--synergistic stimulation of RNA polymerase II basal transcription in vitro. Eur J Biochem *247*, 1166-1173.

Chiu, C.P., Dragowska, W., Kim, N.W., Vaziri, H., Yui, J., Thomas, T.E., Harley, C.B., and Lansdorp, P.M. (1996). Differential expression of telomerase activity in hematopoietic progenitors from adult human bone marrow. Stem Cells *14*, 239-248.

Cobianchi, F., Calvio, C., Stoppini, M., Buvoli, M., and Riva, S. (1993). Phosphorylation of human hnRNP protein A1 abrogates in vitro strand annealing activity. Nucleic Acids Res *21*, 949-955.

de Lange, T. (2005). Shelterin: the protein complex that shapes and safeguards human telomeres. Genes Dev *19*, 2100-2110.

de Silanes, I.L., d'Alcontres, M.S., and Blasco, M.A. (2010). TERRA transcripts are bound by a complex array of RNA-binding proteins. Nat Commun *1*, 33.

Deng, Z., Norseen, J., Wiedmer, A., Riethman, H., and Lieberman, P.M. (2009). TERRA RNA binding to TRF2 facilitates heterochromatin formation and ORC recruitment at telomeres. Mol Cell *35*, 403-413.

Dvir, A., Peterson, S.R., Knuth, M.W., Lu, H., and Dynan, W.S. (1992). Ku autoantigen is the regulatory component of a template-associated protein kinase that phosphorylates RNA polymerase II. Proc Natl Acad Sci U S A *89*, 11920-11924.

Flynn, R.L., Centore, R.C., O'Sullivan, R.J., Rai, R., Tse, A., Songyang, Z., Chang, S., Karlseder, J., and Zou, L. (2011). TERRA and hnRNPA1 orchestrate an RPA-to-POT1 switch on telomeric single-stranded DNA. Nature *471*, 532-536.

Gao, Z.H., Metherall, J., and Virshup, D.M. (2000). Identification of casein kinase I substrates by in vitro expression cloning screening. Biochem Biophys Res Commun *268*, 562-566.

Gately, D.P., Hittle, J.C., Chan, G.K., and Yen, T.J. (1998). Characterization of ATM expression, localization, and associated DNA-dependent protein kinase activity. Mol Biol Cell *9*, 2361-2374.

Gottlieb, T.M., and Jackson, S.P. (1993). The DNA-dependent protein kinase: requirement for DNA ends and association with Ku antigen. Cell *72*, 131-142.

Guil, S., Long, J.C., and Caceres, J.F. (2006). hnRNP A1 relocalization to the stress granules reflects a role in the stress response. Mol Cell Biol *26*, 5744-5758.

Hamilton, B.J., Burns, C.M., Nichols, R.C., and Rigby, W.F. (1997). Modulation of AUUUA response element binding by heterogeneous nuclear ribonucleoprotein A1 in human T lymphocytes. The roles of cytoplasmic location, transcription, and phosphorylation. J Biol Chem *272*, 28732-28741.

Harley, C.B., and Villeponteau, B. (1995). Telomeres and telomerase in aging and cancer. Curr Opin Genet Dev *5*, 249-255.

He, Y., and Smith, R. (2009). Nuclear functions of heterogeneous nuclear ribonucleoproteins A/B. Cell Mol Life Sci *66*, 1239-1256.

Hiyama, E., Tatsumoto, N., Kodama, T., Hiyama, K., Shay, J., and Yokoyama, T. (1996). Telomerase activity in human intestine. Int J Oncol *9*, 453-458.

Hollick, J.J., Golding, B.T., Hardcastle, I.R., Martin, N., Richardson, C., Rigoreau, L.J., Smith, G.C., and Griffin, R.J. (2003). 2,6-disubstituted pyran-4-one and thiopyran-4-one inhibitors of DNA-Dependent protein kinase (DNA-PK). Bioorg Med Chem Lett *13*, 3083-3086.

Iijima, S., Teraoka, H., Date, T., and Tsukada, K. (1992). DNA-activated protein kinase in Raji Burkitt's lymphoma cells. Phosphorylation of c-Myc oncoprotein. Eur J Biochem *206*, 595-603.

Kafatos, F.C., Jones, C.W., and Efstratiadis, A. (1979). Determination of nucleic acid sequence homologies and relative concentrations by a dot hybridization procedure. Nucleic Acids Res *7*, 1541-1552.

Kim, N.W., Piatyszek, M.A., Prowse, K.R., Harley, C.B., West, M.D., Ho, P.L., Coviello, G.M., Wright, W.E., Weinrich, S.L., and Shay, J.W. (1994). Specific association of human telomerase activity with immortal cells and cancer. Science *266*, 2011-2015.

Mantell, L.L., and Greider, C.W. (1994). Telomerase activity in germline and embryonic cells of Xenopus. Embo J *13*, 3211-3217.

Martinez-Contreras, R., Cloutier, P., Shkreta, L., Fisette, J.F., Revil, T., and Chabot, B. (2007). hnRNP proteins and splicing control. Adv Exp Med Biol *623*, 123-147.

Mayeda, A., and Krainer, A.R. (1992). Regulation of alternative pre-mRNA splicing by hnRNP A1 and splicing factor SF2. Cell *68*, 365-375.

Moyzis, R.K., Buckingham, J.M., Cram, L.S., Dani, M., Deaven, L.L., Jones, M.D., Meyne, J., Ratliff, R.L., and Wu, J.R. (1988). A highly conserved repetitive DNA sequence, (TTAGGG)n, present at the telomeres of human chromosomes. Proc Natl Acad Sci U S A *85*, 6622-6626.

Municio, M.M., Lozano, J., Sanchez, P., Moscat, J., and Diaz-Meco, M.T. (1995). Identification of heterogeneous ribonucleoprotein A1 as a novel substrate for protein kinase C zeta. J Biol Chem *270*, 15884-15891.

Okayasu, R., Suetomi, K., and Ullrich, R.L. (1998). Wortmannin inhibits repair of DNA double-strand breaks in irradiated normal human cells. Radiat Res *149*, 440-445.

Okayasu, R., Suetomi, K., Yu, Y., Silver, A., Bedford, J.S., Cox, R., and Ullrich, R.L. (2000). A deficiency in DNA repair and DNA-PKcs expression in the radiosensitive BALB/c mouse. Cancer Res *60*, 4342-4345.

Peng, Y., Woods, R.G., Beamish, H., Ye, R., Lees-Miller, S.P., Lavin, M.F., and Bedford, J.S. (2005). Deficiency in the catalytic subunit of DNA-dependent protein kinase causes down-regulation of ATM. Cancer Res *65*, 1670-1677.

Peng, Y., Zhang, Q., Nagasawa, H., Okayasu, R., Liber, H.L., and Bedford, J.S. (2002). Silencing expression of the catalytic subunit of DNA-dependent protein kinase by small interfering RNA sensitizes human cells for radiation-induced chromosome damage, cell killing, and mutation. Cancer Res *62*, 6400-6404.

Peterson, S.R., Dvir, A., Anderson, C.W., and Dynan, W.S. (1992). DNA binding provides a signal for phosphorylation of the RNA polymerase II heptapeptide repeats. Genes Dev *6*, 426-438.

Peterson, S.R., Jesch, S.A., Chamberlin, T.N., Dvir, A., Rabindran, S.K., Wu, C., and Dynan, W.S. (1995). Stimulation of the DNA-dependent protein kinase by RNA polymerase II transcriptional activator proteins. J Biol Chem *270*, 1449-1454.

Porro, A., Feuerhahn, S., Reichenbach, P., and Lingner, J. Molecular dissection of TERRA biogenesis unveils the presence of distinct and multiple regulatory pathways. Mol Cell Biol.

Ramachandran, C., Fonseca, H.B., Jhabvala, P., Escalon, E.A., and Melnick, S.J. (2002). Curcumin inhibits telomerase activity through human telomerase reverse transcritpase in MCF-7 breast cancer cell line. Cancer Lett *184*, 1-6.

Schoeftner, S., and Blasco, M.A. (2008). Developmentally regulated transcription of mammalian telomeres by DNA-dependent RNA polymerase II. Nat Cell Biol *10*, 228-236.

Sheppard, H.M., and Liu, X. (2000). Transcription by RNA polymerase II in DNA-PK deficient scid mouse cells. Biochim Biophys Acta *1493*, 41-47.

Shimada, N., Rios, I., Moran, H., Sayers, B., and Hubbard, K. (2009). p38 MAP kinase-dependent regulation of the expression level and subcellular distribution of heterogeneous nuclear ribonucleoprotein A1 and its involvement in cellular senescence in normal human fibroblasts. RNA Biol *6*, 293-304.

Ting, N.S., Pohorelic, B., Yu, Y., Lees-Miller, S.P., and Beattie, T.L. (2009). The human telomerase RNA component, hTR, activates the DNA-dependent protein kinase to phosphorylate heterogeneous nuclear ribonucleoprotein A1. Nucleic Acids Res *37*, 6105-6115.

van der Houven van Oordt, W., Diaz-Meco, M.T., Lozano, J., Krainer, A.R., Moscat, J., and Caceres, J.F. (2000). The MKK(3/6)-p38-signaling cascade alters the subcellular distribution of hnRNP A1 and modulates alternative splicing regulation. J Cell Biol *149*, 307-316.

Wang, H., Wang, M., Wang, H., Bocker, W., and Iliakis, G. (2005). Complex H2AX phosphorylation patterns by multiple kinases including ATM and DNA-PK in human cells exposed to ionizing radiation and treated with kinase inhibitors. J Cell Physiol *202*, 492-502.

Watson, J.D. (1972). Origin of concatemeric T7 DNA. Nat New Biol *239*, 197-201.

Williams, E.S., Klingler, R., Ponnaiya, B., Hardt, T., Schrock, E., Lees-Miller, S.P., Meek, K., Ullrich, R.L., and Bailey, S.M. (2009). Telomere dysfunction and DNA-PKcs deficiency: characterization and consequence. Cancer Res *69*, 2100-2107.

Xu, Y., Suzuki, Y., Ito, K., and Komiyama, M. (2010). Telomeric repeat-containing RNA structure in living cells. Proc Natl Acad Sci U S A *107*, 14579-14584.

Xu, Y., Suzuki, Y., Kaminaga, K., and Komiyama, M. (2009). Molecular basis of human telomere DNA/RNA structure and its potential application. Nucleic Acids Symp Ser (Oxf), 63-64.

Zhang, Q.S., Manche, L., Xu, R.M., and Krainer, A.R. (2006). hnRNP A1 associates with telomere ends and stimulates telomerase activity. Rna *12*, 1116-1128.

Zhang, S., Schlott, B., Gorlach, M., and Grosse, F. (2004). DNA-dependent protein kinase (DNA-PK) phosphorylates nuclear DNA helicase II/RNA helicase A and hnRNP proteins in an RNA-dependent manner. Nucleic Acids Res *32*, 1-10.

CHAPTER 4

THE RNA BINDING PROTEIN, hnRNP A1, IN TELOMERE STRUCTURE AND FUNCTION

Chapter 4

The RNA binding protein, hnRNP A1, in telomere structure and function

Phuong N. Le, David G. Maranon, Noeila H. Altina, Christine L.R. Battaglia and Susan M. Bailey

Department of Environmental and Radiological Health Sciences, Colorado State University, Fort Collins, CO 80538, USA

Overview

Telomeres are highly repetitive features that serve to protect the ends of linear chromosomes, which have been regarded as transcriptionally silent until recently. Telomeres are transcribed into telomere repeat-containing RNA (TERRA) (Azzalin et al., 2007; Schoeftner and Blasco, 2008), and TERRA serves to help maintain the condensed, heterochromatic state of telomeres (Deng et al., 2009). The RNA binding protein, heterogeneous nuclear ribonucleoprotein (hnRNP A1) associates with TERRA (de Silanes et al., 2010). hnRNP A1 has also been shown to bind telomeric DNA sequences and influence telomerase activity (Ford et al., 2002; LaBranche et al., 1998; Zhang et al., 2006). We examined hnRNP A1 dependence of TERRA localization to telomeres and found no connection, demonstrating that hnRNP A1 does not act to "tether" TERRA to telomeric DNA. It has also been suggested that hnRNPs influence TERRA stability. Therefore, we examined TERRA levels using RNA dot blots. We observed no significant changes in TERRA levels following siRNA depletion of hnRNP A1. Following siRNA depletion of hnRNP A1 in human mammary epithelial cells, we also investigated telomere function and observed increased frequencies of what has previously been termed "fragile" telomeres (Sfeir et al., 2009) and telomere sister chromatid exchanges (T-SCE), suggesting a role for hnRNP A1 in facilitating telomere replication. Our results provide important insights into the roles of the RNA binding protein, hnRNP A1, in human telomere structure and function.

Introduction

Telomeres are repetitive, well conserved G-rich TTAGGG repeats at the ends of chromosomes in vertebrates (Moyzis et al., 1988). Functional telomeres solve both the end-protection problem by preventing fusions (McClintock, 1939) and protecting from loss of genetic information (Watson, 1972). Because they are heterochromatic and repetitive, telomeres have long been thought to be transcriptionally silent. However, telomeres have recently been shown to be transcribed into UUAGGG sequences (Azzalin et al., 2007), partly by RNA polymerase II (Schoeftner and Blasco, 2008). Telomeric repeat-containing RNA (TERRA) or telomeric RNA (TelRNA), has been shown to localize to telomere ends and is associated with heterochromatin maintenance, telomerase activity and G-quadruplex formation (Azzalin et al., 2007; Deng et al., 2009; Schoeftner and Blasco, 2008; Xu et al., 2010; Xu et al., 2009). TERRA has been shown to be conserved in yeast and partly regulated by suppressors with morphogenetic defects in genitalia (SMG) proteins (Azzalin et al., 2007). SMG proteins are important in nonsense-mediated mRNA decay (NMD) in *caenorhabditis elegans* (Anders et al., 2003; Page et al., 1999). Furthermore, EST1a, EST1b and EST1c, the human orthologues of SMG proteins in C. elegans (Chiu et al., 2003; Gatfield et al., 2003) have been shown to interact with telomerase (Reichenbach et al., 2003). In humans, CpG island rich promoters have been shown to influence TERRA transcription (Schoeftner and Blasco, 2008; Yehezkel et al., 2008). TERRA function and how it is maintained at telomeres are currently areas of intense investigation.

Heterogenous nuclear ribonucleoprotein A1 (hnRNP A1) is a member of a large family of RNA binding proteins. This family is made up of over 20 proteins, including

hnRNP A1-U, some of which bind pre-mRNA and packages them for transport (He et al., 2005). hnRNPs have also been shown to play a role in mRNA alternative splicing (Martinez-Contreras et al., 2007; Mayeda and Krainer, 1992). hnRNP A1 is one of the most abundant proteins in this family (Beyer et al., 1977) and has been shown to bind telomeric repeats and influence telomerase activity (Dallaire et al., 2000; LaBranche et al., 1998; Zhang et al., 2006). It has been shown to preferentially bind UAGGGA/U sequences, a sequence similar to that of TERRA (Burd and Dreyfuss, 1994; Hamilton et al., 1997). In addition, recent studies suggest that hnRNP A1 interacts with TERRA (de Silanes et al., 2010; Deng et al., 2009).

Telomeres are known to be inherently difficult to replicate due to their highly repetitive sequence and propensity to form secondary structures, including G-quadruplex structure. Thus, replication fork stalling has been shown to naturally occur at telomeres and is exacerbated when lacking the necessary helicases (Ivessa et al., 2002; Ivessa et al., 2000; Makovets et al., 2004). A recent study demonstrated that Telomere Repeat Factor 1 (TRF1) was required to prevent the "fragile" telomere phenotype, an extended or doublet telomeric signal when using Fluorescence *In Situ* Hybridization (FISH) with a telomere specific probe (Sfeir et al., 2009). This study also provided evidence suggesting that "fragile" telomeres were the result of aberrant telomere replication.

We hypothesized that hnRNP A1 may contribute to "tethering" TERRA to telomere ends. We examined such a possibility following siRNA depletion of hnRNP A1 in two human mammary epithelial cell lines, non-tumorigenic MCF 10a and tumorigenic MCF7 cell lines. In conjunction, we utilized RNA FISH with a probe specific for TERRA and immunocytochemisty with an antibody against telomere repeat factor 2 (TRF2), a

telomere specific protein. We found little to no change in localization of TERRA to telomeres following siRNA depletion of hnRNP A1, suggesting that hnRNP A1 does not function to "tether" TERRA to telomeres. Because hnRNPs have also been shown to influence TERRA stability (de Silanes et al., 2010), we also monitored changes in TERRA levels following hnRNP A1 depletion by RNA dot blot. We found no significant changes in TERRA levels following siRNA treatment, suggesting that hnRNP A1 does not affect TERRA levels, at least at our time point.

Because hnRNP A1 has also been tightly linked with telomere lengthening via telomerase (Zhang et al., 2006), we further examined telomere function following siRNA knockdown of hnRNP A1 using Fluorescence *In Situ* Hybridization (FISH) and Chromosome-Orientation (CO-) FISH with a telomere specific probe. We observed increased frequencies of "fragile" telomeres, as previously described (Sfeir et al., 2009) and increased Telomere Sister Chromatid Eschange (T-SCE), approaching significance, with loss of hnRNP A1. These results suggest a role for hnRNP A1 in facilitating telomere replication.

Materials and methods

Cell culture

The MCF7 cell line, a gift from Laura Chubb at Colorado State University Veterinary Teaching Hospital, was originally derived from a human metastatic mammary carcinoma and grown in Minimum Essential Media/Earle's Balanced Salt Solution (MEM/EBSS; Hyclone) media supplemented with 10% fetal bovine serum (FBS; Sigma). The epithelial mammary non-tumorigenic cell line, MCF 10A, was purchased from

ATCC and cultured in 1:1 Dulbecco's Modified Eagle's Medium (DMEM) / Ham's F12 growth media (Hyclone) supplemented with 5% FBS , 20ng/ml Epidermal Growth Factor (EGF; Sigma), 0.5ug/ml hydrocortisone (Sigma), 0.1ug/ml cholera toxin (Sigma), 10ug/ml insulin (Sigma), 1% Glutamax (Gibco) and 1% penicillin/streptomycin (Hyclone). The normal human foreskin fibroblasts, BJ 1, were maintained in high glucose DMEM (Gibco) with 10% FBS and 1% penicillin/streptomycin. The isogenic BJ-hTERT cell line, parental BJ 1 transfected with the catalytic subunit of telomerase, was maintained in α-MEM (Gibco) supplemented with 10% FBS, 1% glutamax 1% pennicillin/streptomycin. Both BJ 1 and BJ-hTERT were generous gifts from Dr. Jerry Shay at the University of Texas Southwestern Medical Center in Dallas, TX. Normal human fibroblasts, 5C, were bought from Cascade Biologicals and maintained in α-MEM with 10% FBS, 1% glutamax 1% pennicillin/streptomycin. Cell media was changed every 3-4 days, and cells were passaged 1-2 times per week.

Fluorescence In Situ Hybridization (FISH) and two-color Chromosome-Orientation (CO-) FISH

Metaphase spreads were collected using standard cytogenetic techniques (Henegariu et al., 2001). Briefly, cells were incubated with 0.1ug/mL colcemid, harvested and lysed with 75mM KCL, fixed in 3:1 methanol: acetic acid and added to pre-cleaned slides. Slides were fixed in 3% paraformaldehyde, dehydrated in an ethanol series (75%, 85% and 100%) and denatured in 70% formamide/2x saline sodium citrate (SSC) at 70ºC for 2 minutes. A G-rich telomere Peptide Nucleic Acid (PNA) probe $(TTAGGG)_7$ labelled with Cy-3 was subsequently hybridized onto the slides at 37ºC for 30-60

minutes, and for CO-Fish the C-rich telomere probe $(CCCTAA)_7$ labelled with FITC was also hybridized onto the slide at 37ºC overnight. Slides were then washed in 50% formamide/2xSSC, 2X SSC and 0.1% NP-40/2X SSC at 43ºC for 2.5 minutes each. Lastly, slides were mounted in Prolong Gold Antifade (Invitrogen) with 4',6-diamidino-2-phenylindole, dihydrochloride (DAPI).

For CO-FISH, in addition to the steps described above, cells were also incubated for a single round of replication in 5-bromo-2'-deoxyuridine and 5-bromo-2'-deoxy-cytosine (BrdU/BrdC) at a 3:1 ratio for a final concentration of 5×10^{-5}M. Prior to denaturing, slides were stained with Hoescht 33258 (0.5ug/mL), exposed to Ultraviolet (UV) light using Stratagene Stratalinker outfitted with 365nM bulbs for 35 minutes, and then incubated with Exonuclease III (~10U) for 20 minutes at 25ºC. Lastly, slides were hybridized with telomere probes as described above. Three independent experiments were performed and 30 metaphases scored per experiment. Because there was no significant difference between the individual means, experimental data were combined for statistical analysis. Immunoblotting was done to confirm siRNA depletion of hnRNP A1 for each experiment. Statistical analysis was done using the student T-test.

Chromosome and telomere aberration scoring criteria

Clonal chromosome-type aberrations were not included in the final aberration frequencies. Chromatid-type gaps were defined as discontinuities in DAPI staining greater than the width of a chromatid arm. Chromatid-type breaks were defined as a discontinuity in DAPI equal to or greater than the width of a chromatid.

Telomere function was evaluated using several endpoints. Signal free ends (SFE) were assessed following both FISH and CO-FISH using two scoring criteria. First, SFEs were scored as a complete lack of telomere signal on one chromatid arm. Secondly, SFEs were scored as a single event only if the signal was missing from both sister chromatid arms, as would be expected with telomere shortening and subsequent replication. "Fragile" telomeres were defined as one extended telomere signal and/or duplicated telomere signals. Scoring criteria included that the duplicate telomere signals were within one signal width of each other. All signals that did not meet this criterion were subsequently scored as interstitial telomere signals (ITS) and were not included as a "fragile" telomere.

RNA FISH and Immunocytochemistry (ICC)

Cells grown on chamber slides were washed at room temperature with cytoskeleton (CSK) buffer for 30 seconds, permeabilized with 0.5% Triton X-100 in CSK/vanadyl for 5 minutes and subsequently fixed in 3% paraformaldehyde for 10 minutes at room temperature. Following fixation, slides were blocked in 3% Bovine Serum Albumin (BSA) for 1 hour at room temperature. Slides were then incubated for 1 hour with mouse anti-TRF-2 primary antibody (Imgenex) at room temperature followed by incubation with anti-mouse Alexa 594 secondary antibody (Invitrogen) for 45 minutes. Slides were washed once with 1X Phosphate Buffer Saline (PBS), incubated overnight with a FITC labeled PNA probe $(CCCTAA)_7$ complementary to TERRA and sequentially washed in 50% formamide/2XSSC, 2X SSC, 2X SSC/NP-40 for 2.3 min

each at 39°C. Lastly, slides were mounted with ProLong Gold Antifade with DAPI (Invitrogen).

Microscopy and imaging

A Nikon Eclipse E600 epifluorescent microscope was used to acquire stacked images, and Metamorph software was used for 3-D deconvolution and reconstruction of the acquired images. Colocalization of TERRA and TRF2 signals was established using different statistical parameters to measure 3-D images and generate the colocalization profile for each particular cell. Metamorph and Image J software were used to measure the co-localization signals from the acquired 3-D images in both channels, green (TERRA) and red (TRF-2), using colocalization coefficients, including Pearson's and Mander's Coefficient.

Small interfering RNA (siRNA) knockdown of hnRNP A1

Cells were transfected using the reverse transfection method with lipofectamine RNAimax (Invitrogen) as recommended by the manufacturer. Briefly, cells were passed and seeded at approximately 50% confluency with non-antibiotic media and were simultaneously treated with lipofectamine alone (mock) or lipofectamine and siRNA oligonucleotides (siRNA treated) targeted to hnRNP A1. ON-TARGET plus SMARTpool siRNA (Dharmacon) oligo sequences used were as follows: CGGAAACCUUGGUGUAGUU, GGGAAUGAAGCUUGUGUAU, CAACUUCGGUCGUGGAGGA and UAGAAUUCCUUCAGGGUGA. Cells were incubated with siRNA at a final concentration of 10nM and harvested at different time

points to monitor knockdown efficiency. Cells were treated with a non-target sequence to assess for siRNA specificity to hnRNP A1 using ON-TARGETplus non-targeting pool (Dharmacon). siRNA silencing was subsequently confirmed by immunoblotting (below).

Cell lysis and protein quantification

Cells were harvested by trypsinization and pellets washed with 1X PBS. Pellets were subsequently incubated in lysis buffer for 10 minutes over ice with periodic flicking. Lysis buffer included 50mM Tris-HCL, 150mM NaCL, 2mM ethylenediaminetetraacetic acid (EDTA), 2mM ethylene glycol tetraacetic acid (EGTA), 25mM NaF, 25mM β-glycerophosphate, 0.2% triton x-100, 0.3% NP-40, and 0.1mM sodium ortho-vanadate in water. Protease inhibitors were added directly before use, including 0.1mM phenylmethylsulfonyl fluoride (PMSF), 5µg/mL leupeptin and 5µg/mL aprotinin. The Bradford Assay was used to quantify protein in whole cell lysate using Bradford Dye (Bio-Rad).

Immunoblotting

Protein samples were separated via Sodium Dodecyl Sulfate Solution Polyacrylamide Gel Electrophoresis (SDS-PAGE) and transferred to a methanol activated Polyvinylidene Fluoride (PVDF) membrane. The membrane was blocked for 1 hour with 4% milk in Tris-buffered saline with 0.1% Tween (TBST) at room temperature with shaking. Membrane was rinsed once in TBST before incubating with primary antibody in 1% milk in TBST for 1 hour at room temperature or overnight at 4ºC with shaking. Primary antibody against hnRNP A1 (Abcam ab5832 clone 9H10) was added at 1:1000

concentration, and primary antibody toward β-tubulin (Abcam ab6046) was added at a 1:1000 concentration and used as a loading control. The membrane was subsequently washed 4 times in 1x TBST for 5 minutes each at room temperature with shaking, incubated with secondary antibody in Licor Blocking Buffer for 2 hours at room temp with shaking and subjugated to the 4 TBST washes as described above. Alexa Fluor 680 (Invitrogen A21058) and goat anti-rabbit IgG 800 (Thermo Scientific 35571) was added at a 1:10,000 and 1:40,000 dilution respectively. Lastly, the membrane was imaged on the Odyssey Imaging System. Relative protein expression was measured as a ratio of intensity of bands using Odyssey imaging software, which also accounts for background.

RNA dot blot

RNA dot blot was performed as previously described (Kafatos et al., 1979) with some modifications. Total RNA extraction was performed using the Qiagen RNeasy kit (Qiagen), and RNA quality was assessed by gel electrophoresis. Pre-wet GeneScreen Plus Nylon (Perkin Elmer) and Bio-Dot SF filter paper (Biorad) in 20X SSC was assembled into a Biorad biodot apparatus which could be attached to a vacuum source. The membrane was rinsed twice in 10X SSC. 7.5ug of RNA was diluted in ddH_20 with 30uL of RNA denaturing solution (66% formamide, 21% Formaldehyde [37%], 13% 10X MOPs pH 7). RNA was denatured for 5 minutes at 75ºC, and then 20X SSC was added at an equal volume. Samples were subsequently applied to the slots, vacuumed through and washed twice with 10X SSC. Vacuum was applied for 5 minutes to dry the membrane. The membrane was then removed and placed in the UV Stratalinker 2400 (Stratagene) for 25-50 seconds. The membrane was stained in 0.02% Methylene blue,

0.5M Sodium Acetate, pH 5.2 in order to visualize and mark RNA dots. Hybridization solution (2mM vanadyl, 50% formamide, 30% 20xSSC, 1% 50X Denhardt's solution, 0.25% SDS [20%], 0.1 % or 250ug/mL of salmon sperm DNA, brought up to volume with ddH_20) was incubated with the membrane for 2hrs at 42ºC. Fresh hybridization buffer was added with denatured FITC labeled TERRA PNA probe $(CCCTAA)_7$ or denatured FITC labeled-GAPDH PNA probe (DAKO) and incubated overnight at 42ºC. The membrane was washed with shaking: 1) 4 times in 2X SSC at room temperature for 10 minutes each; 2) 2 times in 0.1X SSC 2, 0.1% SDS at 50ºC for 30 minutes each; and 3) 2 times in 0.1X SSC, 0.5% SDS at 68ºC for 30 minutes each. Images were obtained using Storm 860 (GE Healthcare) and image analysis was performed using Image J (National Institute of Health; NIH).

Results

siRNA silencing of hnRNP A1

Following siRNA transfection, relative protein levels of hnRNP A1 in relation to β-tubulin were monitored by immunoblotting in five different cells, including BJ1 human fibroblasts, BJ-hTERT, 5C human fibroblasts, MCF 10a and MCF7 cells (Figure 4.1). Four independent collections were done and immunoblot analysis repeated twice per collection. hnRNP A1 protein expression was consistently higher in the MCF7 cell line in comparison to the other cells, similar to previous reports suggesting increased hnRNP A1 expression in cancer cells (Boukakis et al.; Ma et al., 2009). Cells were harvested at various time points between 24 and 228 hours to monitor protein levels of hnRNP A1 following siRNA treatment. Optimal hnRNP A1 protein knockdown was achieved

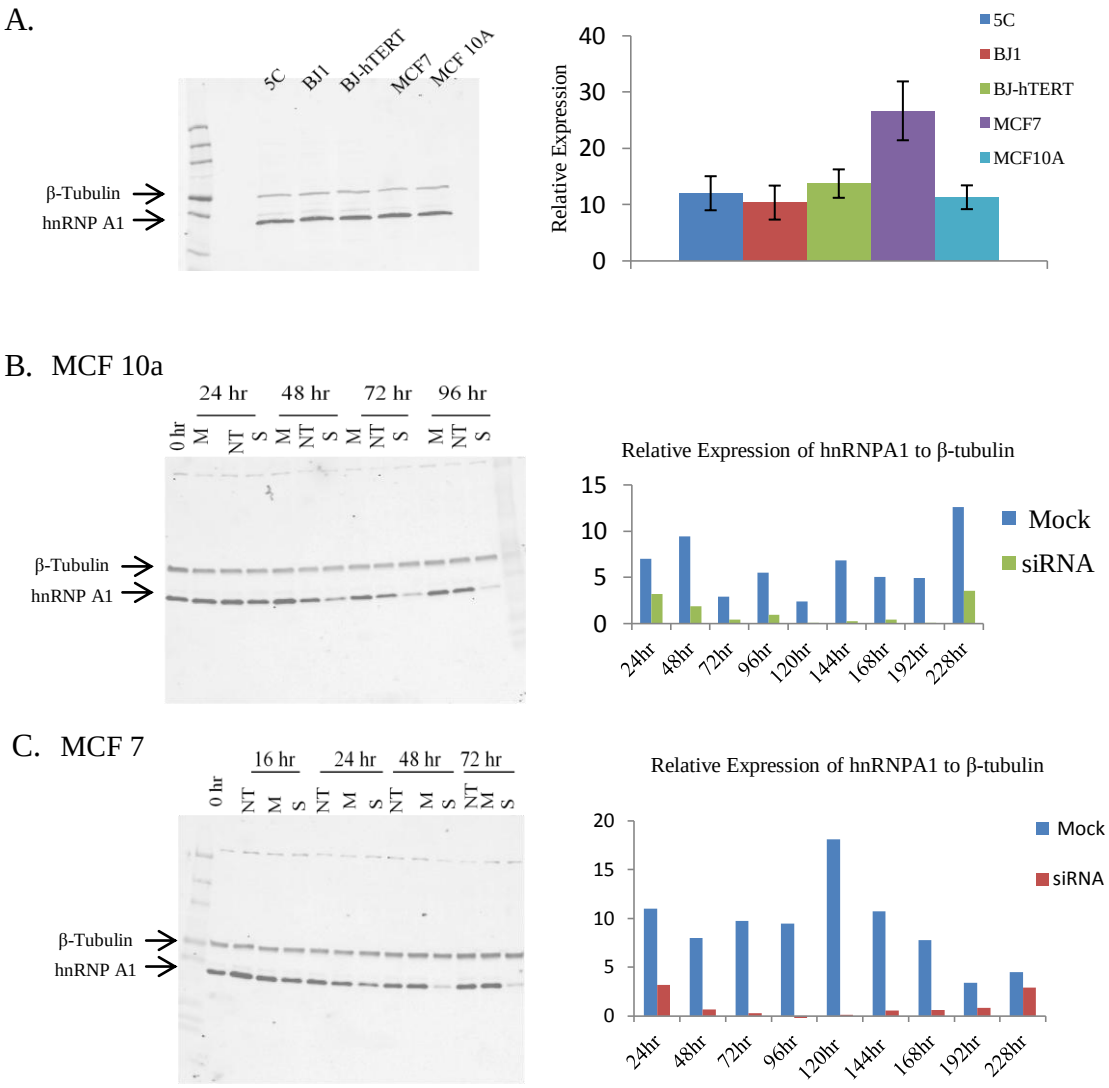

Figure 4.1. siRNA silencing of hnRNP A1 results in MCF7 and MCF 10a cell lines. A) Baseline relative protein expression of hnRNP A1 (34kDa) to β-tubulin (50kDa) in 5 different cell types. Increased expression was consistently observed in the MCF7 tumorigenic cell line as compared to the others. Data was collected from four independent experiments, and immunoblotting repeated twice per experiment. B) Immunoblot depicting siRNA silencing of hnRNP A1 results in MCF 10a cells. Decreased hnRNP A1 protein expression was seen as early as 48 hours post siRNA transfection (S) in comparison to mock (M). Optimal knockdown was seen 72-96 hour. A non-target (NT) effect of approximately 16.6% was seen in this cell line based on 2 independent experiments. C) Immunoblot depicting results of siRNA silencing of hnRNP A1 in MCF7 cells. Optimal knock down was observed 72-96 hours. A non-targeting effect of approximately 3.3% was seen based on two independent experiments.

between 72-96 hours post treatment (Figure 4.1), and therefore subsequent experiments were done at 72 hours. hnRNP A1 siRNA treatment resulted in ~90% knockdown efficiency (Figure 4.1; H-10). An average of a 16.6% decrease (range 5.5-27%) in the MCF 10a cell line and a 3.3% decrease (range -3.6-6.7%) in the MCF7 cell line was seen when including a non-target oligonucleotide sequence (Figure 4.1; NT).

hnRNP A1 is not required for TERRA localization at telomeres

It has been shown that hnRNP A1 interacts with telomeres (Zhang et al., 2006) and binds TERRA (de Silanes et al., 2010). Therefore, we investigated TERRA localization at telomeres following siRNA silencing of hnRNP A1. We performed RNA FISH with a TERRA specific probe FITC-$(CCCTAA)_7$ and immunocytochemistry with an anti-TRF2 antibody, a telomere specific protein. We used a novel 3-dimensional imaging system in order to assess colocalization (Figure 4.2). We observed little to no change in percent colocalization following siRNA knockdown of hnRNP A1 in MCF7 cells, suggesting that hnRNP A1 is not essential for TERRA localization to telomeres (Figure 4.2). Interestingly, we observed a small subset of foci that contained TRF2 and TERRA with differential spacing following siRNA depletion of hnRNP A1; i.e., there was less overlap between the TRF2 and TERRA foci in individual colocalized foci. Colocalization was observed both visually and by using Pearson's Correlation Coefficient, which is a statistical measure of the correlation between the two molecules. A Pearson's Correlation Coefficient of 0.69 is considered to reflect colocalization of the two molecules (Bolte and Cordelieres, 2006). Using Pearson's Correlation Coefficient, a decrease in overlap was seen to correlate when the coefficient was around 0.4. We,

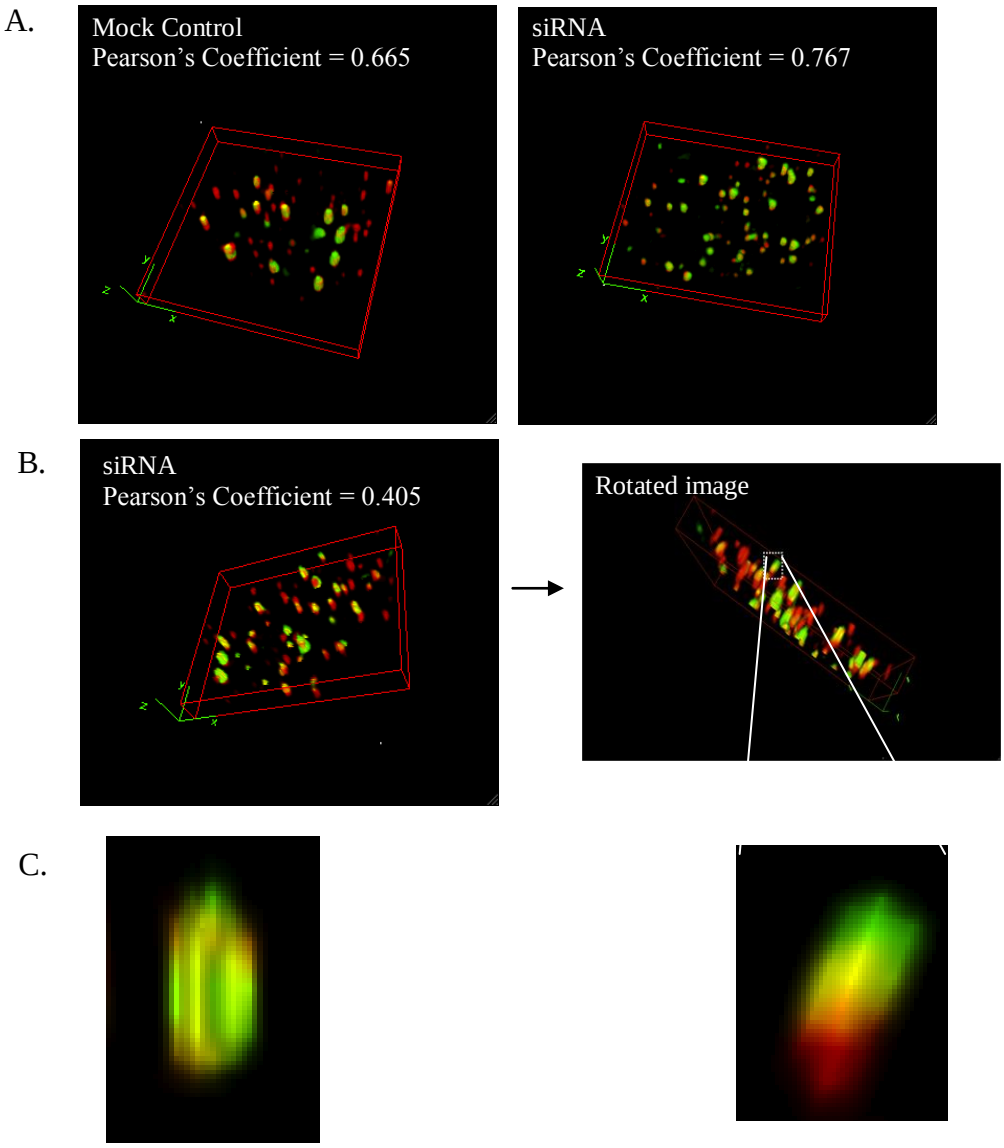

Figure 4.2. TERRA and TRF2 3-D colocalization. A) 3-D images of TERRA (green) and TRF2 (red) colocalization. Every TERRA molecule was colocalized with a TRF2 molecule. No significant change in TERRA localization was seen following siRNA depletion of hnRNP A1. B) A decrease in TERRA and TRF2 foci overlap was observed in a subset of colocalized foci following siRNA treatment. C) Images depicting what is generally observed in a partial colocalization event (left) in comparison to that observed when the shift, i.e. decreased foci overlap, occurs.

therefore, grouped the data into two categories, where data were divided into cells that had an average Pearson's Correlation Coefficient at or above 0.5 and those below 0.5. In the mock treated samples, all cells had an average Pearson's Correlation Coefficient at or above 0.5. However, following siRNA depletion of hnRNP A1, 7.7% of cells examined had Pearson's Correlation Coefficients that were below 0.5. Furthermore, this is reflected in the lower overall mean of Pearson's Correlation Coefficient following siRNA depletion of hnRNP A1 when data were combined (Figure 4.3). Taken together, this suggests that a minor change/shift may be occurring in heterochromatin structure or TERRA and TRF2 interaction at individual telomeres following depletion of hnRNP A1. However, this is a very preliminary finding and other factors, including cell cycle changes need to be accounted for.

hnRNP A1 does not influence TERRA levels

hnRNPs have previously been shown to influence TERRA stability, where siRNA silencing of individual hnRNPs increased TERRA levels (de Silanes et al., 2010). To determine whether our results were influenced by TERRA stability and/or transcription, we examined TERRA levels by RNA dot blot with and without siRNA depletion of hnRNP A1. We performed three independent experiments and observed no significant difference in TERRA RNA levels with decreased hnRNP A1 protein, suggesting that TERRA levels were not influenced by the depletion of hnRNP A1 at our time point (Figure 4.4).

A.

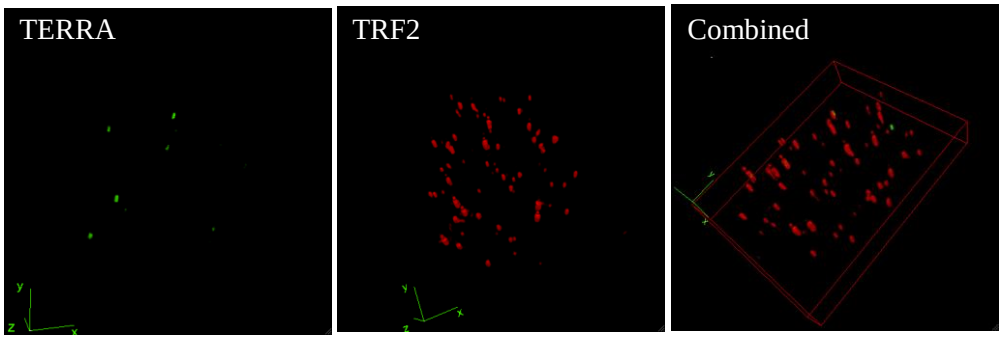

B.

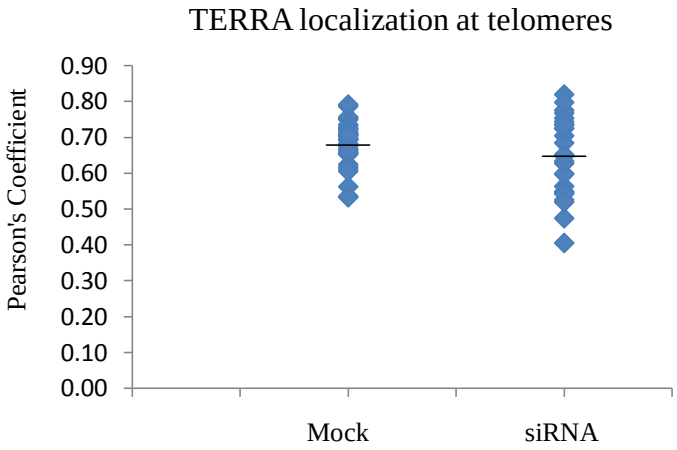

Figure 4.3. A) RNase treatment was done to confirm probe specificity to TERRA. B) The average Pearson's Correlation Coefficient per cell was plotted for mock and hnRNP A1 siRNA treated MCF7 cells. A slight decrease in the mean, represented by the horizontal bars, was observed and reflects a shift in overlap of TRF2 and TERRA following siRNA depletion of hnRNP A1 (right).

A.

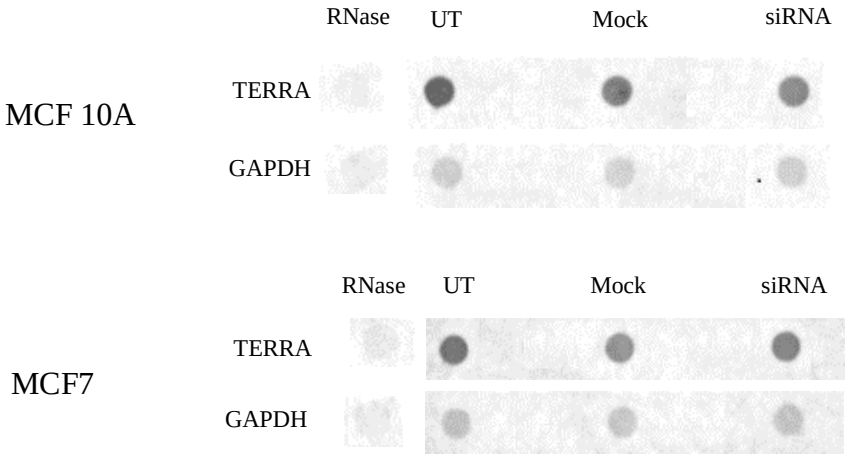

B.

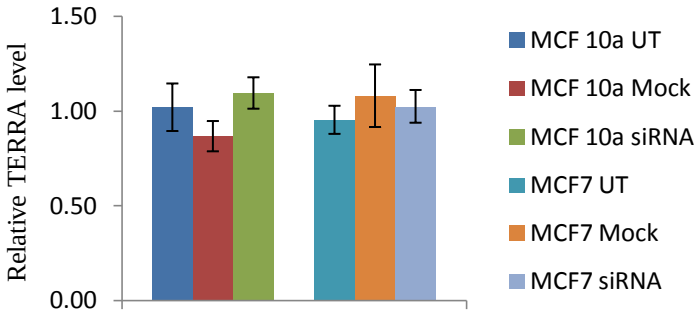

Figure 4.4. No significant change in TERRA levels following siRNA depletion of hnRNP A1 using RNA dot blot analysis. A) RNA dot blots were done using probes specific to TERRA and GAPDH and imaged using Storm imager. RNase treatement was used as a control to show probe specifically labeled RNA. B) TERRA levels relative to GAPDH housekeeping were averaged from three independent experiments. No significant change in TERRA levels was seen between untreated (UT), mock and siRNA in either cell line.

Silencing of hnRNP A1 results in "fragile" telomeres

Previous reports suggest a role for hnRNP A1 in telomere lengthening (Zhang et al., 2006). To evaluate the role of hnRNP A1 in telomere function, we performed FISH following siRNA knockdown of hnRNP A1 in MCF7 and MCF 10a cell lines and scored telomere-, chromatid- and chromosomal-type aberrations. A total of three independent siRNA transfections and metaphase harvests were performed; immunoblotting analysis confirmed efficient knock down of hnRNP A1. The tumorigenic MCF7 cell line displayed increased chromatid-type, chromosomal-type aberrations and interstitial telomere sequences (ITS) in comparison to the non-tumorigenic MCF 10a cell line (data not shown). However, there was no significant increase in these aberration frequencies following hnRNP A1 siRNA treatment. Both MCF 10a and MCF7 cell lines exhibited a clonal aberration involving telomere-ends, seen as two interstitial telomere sequences (Figure 4.5). Most striking was a significant increase in "fragile" telomeres, as previously termed (Figure 4.6) (Sfeir et al., 2009). Here we specifically define "fragile" telomeres as those that exhibit double telomere signals or one extended (stretched out) signal on a single chromatid, where a single punctate signal would normally be seen (Figure 4.5). This phenotype is indicative of aberrant telomere replication and implicates hnRNP A1 in efficient telomere replication. hnRNP A1 has been associated with increased telomerase activity and telomere length (LaBranche et al., 1998; Zhang et al., 2006). However, we did not observe an overall increase in signal free ends (SFE) following siRNA silencing of hnRNP A1 (data not shown). This may be due to our short time course of siRNA depletion, as multiple rounds of replication necessary to visualize telomere shortening was not allowed.

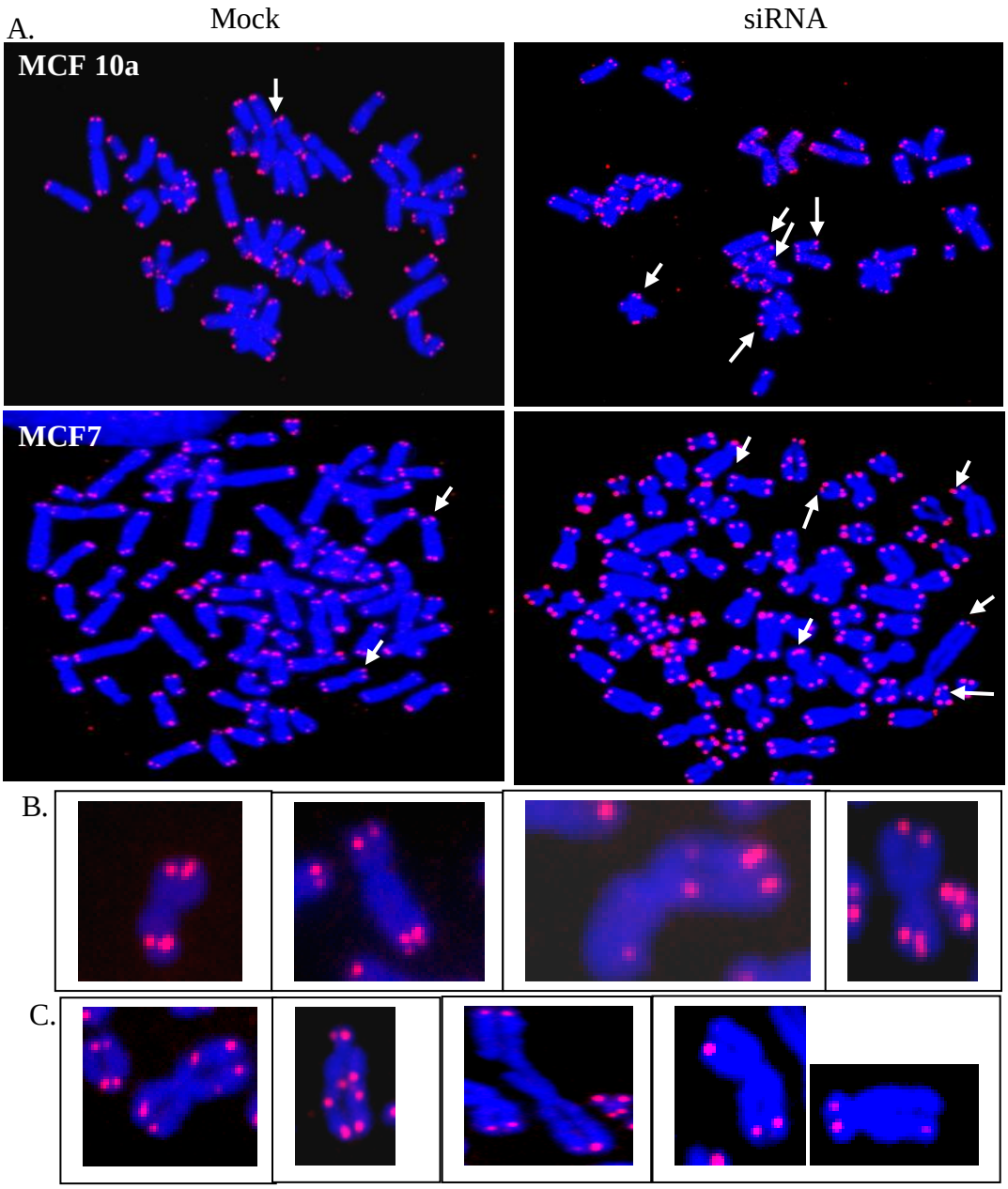

Figure 4.5. A) FISH using a G-rich, telomere specific PNA probe in MCF 10a and MCF7 metaphases. An increase in "fragile" telomeres was observed following siRNA treatment of hnRNP A1 (arrows). B) Examples of "fragile" telomeres. These were defined as a doublet signal, also called telomere duplications, or one extended signal on a single chromatid. C) Common aberrations observed in the MCF7 cell line. Aberrations include a clonal single interstitial telomere sequence on both chromatid arms, two clonal interstitial telomere sequences on each chromatid arm, a chromatid break and signal free ends.

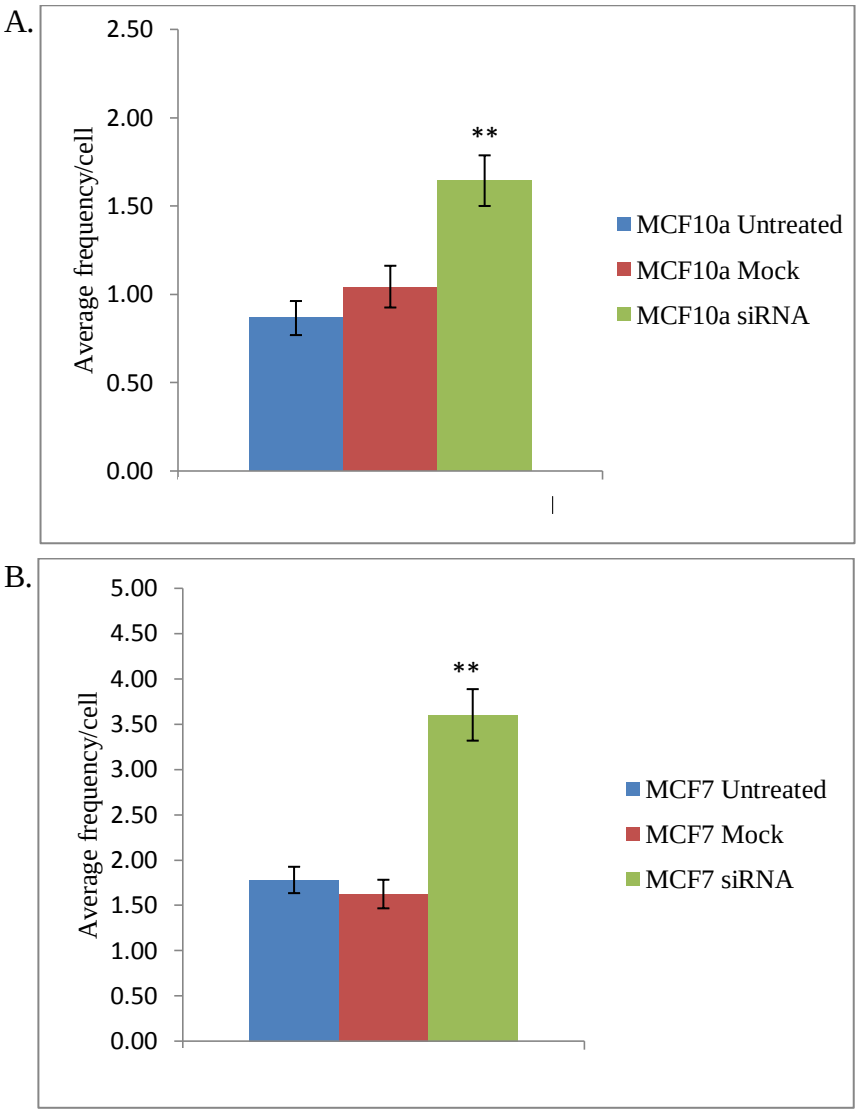

Figure 4.6. A) Increased frequency of "fragile" telomeres in MCF 10a cell line following siRNA of hnRNP A1 in comparison with mock treated or untreated samples ($p<0.01$). B) Increased frequency of "fragile" telomeres in MCF7 cells with siRNA depletion of hnRNP A1. Statistical analysis was done using student T-tests, and error bars represent standard error of the mean (SEM).

siRNA silencing of hnRNP A1 leads to increased Telomere Sister Chromatid Exchange (T-SCE) frequency

An increase in recombination has been reported at common fragile sites (Feichtinger and Schmid, 1989; Glover and Stein, 1987). Although telomeres are not historically defined as a "common" fragile site (Le Beau, 1986; Sutherland and Richards, 1995), we further analyzed telomere integrity by performing two-color CO-FISH. Data were collected from three independent siRNA transfections and metaphase harvests. We observed an increase, approaching significance, in Telomere Sister Chromatid Exchange (T-SCE) frequency following siRNA knockdown of hnRNP A1 as compared to mock or untreated cells in the MCF7 cell line (Figure 4.7). This finding adds additional support to our conclusions in that the loss of hnRNP A1 influences telomere replication, evidenced by increased "fragile" telomeres and increased T-SCE. We note that increased T-SCE frequencies following hnRNP A1 siRNA depletion was not seen in MCF 10a cells. However, this was partly due to the very low frequency of T-SCE observed in general, where only five were seen in the untreated samples when scoring 90 metaphases. It is also likely that MCF7 and MCF 10a cells retain normal telomere regulation of Protection of Telomeres 1 (POT 1) and TRF 2 levels, which have been shown to repress T-SCE frequencies (Celli et al., 2006; Palm et al., 2009). Of the "fragile" telomeres that were observed, a slight, but not significant, bias toward telomeres produced via lagging strand synthesis (FITC-labelled C-rich probe, data not shown) was noted in the MCF7 cell line. Similar to the FISH data, we saw no increase in SFE. However, we observed a greater, not significant, increase in SFE using the Cy-3 probe in all three treatments in comparison to SFE using the FITC probe. This suggests that the differences we observed

A.

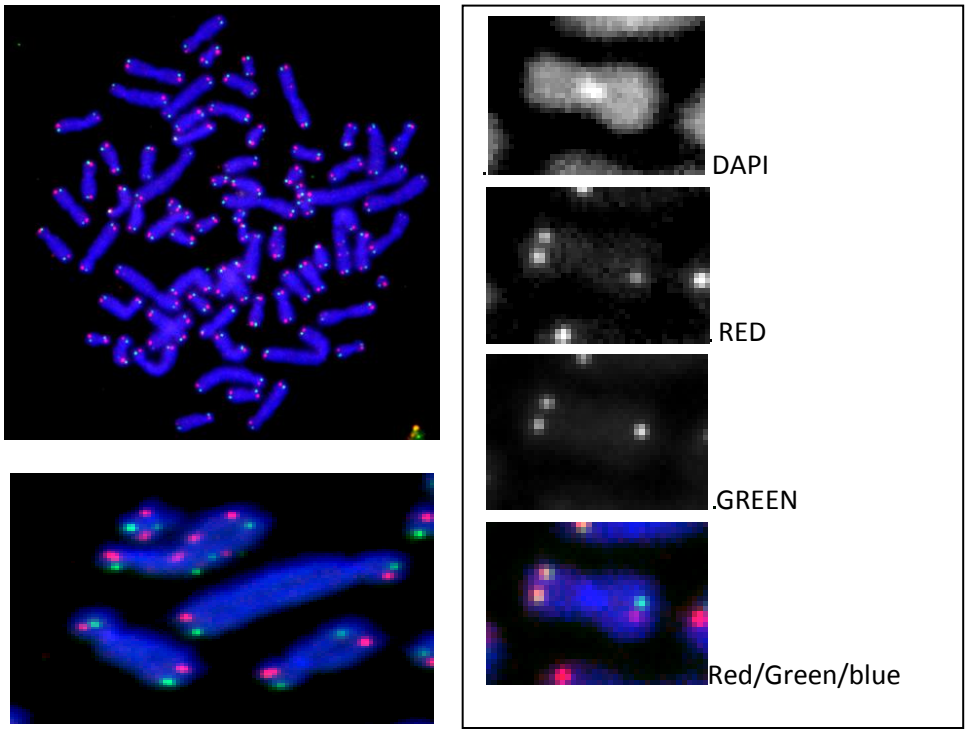

B.

Sample	# T-SCE	T-SCE/Cell	T-SCE/chromosome #
MCF7 Untreated	23	0.256	0.004
MCF7 Mock	23	0.256	0.004
MCF7 siRNA	43	0.478	0.007
MCF 10a Untreated	5	0.056	0.001
MCF 10a Mock	3	0.033	0.001
MCF 10a siRNA	6	0.067	0.001

Figure 4.7. Increased T-SCE frequency in MCF7 cell line following siRNA depletion of hnRNP A1. A). Representative images of 2-color CO-FISH done in MCF7 cells. Panel on the right depicts T-SCE, where an exchange of both telomere sister chromatids was observed (yellow). B) T-SCE frequency in MCF7 cells and MCF 10a cells. T-SCE increases following siRNA of hnRNP A1 in MCF7 cells. This increase was not quite significant (p=0.09) in MCF7 cells. Little difference was observed in T-SCE frequency in the MCF 10a cell line. However, this may be due to the overall low background level of T-SCE. Statistical analysis was performed using Student T-tests.

were largely a reflection of probe and fluor efficiency in binding and not a true difference in strand specificity. Furthermore, the MCF 10a cell line did not exhibit a preference for a strand specific involvement in "fragile" telomeres. Taken together, we conclude that additional studies will be required to confirm/establish any strand-specificity or preference in the "fragile" telomere phenotype. Our results suggest that the "fragile" telomere phenotype was not strand specific.

Discussion

In this study, we show that the RNA binding protein hnRNP A1 is not essential for TERRA localization at mammalian telomere ends. We utilized a novel 3-D reconstruction strategy to evaluate co-localization of TERRA and TRF2 foci to examine this association. Similar to de Silanes et al. studies (de Silanes et al., 2010), we found no change in the localization pattern of TERRA at telomeres with reduced hnRNP A1 levels. However, using our 3-D imaging technique, we did observe a shift in TERRA/TRF2 interaction at individual telomeres, as reflected in a lower Pearson's Correlation Coefficient, following siRNA depletion of hnRNP A1. This change may be due to changes in telomeric heterochromatin or a change in the interaction between TERRA and telomere ends (TRF2). In the de Silanes et al. study other members of the hnRNP family were also examined and shown to affect the localization of TERRA at telomeres, including hnRNP F, hnRNP M, hnRNP A2/B1and hnRNP D/AUF1 (de Silanes et al., 2010). siRNA depletion of these hnRNPs increased the percent colocalization of TERRA with telomeres. They suggested this was due to the role of hnRNPs in repressing TERRA stability through their involvement in pre-mRNA cleavage. We cannot exclude

redundancy in function between the hnRNPs. For example although hnRNP A1 plays a critical role in mRNA splicing and shuttling, it is not essential for cell growth (Ben-David et al., 1992), suggesting other hnRNPs may also be involved in this function. Another possibility would be that hnRNP A1 is not completely silenced in our experiments. However, because our siRNA knockdown efficiency was high, ~90%, we find this unlikely.

hnRNPs have been suggested to influence TERRA RNA stability, where loss of hnRNPs resulted in an increase in TERRA RNA levels (de Silanes et al., 2010). In order to examine if hnRNP A1 affected total TERRA expression levels, we performed RNA dot blots following siRNA silencing of hnRNP A1. We observed no changes in TERRA RNA levels following hnRNP A1 depletion (Figure 4.4). In contrast to the de Silanes studies, we did not examine changes in TERRA RNA levels at different time points following transcription inhibition. Therefore our results do not argue against a possible role for hnRNP A1 in enhancing TERRA RNA stability. Rather, this suggests that hnRNP A1 depletion does not affect TERRA RNA levels at 72 hours post treatment. In addition, in the de Silanes study, the observed increase in TERRA levels following the specific inhibition of hnRNP A1 was nominal and not significant. This suggests that of the hnRNPs, perhaps hnRNP A1 plays only a minimal role in TERRA stability.

Because hnRNP A1 has been shown to influence telomere length and telomerase activity (Zhang et al., 2006), we also examined telomere function following siRNA silencing of hnRNP A1. We provide evidence that hnRNP A1 plays an important role in the efficient replication of telomeres in human mammary epithelial cells. We observed a significant increase in duplicated telomere signals or a single extended telomere signal,

previously termed “fragile” telomeres, in hnRNP A1 depleted cells (Sfeir et al., 2009). Sfeir et al. showed that this phenotype resembled that which is commonly seen when cells are treated with amphidicolin, a DNA polymerase-α inhibitor, thus further linking this phenotype to replication. An increase in sister chromatid recombination has previously been observed at fragile sites (Feichtinger and Schmid, 1989; Glover and Stein, 1987). An increase in exchange frequency has been proposed to result from unreplicated single stranded regions created by stalled fork progression (Painter, 1980). In this model, cells treated with agents that reduce fork progression maintain either single stranded regions or regions that replicate late in the cell cycle and have not fully condensed, making the area prone to exchanges. Consistent with this view, we observed an increase in T-SCE frequency that approached significance following siRNA treatment of hnRNP A1 in MCF7 cells. We observed little to no change in T-SCE frequencies in the MCF 10a cell line. However, this may be due to the overall low levels of T-SCE in the MCF 10a cell line. Because of this low number, a large number of metaphases may have to be analyzed before any difference in T-SCE frequency can be definitely determined. Furthermore, the low number of T-SCE frequency in MCF 10a, as well as the relatively low frequency in MCF7, may reflect other factors that regulate telomere recombination. For example, POT 1 and TRF2 have also been shown to repress T-SCE events (Celli et al., 2006; Palm et al., 2009).

A role for hnRNP A1 in telomere replication has recently been suggested, as hnRNP A1 was observed to play a role in the removal of Replication Protein A (RPA) from telomere ends, thereby allowing access for Protection Of Telomeres 1 (POT 1) binding (Flynn et al., 2011). An increase in telomere induced foci (TIF) has previously

been observed following siRNA of hnRNP A1, suggesting that removal of this hnRNP A1 initiates a damage response (de Silanes et al., 2010). RPA is vital in the activation of Ataxia-Telagectasia mutated and Rad 3 related (ATR) pathway, and it has been suggested that binding of POT 1 blocks access to RPA, preventing the activation of ATR signaling at telomere ends (Gong and de Lange, 2010). hnRNP A1 has also been shown to unwind G-quadruplex structures, common in G-rich sequences (Fukuda et al., 2002; Zhang et al., 2006), such as telomeres. Therefore, hnRNP A1 may act to allow access to replication proteins during telomere replication.

The question of how TERRA is associated with telomeres is poorly understood and an active area of investigation. Other members of hnRNP family have been implicated (de Silanes et al., 2010). Possible TERRA associations with Shelterin, the complex of proteins involved in protecting telomeres and t-loop formation (Griffith et al., 1999), have also been suggested and may involve TRF1 and/or TRF2 (Deng et al., 2009). Here, we demonstrate that hnRNP A1 is not necessary in TERRA localization at telomeres, and hnRNP A1 does not influence overall TERRA levels. In addition, we show hnRNP A1 is important in efficient telomere replication.

Acknowledgements

We thank Andrea Herdon and Alena Campbell for their assistance in imaging and microscopy work. We would also like to thank Dr. Jerry Shay for the generous donation of BJ1 cells and BJ-hTERT cell line used in this study. We also thank Laura Chubb for the generous donation of the MCF7 cell line.

References

Anders, K.R., Grimson, A., and Anderson, P. (2003). SMG-5, required for C.elegans nonsense-mediated mRNA decay, associates with SMG-2 and protein phosphatase 2A. Embo J *22*, 641-650.

Azzalin, C.M., Reichenbach, P., Khoriauli, L., Giulotto, E., and Lingner, J. (2007). Telomeric repeat containing RNA and RNA surveillance factors at mammalian chromosome ends. Science *318*, 798-801.

Ben-David, Y., Bani, M.R., Chabot, B., De Koven, A., and Bernstein, A. (1992). Retroviral insertions downstream of the heterogeneous nuclear ribonucleoprotein A1 gene in erythroleukemia cells: evidence that A1 is not essential for cell growth. Mol Cell Biol *12*, 4449-4455.

Beyer, A.L., Christensen, M.E., Walker, B.W., and LeStourgeon, W.M. (1977). Identification and characterization of the packaging proteins of core 40S hnRNP particles. Cell *11*, 127-138.

Bolte, S., and Cordelieres, F.P. (2006). A guided tour into subcellular colocalization analysis in light microscopy. J Microsc *224*, 213-232.

Boukakis, G., Patrinou-Georgoula, M., Lekarakou, M., Valavanis, C., and Guialis, A. Deregulated expression of hnRNP A/B proteins in human non-small cell lung cancer: parallel assessment of protein and mRNA levels in paired tumour/non-tumour tissues. BMC Cancer *10*, 434.

Burd, C.G., and Dreyfuss, G. (1994). RNA binding specificity of hnRNP A1: significance of hnRNP A1 high-affinity binding sites in pre-mRNA splicing. Embo J *13*, 1197-1204.

Celli, G.B., Denchi, E.L., and de Lange, T. (2006). Ku70 stimulates fusion of dysfunctional telomeres yet protects chromosome ends from homologous recombination. Nat Cell Biol *8*, 885-890.

Chiu, S.Y., Serin, G., Ohara, O., and Maquat, L.E. (2003). Characterization of human Smg5/7a: a protein with similarities to Caenorhabditis elegans SMG5 and SMG7 that functions in the dephosphorylation of Upf1. Rna *9*, 77-87.

Dallaire, F., Dupuis, S., Fiset, S., and Chabot, B. (2000). Heterogeneous nuclear ribonucleoprotein A1 and UP1 protect mammalian telomeric repeats and modulate telomere replication in vitro. J Biol Chem *275*, 14509-14516.

de Silanes, I.L., d'Alcontres, M.S., and Blasco, M.A. (2010). TERRA transcripts are bound by a complex array of RNA-binding proteins. Nat Commun *1*, 33.

Deng, Z., Norseen, J., Wiedmer, A., Riethman, H., and Lieberman, P.M. (2009). TERRA RNA binding to TRF2 facilitates heterochromatin formation and ORC recruitment at telomeres. Mol Cell *35*, 403-413.

Feichtinger, W., and Schmid, M. (1989). Increased frequencies of sister chromatid exchanges at common fragile sites (1)(q42) and (19)(q13). Hum Genet *83*, 145-147.

Flynn, R.L., Centore, R.C., O'Sullivan, R.J., Rai, R., Tse, A., Songyang, Z., Chang, S., Karlseder, J., and Zou, L. (2011). TERRA and hnRNPA1 orchestrate an RPA-to-POT1 switch on telomeric single-stranded DNA. Nature *471*, 532-536.

Ford, L.P., Wright, W.E., and Shay, J.W. (2002). A model for heterogeneous nuclear ribonucleoproteins in telomere and telomerase regulation. Oncogene *21*, 580-583.

Fukuda, H., Katahira, M., Tsuchiya, N., Enokizono, Y., Sugimura, T., Nagao, M., and Nakagama, H. (2002). Unfolding of quadruplex structure in the G-rich strand of the minisatellite repeat by the binding protein UP1. Proc Natl Acad Sci U S A *99*, 12685-12690.

Gatfield, D., Unterholzner, L., Ciccarelli, F.D., Bork, P., and Izaurralde, E. (2003). Nonsense-mediated mRNA decay in Drosophila: at the intersection of the yeast and mammalian pathways. Embo J *22*, 3960-3970.

Glover, T.W., and Stein, C.K. (1987). Induction of sister chromatid exchanges at common fragile sites. Am J Hum Genet *41*, 882-890.

Gong, Y., and de Lange, T. (2010). A Shld1-controlled POT1a provides support for repression of ATR signaling at telomeres through RPA exclusion. Mol Cell *40*, 377-387.

Griffith, J.D., Comeau, L., Rosenfield, S., Stansel, R.M., Bianchi, A., Moss, H., and de Lange, T. (1999). Mammalian telomeres end in a large duplex loop. Cell *97*, 503-514.

Hamilton, B.J., Burns, C.M., Nichols, R.C., and Rigby, W.F. (1997). Modulation of AUUUA response element binding by heterogeneous nuclear ribonucleoprotein A1 in human T lymphocytes. The roles of cytoplasmic location, transcription, and phosphorylation. J Biol Chem *272*, 28732-28741.

He, Y., Brown, M.A., Rothnagel, J.A., Saunders, N.A., and Smith, R. (2005). Roles of heterogeneous nuclear ribonucleoproteins A and B in cell proliferation. J Cell Sci *118*, 3173-3183.

Henegariu, O., Heerema, N.A., Lowe Wright, L., Bray-Ward, P., Ward, D.C., and Vance, G.H. (2001). Improvements in cytogenetic slide preparation: controlled chromosome spreading, chemical aging and gradual denaturing. Cytometry *43*, 101-109.

Ivessa, A.S., Zhou, J.Q., Schulz, V.P., Monson, E.K., and Zakian, V.A. (2002). Saccharomyces Rrm3p, a 5' to 3' DNA helicase that promotes replication fork progression through telomeric and subtelomeric DNA. Genes Dev *16*, 1383-1396.

Ivessa, A.S., Zhou, J.Q., and Zakian, V.A. (2000). The Saccharomyces Pif1p DNA helicase and the highly related Rrm3p have opposite effects on replication fork progression in ribosomal DNA. Cell *100*, 479-489.

Kafatos, F.C., Jones, C.W., and Efstratiadis, A. (1979). Determination of nucleic acid sequence homologies and relative concentrations by a dot hybridization procedure. Nucleic Acids Res *7*, 1541-1552.

LaBranche, H., Dupuis, S., Ben-David, Y., Bani, M.R., Wellinger, R.J., and Chabot, B. (1998). Telomere elongation by hnRNP A1 and a derivative that interacts with telomeric repeats and telomerase. Nat Genet *19*, 199-202.

Le Beau, M.M. (1986). Chromosomal fragile sites and cancer-specific rearrangements. Blood *67*, 849-858.

Ma, Y.L., Peng, J.Y., Zhang, P., Huang, L., Liu, W.J., Shen, T.Y., Chen, H.Q., Zhou, Y.K., Zhang, M., Chu, Z.X., *et al.* (2009). Heterogeneous nuclear ribonucleoprotein A1 is identified as a potential biomarker for colorectal cancer based on differential proteomics technology. J Proteome Res *8*, 4525-4535.

Makovets, S., Herskowitz, I., and Blackburn, E.H. (2004). Anatomy and dynamics of DNA replication fork movement in yeast telomeric regions. Mol Cell Biol *24*, 4019-4031.

Martinez-Contreras, R., Cloutier, P., Shkreta, L., Fisette, J.F., Revil, T., and Chabot, B. (2007). hnRNP proteins and splicing control. Adv Exp Med Biol *623*, 123-147.

Mayeda, A., and Krainer, A.R. (1992). Regulation of alternative pre-mRNA splicing by hnRNP A1 and splicing factor SF2. Cell *68*, 365-375.

McClintock, B. (1939). The Behavior in Successive Nuclear Divisions of a Chromosome Broken at Meiosis. Proc Natl Acad Sci U S A *25*, 405-416.

Moyzis, R.K., Buckingham, J.M., Cram, L.S., Dani, M., Deaven, L.L., Jones, M.D., Meyne, J., Ratliff, R.L., and Wu, J.R. (1988). A highly conserved repetitive DNA sequence, (TTAGGG)n, present at the telomeres of human chromosomes. Proc Natl Acad Sci U S A *85*, 6622-6626.

Page, M.F., Carr, B., Anders, K.R., Grimson, A., and Anderson, P. (1999). SMG-2 is a phosphorylated protein required for mRNA surveillance in Caenorhabditis elegans and related to Upf1p of yeast. Mol Cell Biol *19*, 5943-5951.

Painter, R.B. (1980). A replication model for sister-chromatid exchange. Mutat Res *70*, 337-341.

Palm, W., Hockemeyer, D., Kibe, T., and de Lange, T. (2009). Functional dissection of human and mouse POT1 proteins. Mol Cell Biol *29*, 471-482.

Reichenbach, P., Hoss, M., Azzalin, C.M., Nabholz, M., Bucher, P., and Lingner, J. (2003). A human homolog of yeast Est1 associates with telomerase and uncaps chromosome ends when overexpressed. Curr Biol *13*, 568-574.

Schoeftner, S., and Blasco, M.A. (2008). Developmentally regulated transcription of mammalian telomeres by DNA-dependent RNA polymerase II. Nat Cell Biol *10*, 228-236.

Sfeir, A., Kosiyatrakul, S.T., Hockemeyer, D., MacRae, S.L., Karlseder, J., Schildkraut, C.L., and de Lange, T. (2009). Mammalian telomeres resemble fragile sites and require TRF1 for efficient replication. Cell *138*, 90-103.

Sutherland, G.R., and Richards, R.I. (1995). The molecular basis of fragile sites in human chromosomes. Curr Opin Genet Dev *5*, 323-327.

Watson, J.D. (1972). Origin of concatemeric T7 DNA. Nat New Biol *239*, 197-201.

Xu, Y., Suzuki, Y., Ito, K., and Komiyama, M. (2010). Telomeric repeat-containing RNA structure in living cells. Proc Natl Acad Sci U S A *107*, 14579-14584.

Xu, Y., Suzuki, Y., Kaminaga, K., and Komiyama, M. (2009). Molecular basis of human telomere DNA/RNA structure and its potential application. Nucleic Acids Symp Ser (Oxf), 63-64.

Yehezkel, S., Segev, Y., Viegas-Pequignot, E., Skorecki, K., and Selig, S. (2008). Hypomethylation of subtelomeric regions in ICF syndrome is associated with abnormally short telomeres and enhanced transcription from telomeric regions. Hum Mol Genet *17*, 2776-2789.

Zhang, Q.S., Manche, L., Xu, R.M., and Krainer, A.R. (2006). hnRNP A1 associates with telomere ends and stimulates telomerase activity. Rna *12*, 1116-1128.

CHAPTER 5

CONCLUSIONS AND DISCUSSION

Overrview

Since Barbara McClintock and Herman Muller first identified telomeres, researchers have been seeking to define the mechanisms that maintain these unique structures and their critical functions (McClintock, 1941; Muller, 1938). With the identification of telomerase (Greider and Blackburn, 1985), the enzyme that extends telomere sequences, and its upregulation in cancer (Kim et al., 1994), the telomere biology field quickly expanded into and integrated with cancer research. The field continues to evolve as evidenced by the recent discovery of Telomere Repeat-containing RNA or Telomeric RNA (TERRA/TelRNA), which is transcribed from the telomere sequence (Azzalin et al., 2007; Schoeftner and Blasco, 2008). Telomere structure and function is maintained by a complex of proteins termed Shelterin, a host of associated proteins (de Lange, 2005). Critical loss of telomere length and/or the disruption of the telomere structure may result in chromosomal fusions and contribute to carcinogenesis. In these studies, we investigated the mechanisms of human telomere structure and function.

The goal of the studies presented here was to 1) investigate the role of telomeres in radiation induced murine Acute Myeloid Leukemia (AML), 2) examine the effects of DNA Protein Kinase catalytic subunit (DNA-PKcs) kinase activity on TERRA localization to telomeres and 3) characterize the role of heterogeneous ribonuclear protein A1 (hnRNP A1) in TERRA localization at telomeres and telomere function.

Increased genomic instability in radiation-induced murine AML

Chapter I described the dangers to astronauts during space travel, which includes exposure to highly ionizing, high energy (HZE) radiation. The risk of carcinogenesis due

to such a radiation exposure is largely uncertain. We provide evidence supportive of an association between genomic instability, seen as increased chromatid-type aberrations, and radiation-induced AML in CBA/Ca mice. Interestingly, increased frequencies of chromatid-type aberrations were specific to mice that developed AML and were seen in tumors following both ɣ- and ^{56}Fe ion exposure. These results suggest that the increased frequencies of chromatid-type aberrations were not influenced by radiation quality, but rather are linked with AML development itself. Furthermore, we observed an initial increase in chromatid-type aberrations in spleen colonies, using the Colony Forming Unit-Spleen (CFU-S) assay, suggesting that such instability may occur early in tumor initiation. Chromatid-type aberration frequencies were not significantly different in ɣ- or (1 GeV/n) ^{56}Fe-induced AML tumor samples. A slight relative biological effectiveness (RBE) was seen when examining AML induction following ɣ- or (1GeV/n) ^{56}Fe irradiation in CBA/CaJ mice (Weil et al., 2009).

We observed little to no change in the frequency of telomere aberrations in murine AML tumor samples. Critically short telomeres have frequently been observed in carcinogenesis (Gisselsson et al., 2001). However, active telomerase in mice masks such telomere defects (Chadeneau et al., 1995; Prowse and Greider, 1995). Therefore, we also examined two human AML cell lines, KG-1a and UoC-M1. We observed a clonal aberration in the KG-1a cell line involving interstital telomeres. Evidence suggests that this telomere fusion event involves chromosomes 5 and 17 [(Mrozek et al., 2003) and personal correspondence with Michelle LeBeau]. This telomere fusion event provides evidence supporting the ability of a single dysfunctional telomere to contribute to

chromosomal instability and emphasizes the importance of functional telomere structure and function.

Implications and Future Directions

Because chromosomal instability was specifically linked to tumor samples, it is possible that such instability provides a valuable measure of risk for radiation-induced AML. However, in order to more confidently assess cancer risk following radiation exposure, a stronger prognostic assessment could be achieved through the combination of chromatid-type aberration induction and genomic changes, such as the loss of *PU.1* (Peng et al., 2009).

There is a vital need for a means to better assess AML risk following radiation exposure. In order to better define this risk, an assessment of chromatid-type aberrations in human radiation-induced AML is essential. ^{56}Fe exposure to humans is limited. Therefore, other types of radiation must be examined. For example, chromatid-type aberrations should be assessed in patients treated following radiotherapy. Patients that develop AML as a secondary cancer would need to be examined. Unfortunately, the collection of this data are confounded by chemotherapy.

The interactions of DNA dependent protein kinase catalytic subunit (DNA-PKcs), telomere repeat-containing RNA (TERRA), and heterogenous nuclear ribonucleoprotein A1 (hnRNP A1) in telomere function and structure

DNA-PKcs dependent phosphorylation of hnRNP A1

We confirmed decreased phosphorylation of hnRNP A1 following siRNA silencing of DNA-PKcs in two human mammary epithelial cell lines, MCF7 (tumorigenic) and MCF 10a (non-tumorigenic), by examining metabolic Phosphorus-32 (^{32}P) uptake followed by immunoprecipitation of hnRNP A1. We observed decreased phosphorylation of hnRNP A1 in MCF7 cells following inhibition of DNA-PKcs kinase activity with 2-(Morpholin-4-yl)-benzo[h]chromen-4-one (NU7026) but did not see a significant change in hnRNP A1 phosphorylation in MCF 10a cells. This finding is consistent with the previous observation that DNA-PKcs phosphorylation of hnRNP A1 is influenced by the presence of the human telomerase RNA component (hTR) (Ting et al., 2009), and MCF 10a cells have been shown to have decreased hTR expression and telomerase activity (Ramachandran et al., 2002). Furthermore, the decrease in ^{32}P-labelled hnRNP A1 following siRNA silencing of DNA-PKcs may be due to an indirect affect on related kinases, such as ATM (Peng et al., 2005). It is likely that other kinases target hnRNP A1, as ^{32}P-labelled signal remains following the siRNA depletion of DNA-PKcs. Many kinases have been implicated in phosphorylating hnRNP A1, including protein kinase A (Cobianchi et al., 1993), p38 MAP kinase (Shimada et al., 2009), protein kinase C (Municio et al., 1995) and casein kinase (Gao et al., 2000).

DNA-PKcs kinase activity and TERRA localization at telomeres

DNA-PKcs has previously been shown to phosphorylate hnRNP A1 (Ting et al., 2009; Zhang et al., 2004) and play a role in telomere end capping function (Bailey et al., 2004; Bailey et al., 1999). We, therefore, also examined the affects of DNA-PKcs kinase activity on the localization of TERRA to telomeres, hypothesizing a mechanism of action through hnRNP A1.

siRNA depletion of DNA-PKcs has been previously shown to also decrease levels of ATM (Peng et al., 2005). We, therefore, treated cells with NU7026, a specific DNA-PKcs kinase activity inhibitor at low concentrations (Hollick et al., 2003) and examined TERRA localization at telomeres. We combined RNA Fluorescence *In Situ* Hybridization (FISH) and immunocytochemistry (ICC) with a probe specific to TERRA and an antibody against telomere repeat factor 2 (TRF2). We did not observe a significant change in TERRA localization to telomeres following NU7026 treatment in the MCF7 cell line. These results suggest that DNA-PKcs kinase activity is not required for TERRA localization at telomeres. Interestingly, we did observe a slight decrease in TRF2 and TERRA foci overlap at individual telomeres following DNA-PKcs kinase inhibition. This was observed both visually and by a lower Pearson's Correlation Coefficient when using 3-D imaging. This suggests that DNA-PKcs may indirectly facilitate telomeric heterochromatin or TERRA/TRF2 interaction. These findings are preliminary and more research is needed in order to explore this possible interaction.

TERRA levels decrease following DNA-PKcs kinase inhibition

We examined overall effects on TERRA levels following DNA-PKcs kinase activity inhibition using RNA dot blots. TERRA levels in the MCF 10a cell line were sensitive to Dimethyl Sulfoxide (DMSO) treatment, as TERRA levels were decreased in both the DMSO control and NU7026 treated. However, we observed little to no change in TERRA levels following kinase inhibition in the MCF 10a cell line. Various members of the hnRNPs have been implicated in TERRA stability, where loss of hnRNP F led to increased levels of TERRA (de Silanes et al., 2010). This was believed to be due to the role of hnRNP F in pre-mRNA cleavage. Similarly, hnRNP A1 also plays a role in pre-mRNA processing (He and Smith, 2009). Because transcription has been shown to be affected by DNA-PKcs (Chibazakura et al., 1997; Dvir et al., 1992; Peterson et al., 1992; Peterson et al., 1995; Sheppard and Liu, 2000) and hnRNP A1 mRNA binding affected by phosphorylation (Buxade et al., 2005), decreases in TERRA levels following DNA-PKcs kinase inhibition in the MCF7 cell line may be due to a combination of decreased transcription and decreased hnRNP A1 interaction with TERRA (Figure 5.1).

The role of hnRNP A1 in telomere structure and function

hnRNP A1 is not necessary for TERRA localization at telomeres

Because hnRNP A1 preferentially binds UUAGGG/U sequences (Burd and Dreyfuss, 1994) and has been shown to play a role in telomere biology (Zhang et al., 2006), we hypothesized that hnRNP A1 plays a role in "tethering" TERRA at telomere ends. In support of this, recent evidence has demonstrated the *in* vivo interaction of

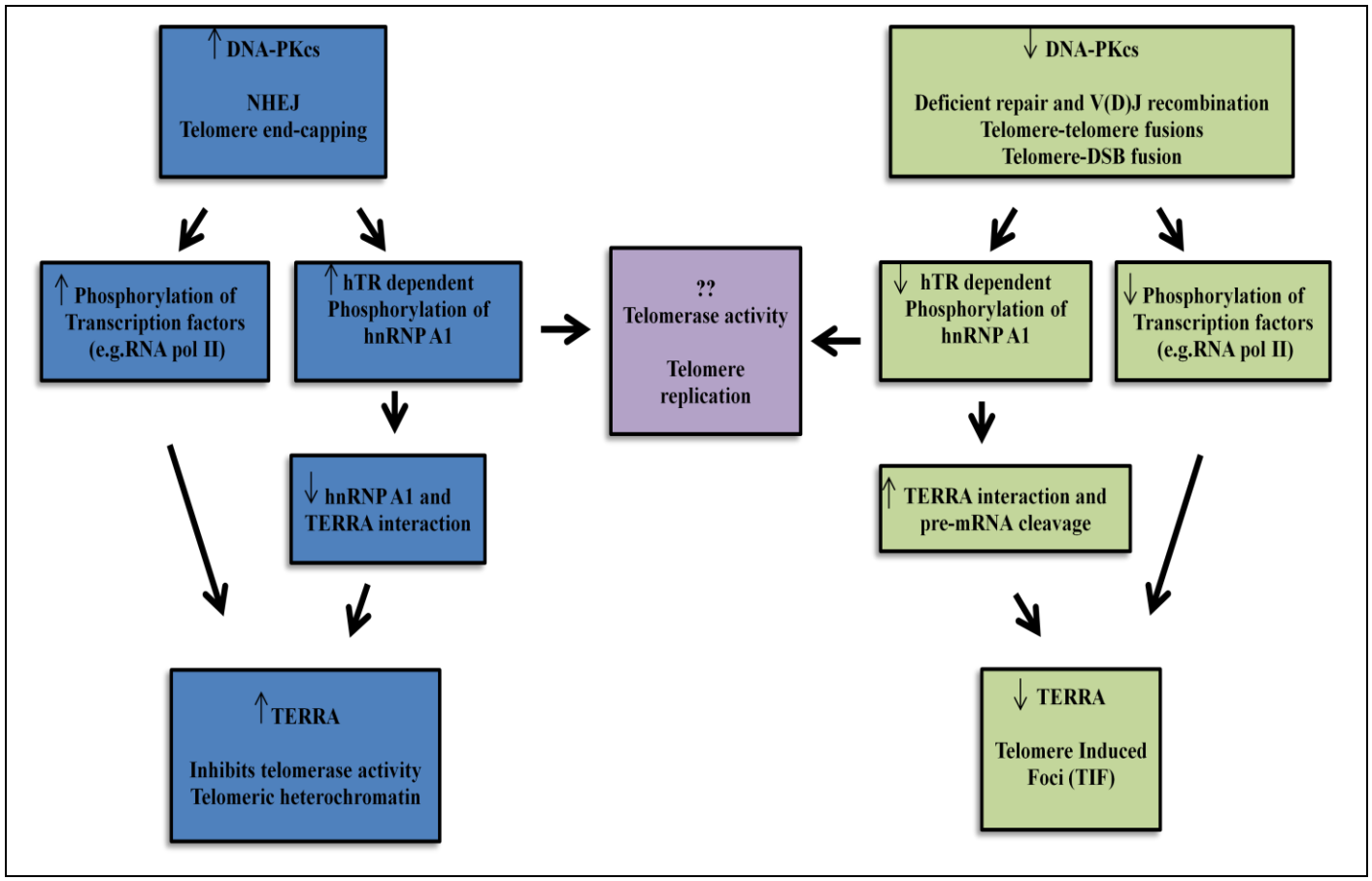

Figure 5.1. Diagram depicting DNA-PKcs, hnRNP A1 and TERRA interactions. The hTR dependent phosphorylation of hnRNP A1 by DNA-PKcs leads to decreased hnRNP A1 interaction. hnRNP A1 has been shown to enhance telomerase activity, and we propose it is important in efficient telomere replication. Furthermore, DNA-PKcs kinase activity may be important in regulating TERRA levels through its roles in transcription. Future directions include examining how DNA-PKcs dependent (de)-phosphorylation of hnRNP A1 affects telomerase activity and/or replication.

hnRNP A1 with TERRA (de Silanes et al., 2010). We investigated the role of hnRNP A1 in TERRA localization at telomeres by combining RNA FISH with ICC using a probe specific to TERRA and an antibody toward TRF2. In order to evaluate the role of hnRNP A1 in TERRA localization, we targeted hnRNP A1 using small interfering (si) RNA transfection with an oligonucleotide specific to hnRNP A1. We saw little to no change in TERRA localization at telomeres, suggesting that hnRNP A1 is not necessary in TERRA localization at telomere ends. However, we cannot exclude redundancy in function among the hnRNP family of proteins, as supported by data showing that cells may still proliferate with silencing of hnRNP A1 although it plays a vital role in mRNA splicing (Ben-David et al., 1992). This is suggested in the Silanes et al. study, where siRNA depletion of other hnRNP members led to a significant increase in TERRA localization to telomeres, including hnRNP F, hnRNP M, hnRNP A2/B1 and hnRNP A1 and D/AUF1 (de Silanes et al., 2010).

Interestingly, we did observe minor decreases in TRF2 and TERRA overlap using our 3-D imaging technique following siRNA targeting of hnRNP A1 in colocalized foci. This was reflected in a decreased average of Pearson's Correlation Coefficient for a small subset of the cells and suggests a possible shift in telomeric heterochromatin structure and/or TERRA and telomere (TRF2) interactions. In addition, we observed a similar, less dramatic, change in TERRA and TRF2 foci overlap following DNA-PKcs kinase inhibition. This suggests that this decrease in TRF2 and TERRA foci overlap may be due to changes targeting hnRNP A1, where its depletion leads to a more notable change. These preliminary results imply that hnRNP A1 may function to facilitate telomeric heterochromatin structure or the interaction of TERRA with telomeres (TRF2). More

research is required, as we cannot discount changes in cell cycle, where heterochromatin structure naturally shifts. Telomeres of replicating cells in S-phase would be expected to lose telomere associated proteins due to unraveling of the telomere structure to allow access of replication machinery. Because TERRA is found to be decreased during S-phase (Flynn et al., 2011; Porro et al.), we are naturally selecting cells outside of S-phase. However, we cannot disregard the concern that we are not excluding cells in early S-phase, where shifts in heterochromatin and protein interactions may occur.

hnRNP A1 does not influence TERRA levels

A previous study found that TERRA levels increased with siRNA knockdown of various hnRNPs, particularly hnRNP F (de Silanes et al., 2010). We, therefore, examined TERRA levels following hnRNP A1 depletion but found no significant change in TERRA levels with decreased hnRNP A1. Similarly in the de Silanes et al. study, hnRNP A1 knock down showed only nominal effects on TERRA levels, where as hnRNP F exerted a stronger influence on TERRA levels (de Silanes et al., 2010).

Silencing of hnRNP A1 leads to "fragile" telomeres

Telomere replication is inherently difficult due to the highly repetitive sequence and propensity to form secondary structures, including G-quadruplex structures (Gilson and Geli, 2007). Recently, it was shown that TRF1 is required for efficient telomere replication, where conditional knockout of TRF1 led to a "fragile" telomere phenotype (Sfeir et al., 2009). This phenotype was also increased following treatment with

aphidicolin, a DNA polymerase α inhibitor, which is frequently used to identify common fragile sites.

In Chapter 4, we observed a similar "fragile" telomere phenotype following siRNA silencing of hnRNP A1 in two human mammary epithelial cell lines, defined as telomere duplicates or extended telomere signal on a single chromatid. hnRNP A1 has recently been proposed to be important in the displacement of Replication Protein A (RPA) at telomere ends (Flynn et al., 2011), providing one possible role for hnRNP A1 in replication. Another possible role for hnRNP A1 in replication may involve its role in unwinding G-quadruplex structures (Zhang et al., 2006). Here we propose that hnRNP A1 is important in efficient telomere replication. Furthermore, it is interesting to postulate that this interaction may be intimately linked to its ability to stimulate telomerase activity (Zhang et al., 2006), functioning to allow access to telomerase and/or recruit telomerase to telomere ends.

We observed a bias towards the "fragile" telomere phenotype in telomeres produced via lagging strand synthesis in MCF7 cells. We also noted an increase in signal free ends (SFE) involving the telomere produced via leading strand synthesis. Furthermore, the FITC-labeled C-rich probe that labels the telomeres produced via lagging strand synthesis has an inherently higher background than the Cy-3 fluor used in labeling the strand produced via leading strand synthesis. In addition, we did not observe a strand bias for the "fragile" telomere phenotype in the MCF 10a cell line. Taken together, our data suggests that the "fragile" telomere phenotype was not strand specific, and a similar conclusion was reached following conditional knockout of TRF1 (Sfeir et al., 2009). In order to confidently establish strand specificity, reversing the fluors, i.e.

label the G-rich probe with FITC and the C-rich probe with Cy-3, and re-examination of "fragile" telomeres would be necessary.

Future Directions

DNA-PKcs is an multifunctional protein involved in Non-Homologous End Joining (NHEJ) (Allalunis-Turner et al., 1995; Okayasu et al., 1998), DNA replication (Allen et al., 2011), telomere end-capping function (Bailey et al., 2001; Bailey et al., 1999) and transcription (Chibazakura et al., 1997; Peng et al., 2005; Peterson et al., 1995). We examined possible mechanisms underlying DNA-PKcs mediated telomere function. Although we did not observe decreased TERRA localization to telomere following either DNA-PKcs kinase activity inhibition or siRNA depletion of hnRNP A1, we did observe a decrease in the degree of overlap between TERRA and individual telomeres in MCF7 cells. We are actively collecting data in the MCF 10a cells. Our future directions include exploring this interaction. We found that DNA-PKcs does influence TERRA levels, therefore a future direction would be to determine how. One possible target is RNA polymerase II, a known phosphorylation target for DNA-PKcs (Dvir et al., 1992) which has been shown to partially transcribe TERRA (Azzalin et al., 2007; Schoeftner and Blasco, 2008). In order to examine this possibility, phosphorylation mutants of RNA polymerase II could be used to examine TERRA levels.

hnRNP A1 has been shown to bind TERRA *in vivo* and affect TERRA stability (de Silanes et al., 2010). We showed that hnRNP A1 was not necessary for the localization of TERRA at telomere ends. However, the question of whether or not hnRNP A1 affects the stability or the transcription of TERRA remains unanswered. In order to

examine this, one possible experiment would be to inhibit transcription via treatment with α-amanitin, an RNA polymerase II inhibitor combined with siRNA silencing of hnRNP A1, then examine TERRA expression over time. If hnRNP A1 indeed affects stability, one would imagine increased TERRA degradation over time in comparison to sample with normal hnRNP A1 expression. Furthermore, the question of whether phosphorylation of hnRNP A1 affects its binding to TERRA also remains unanswered. Use of phosphorylation mutants of hnRNP A1, such as those developed by Ting et al. (Ting et al., 2009) and performing gel shift assays in order to examine TERRA binding changes *in vitro* would be informative in this regard.

MicroRNA (miRNA) expression following hnRNP A1 depletion

The regulation of miRNA has recently been shown to influence telomeric heterochromatin structure (Benetti et al., 2008). In this study, a deficiency in dicer, a protein vital in mature miRNA processing (Grishok et al., 2001; Hutvagner et al., 2001; Ketting et al., 2001), led to increased levels of mir-290 that targeted and consequently silenced Retinoblastoma-like 2 protein (Rbl2) (Benetti et al., 2008). Decreased Rbl2, in turn, resulted in decreased DNA methyltransferases, decreased DNA methylation and increased telomeric recombination, suggesting telomere heterochromatin structure may be influenced by miRNA. LET-7 is a miRNA correlated with the development and terminal differentiation in caenorhabditis elegans (Reinhart et al., 2000) and a proposed tumor suppressor (Johnson et al., 2007; Yu et al., 2007). Because hnRNP A1 has also been shown to negatively regulate levels of LET- 7 by inhibiting pre-mature LET-7 processing (Michlewski and Caceres, 2010), we examined miRNA expression by miRNA

microarray analysis following siRNA depletion of hnRNP A1 in order to identify possible miRNA that may influence telomere function and/or structure (listed in Appendix II). We observed no significant changes in miRNA expression following siRNA depletion of hnRNP A1 in the MCF7 cell line. However, many miRNA of interest were downregulated following siRNA depletion of hnRNP A1 in the MCF 10a cell line. In contrast to evidence that overexpression of hnRNP A1 leads to decreased LET-7a, we observed nearly a five-fold decrease in miRNA in the LET-7 family following siRNA depletion of hnRNP A1 (Michlewski and Caceres, 2010). We also observed a substantial decrease in miRNA-106b (~four-fold) following siRNA depletion of hnRNP A1. miRNA-106b has also been shown to target Rbl2, suggesting a possible link between hnRNP A1 and telomere heterochromatin structure. Validation of identified miRNA candidates by quantitative real-time Polymerase Chain Reaction (PCR) is still required, and this is an active area of our future research. miRNA expression array data are listed in Appendix II.

Telomere maintenance and regulation continues to be complex and ever evolving. With the recent discovery of telomere repeat-containing RNA (TERRA), another level of regulation has been added to the maintenance of telomere structure. We explored the mechanisms of telomere structure and function, and we provide new insight into possible roles for DNA-PKcs mediated regulation of TERRA and for hnRNP A1 dependent telomere replication.

References

Allalunis-Turner, M.J., Zia, P.K., Barron, G.M., Mirzayans, R., and Day, R.S., 3rd (1995). Radiation-induced DNA damage and repair in cells of a radiosensitive human malignant glioma cell line. Radiat Res *144*, 288-293.

Allen, C., Ashley, A.K., Hromas, R., and Nickoloff, J.A. (2011). More forks on the road to replication stress recovery. J Mol Cell Biol *3*, 4-12.

Azzalin, C.M., Reichenbach, P., Khoriauli, L., Giulotto, E., and Lingner, J. (2007). Telomeric repeat containing RNA and RNA surveillance factors at mammalian chromosome ends. Science *318*, 798-801.

Bailey, S.M., Brenneman, M.A., Halbrook, J., Nickoloff, J.A., Ullrich, R.L., and Goodwin, E.H. (2004). The kinase activity of DNA-PK is required to protect mammalian telomeres. DNA Repair (Amst) *3*, 225-233.

Bailey, S.M., Cornforth, M.N., Kurimasa, A., Chen, D.J., and Goodwin, E.H. (2001). Strand-specific postreplicative processing of mammalian telomeres. Science *293*, 2462-2465.

Bailey, S.M., Meyne, J., Chen, D.J., Kurimasa, A., Li, G.C., Lehnert, B.E., and Goodwin, E.H. (1999). DNA double-strand break repair proteins are required to cap the ends of mammalian chromosomes. Proc Natl Acad Sci U S A *96*, 14899-14904.

Ben-David, Y., Bani, M.R., Chabot, B., De Koven, A., and Bernstein, A. (1992). Retroviral insertions downstream of the heterogeneous nuclear ribonucleoprotein A1 gene in erythroleukemia cells: evidence that A1 is not essential for cell growth. Mol Cell Biol *12*, 4449-4455.

Benetti, R., Gonzalo, S., Jaco, I., Munoz, P., Gonzalez, S., Schoeftner, S., Murchison, E., Andl, T., Chen, T., Klatt, P., *et al.* (2008). A mammalian microRNA cluster controls DNA methylation and telomere recombination via Rbl2-dependent regulation of DNA methyltransferases. Nat Struct Mol Biol *15*, 998.

Burd, C.G., and Dreyfuss, G. (1994). RNA binding specificity of hnRNP A1: significance of hnRNP A1 high-affinity binding sites in pre-mRNA splicing. Embo J *13*, 1197-1204.

Buxade, M., Parra, J.L., Rousseau, S., Shpiro, N., Marquez, R., Morrice, N., Bain, J., Espel, E., and Proud, C.G. (2005). The Mnks are novel components in the control of TNF alpha biosynthesis and phosphorylate and regulate hnRNP A1. Immunity *23*, 177-189.

Chadeneau, C., Siegel, P., Harley, C.B., Muller, W.J., and Bacchetti, S. (1995). Telomerase activity in normal and malignant murine tissues. Oncogene *11*, 893-898.

Chibazakura, T., Watanabe, F., Kitajima, S., Tsukada, K., Yasukochi, Y., and Teraoka, H. (1997). Phosphorylation of human general transcription factors TATA-binding protein and transcription factor IIB by DNA-dependent protein kinase--synergistic stimulation of RNA polymerase II basal transcription in vitro. Eur J Biochem *247*, 1166-1173.

Cobianchi, F., Calvio, C., Stoppini, M., Buvoli, M., and Riva, S. (1993). Phosphorylation of human hnRNP protein A1 abrogates in vitro strand annealing activity. Nucleic Acids Res *21*, 949-955.

de Lange, T. (2005). Shelterin: the protein complex that shapes and safeguards human telomeres. Genes Dev *19*, 2100-2110.

de Silanes, I.L., d'Alcontres, M.S., and Blasco, M.A. (2010). TERRA transcripts are bound by a complex array of RNA-binding proteins. Nat Commun *1*, 33.

Dvir, A., Peterson, S.R., Knuth, M.W., Lu, H., and Dynan, W.S. (1992). Ku autoantigen is the regulatory component of a template-associated protein kinase that phosphorylates RNA polymerase II. Proc Natl Acad Sci U S A *89*, 11920-11924.

Flynn, R.L., Centore, R.C., O'Sullivan, R.J., Rai, R., Tse, A., Songyang, Z., Chang, S., Karlseder, J., and Zou, L. (2011). TERRA and hnRNPA1 orchestrate an RPA-to-POT1 switch on telomeric single-stranded DNA. Nature *471*, 532-536.

Gao, Z.H., Metherall, J., and Virshup, D.M. (2000). Identification of casein kinase I substrates by in vitro expression cloning screening. Biochem Biophys Res Commun *268*, 562-566.

Gilson, E., and Geli, V. (2007). How telomeres are replicated. Nat Rev Mol Cell Biol *8*, 825-838.

Gisselsson, D., Jonson, T., Petersen, A., Strombeck, B., Dal Cin, P., Hoglund, M., Mitelman, F., Mertens, F., and Mandahl, N. (2001). Telomere dysfunction triggers extensive DNA fragmentation and evolution of complex chromosome abnormalities in human malignant tumors. Proc Natl Acad Sci U S A *98*, 12683-12688.

Greider, C.W., and Blackburn, E.H. (1985). Identification of a specific telomere terminal transferase activity in Tetrahymena extracts. Cell *43*, 405-413.

Grishok, A., Pasquinelli, A.E., Conte, D., Li, N., Parrish, S., Ha, I., Baillie, D.L., Fire, A., Ruvkun, G., and Mello, C.C. (2001). Genes and mechanisms related to RNA interference regulate expression of the small temporal RNAs that control C. elegans developmental timing. Cell *106*, 23-34.

He, Y., and Smith, R. (2009). Nuclear functions of heterogeneous nuclear ribonucleoproteins A/B. Cell Mol Life Sci *66*, 1239-1256.

Hollick, J.J., Golding, B.T., Hardcastle, I.R., Martin, N., Richardson, C., Rigoreau, L.J., Smith, G.C., and Griffin, R.J. (2003). 2,6-disubstituted pyran-4-one and thiopyran-4-one inhibitors of DNA-Dependent protein kinase (DNA-PK). Bioorg Med Chem Lett *13*, 3083-3086.

Hutvagner, G., McLachlan, J., Pasquinelli, A.E., Balint, E., Tuschl, T., and Zamore, P.D. (2001). A cellular function for the RNA-interference enzyme Dicer in the maturation of the let-7 small temporal RNA. Science *293*, 834-838.

Johnson, C.D., Esquela-Kerscher, A., Stefani, G., Byrom, M., Kelnar, K., Ovcharenko, D., Wilson, M., Wang, X., Shelton, J., Shingara, J., *et al.* (2007). The let-7 microRNA represses cell proliferation pathways in human cells. Cancer Res *67*, 7713-7722.

Ketting, R.F., Fischer, S.E., Bernstein, E., Sijen, T., Hannon, G.J., and Plasterk, R.H. (2001). Dicer functions in RNA interference and in synthesis of small RNA involved in developmental timing in C. elegans. Genes Dev *15*, 2654-2659.

Kim, N.W., Piatyszek, M.A., Prowse, K.R., Harley, C.B., West, M.D., Ho, P.L., Coviello, G.M., Wright, W.E., Weinrich, S.L., and Shay, J.W. (1994). Specific association of human telomerase activity with immortal cells and cancer. Science *266*, 2011-2015.

McClintock, B. (1941). The Stability of Broken Ends of Chromosomes in Zea Mays. Genetics *26*, 234-282.

Michlewski, G., and Caceres, J.F. (2010). Antagonistic role of hnRNP A1 and KSRP in the regulation of let-7a biogenesis. Nat Struct Mol Biol *17*, 1011-1018.

Mrozek, K., Tanner, S.M., Heinonen, K., and Bloomfield, C.D. (2003). Molecular cytogenetic characterization of the KG-1 and KG-1a acute myeloid leukemia cell lines by use of spectral karyotyping and fluorescence in situ hybridization. Genes Chromosomes Cancer *38*, 249-252.

Muller, H.J. (1938). The remaking of chromosomes. Collecting Net *13*, 182-198.

Municio, M.M., Lozano, J., Sanchez, P., Moscat, J., and Diaz-Meco, M.T. (1995). Identification of heterogeneous ribonucleoprotein A1 as a novel substrate for protein kinase C zeta. J Biol Chem *270*, 15884-15891.

Okayasu, R., Suetomi, K., and Ullrich, R.L. (1998). Wortmannin inhibits repair of DNA double-strand breaks in irradiated normal human cells. Radiat Res *149*, 440-445.

Peng, Y., Brown, N., Finnon, R., Warner, C.L., Liu, X., Genik, P.C., Callan, M.A., Ray, F.A., Borak, T.B., Badie, C., *et al.* (2009). Radiation leukemogenesis in mice: loss of PU.1 on chromosome 2 in CBA and C57BL/6 mice after irradiation with 1 GeV/nucleon 56Fe ions, X rays or gamma rays. Part I. Experimental observations. Radiat Res *171*, 474-483.

Peng, Y., Woods, R.G., Beamish, H., Ye, R., Lees-Miller, S.P., Lavin, M.F., and Bedford, J.S. (2005). Deficiency in the catalytic subunit of DNA-dependent protein kinase causes down-regulation of ATM. Cancer Res *65*, 1670-1677.

Peterson, S.R., Dvir, A., Anderson, C.W., and Dynan, W.S. (1992). DNA binding provides a signal for phosphorylation of the RNA polymerase II heptapeptide repeats. Genes Dev *6*, 426-438.

Peterson, S.R., Jesch, S.A., Chamberlin, T.N., Dvir, A., Rabindran, S.K., Wu, C., and Dynan, W.S. (1995). Stimulation of the DNA-dependent protein kinase by RNA polymerase II transcriptional activator proteins. J Biol Chem *270*, 1449-1454.

Porro, A., Feuerhahn, S., Reichenbach, P., and Lingner, J. Molecular dissection of TERRA biogenesis unveils the presence of distinct and multiple regulatory pathways. Mol Cell Biol.

Prowse, K.R., and Greider, C.W. (1995). Developmental and tissue-specific regulation of mouse telomerase and telomere length. Proc Natl Acad Sci U S A *92*, 4818-4822.

Ramachandran, C., Fonseca, H.B., Jhabvala, P., Escalon, E.A., and Melnick, S.J. (2002). Curcumin inhibits telomerase activity through human telomerase reverse transcritpase in MCF-7 breast cancer cell line. Cancer Lett *184*, 1-6.

Reinhart, B.J., Slack, F.J., Basson, M., Pasquinelli, A.E., Bettinger, J.C., Rougvie, A.E., Horvitz, H.R., and Ruvkun, G. (2000). The 21-nucleotide let-7 RNA regulates developmental timing in Caenorhabditis elegans. Nature *403*, 901-906.

Schoeftner, S., and Blasco, M.A. (2008). Developmentally regulated transcription of mammalian telomeres by DNA-dependent RNA polymerase II. Nat Cell Biol *10*, 228-236.

Sfeir, A., Kosiyatrakul, S.T., Hockemeyer, D., MacRae, S.L., Karlseder, J., Schildkraut, C.L., and de Lange, T. (2009). Mammalian telomeres resemble fragile sites and require TRF1 for efficient replication. Cell *138*, 90-103.

Sheppard, H.M., and Liu, X. (2000). Transcription by RNA polymerase II in DNA-PK deficient scid mouse cells. Biochim Biophys Acta *1493*, 41-47.

Shimada, N., Rios, I., Moran, H., Sayers, B., and Hubbard, K. (2009). p38 MAP kinase-dependent regulation of the expression level and subcellular distribution of heterogeneous nuclear ribonucleoprotein A1 and its involvement in cellular senescence in normal human fibroblasts. RNA Biol *6*, 293-304.

Ting, N.S., Pohorelic, B., Yu, Y., Lees-Miller, S.P., and Beattie, T.L. (2009). The human telomerase RNA component, hTR, activates the DNA-dependent protein kinase to phosphorylate heterogeneous nuclear ribonucleoprotein A1. Nucleic Acids Res *37*, 6105-6115.

Weil, M.M., Bedford, J.S., Bielefeldt-Ohmann, H., Ray, F.A., Genik, P.C., Ehrhart, E.J., Fallgren, C.M., Hailu, F., Battaglia, C.L., Charles, B., *et al.* (2009). Incidence of acute myeloid leukemia and hepatocellular carcinoma in mice irradiated with 1 GeV/nucleon (56)Fe ions. Radiat Res *172*, 213-219.

Yu, F., Yao, H., Zhu, P., Zhang, X., Pan, Q., Gong, C., Huang, Y., Hu, X., Su, F., Lieberman, J., *et al.* (2007). let-7 regulates self renewal and tumorigenicity of breast cancer cells. Cell *131*, 1109-1123.

Zhang, Q.S., Manche, L., Xu, R.M., and Krainer, A.R. (2006). hnRNP A1 associates with telomere ends and stimulates telomerase activity. Rna *12*, 1116-1128.

Zhang, S., Schlott, B., Gorlach, M., and Grosse, F. (2004). DNA-dependent protein kinase (DNA-PK) phosphorylates nuclear DNA helicase II/RNA helicase A and hnRNP proteins in an RNA-dependent manner. Nucleic Acids Res *32*, 1-10.

APPENDIX

APPENDIX I

MicroRNA array methods

Total RNA was collected using a Qiagen RNeasy Plus Mini Kit (Qiagen 74134), which includes the collection of small RNAs. DNA-free RNA quality was tested by gel electrophoresis. miRCURY LNA microRNA Array Spike-in kit v2 (Exiqon) was used as a control for the labeling reaction and hybridization. A total of 1.5 ug of RNA was labeled with Hy 3 fluor using the Hi-Power labeling kit (Exiqon), as suggested by the manufacturer. Briefly, 1.5 ug RNA in 3uL volume, 1uL spike-in miRNA kit v2, 0.5uL Calf Intestinal Phosphatase (CIP) buffer and 0.5 uL CIP enzyme was mixed on ice and incubated at 37ºC for 30 minutes. The RNA was then denatured at 95ºC and immediately placed on ice for 2 minutes. This reaction product is then mixed with 3 uL Hi-Power labeling buffer, 1.5 uL Hy3 fluorescent label, 2 uL Dimethyl Sulfoxide (DMSO) and 1 uL Hi-Power labeling enzyme for a total of 12.5 uL total volume. This is incubated for 2 hours at 16ºC. Samples are subsequently hybridized to microarray slides (Exiqon miRCURY LNA microRNA array kit) using the Nimble Gen/MAUI 4-Bay hybridization station, as suggested by the manufacturer. The labeled RNA is brought up to a 25 uL volume and 25 uL of hybridization buffer is added, for a total of 50 uL volume. Following denaturation at 95ºC for 2 minutes, the sample was iced for 2 minutes. The sample is then heated to 56ºC, and the total sample is added to the microarray slide, and hybridization occurs for 16 hours at 56ºC in the hybridization chamber. Slides are then washed for 1 minute at 56ºC in wash buffer A, 1 min at 23ºC in wash buffer B and 1 minute at 23ºC in wash buffer C. Lastly, this is followed by a brief wash in 99% ethanol.

Slides are then dried for 5 minutes. Microaray slides are scanned using the Tecan's Power Scanner. Spot quantification, image and statistical analysis were done using Imagene 9 and Nexus Expression 2 software, both from Exiqon. Background substraction was done by subtracting the median local background, and normalization was done using the Quantile Normalization method.

APPENDIX II

MicroRNA Array Data

Data was collected and analyzed from prepared RNA samples by Dr. Michael Story

*Minor miRNA

**Not all validated target genes provided to us were listed

I. MCF 7 mock transfected versus MCF 7 siRNA depletion of hnRNP A1
   a. N/A: no significant results

II. MCF 10a mock versus siRNA depletion of hnRNP A1
   a. A positive Fold change represents an increase in mock, i.e. decrease in siRNA treated cells
   b. Blank cells are indicate that these miRNA do not yet have experimentally validated targets

miRNA ID	**Symbol**	**Validated Target genes**	**Fold change**	**q-value**
hsa-miR-186	miR-186	FOXO1	5.874	0.021
hsa-miR-454	miR-130a/miR-130b/miR-301a (includes others)	CSF1, TAC1	5.463	0.031
hsa-miR-130b			5.403	0.012
hsa-miR-331-3p	miR-331-3p/miR-331	ERBB2, KIF23	5.231	0.041
hsa-miR-140-5p	miR-140/miR-876-3p/miR-140-5p	CXCL12, HDAC4, IGFBP5, SMAD3, VEGFA,	5.198	0.018
hsa-miR-425			4.994	0.016
hsa-miR-98	let-7a/let-7f/let-7c (includes others)	**ACP1, AKAP8, ANAPC1/LOC100286979, ATP6V0A1, ATP6V1F,	4.986	0.025

		BCL2L1, BCL211, CASP3, CCND1, CDC25A, CDIPT, CDK6		
hsa-miR-96	miR-96/miR-1271	WNT1, ADCY6, CELSR2,FOXO1, HTR1B, IRS1, MITF, RYK	4.981	0.012
hsa-miR-1285	miR-1285/miR-612/miR-3187-5p	TP53	4.926	0.013
hsa-miR-182	miR-182	ADCY6, IGF1R, MITF, RARG	4.840	0.033
hsa-miR-374b			4.820	0.013
hsa-miR-374c			4.783	0.014
hsa-miR-20a*			4.751	0.020
hsa-miR-3660			4.680	0.048
hsa-miR-708			4.606	0.015
hsa-miR-32	miR-92a/miR-92b/miR-32 (includes others)		4.606	0.015
hsa-miR-342-3p			4.598	0.012
hsa-miR-744			4.512	0.021
hsa-miR-99b	miR-100/miR-99a/miR-99b	FGF16, IGF1R, MTOR, PLK1, RPTOR	4.501	0.026
hsa-miR-659			4.368	0.023
hsa-let-7d*			4.308	0.026
hsa-miR-224	miR-224	AP2M1, IL11, KLK1	4.251	0.026
hsa-miR-296-3p			4.202	0.013
hsa-miR-26b	miR-26a/miR-26b	BAK1, EPHA2, SMAD1, TGFBR2	4.128	0.025

hsa-miR-4299			4.099	0.021
hsa-miR-340*			4.081	0.027
hsa-miR-1304			4.057	0.036
hsa-miR-106b	miR-20a/miR-106b/miR-17-5p (includes others)	**BCL2, BCL2L11, E2F1, IL8, JAK1, MAP3K12, PTEN, RB1, RBl2, STAT3, VEGFA	4.036	0.013
hsa-miR-30b	miR-30c/miR-30a/miR-30d (includes others)	**ATRX, BCL6, JUN,MET, RUNX2, THEM4, TP53, WNT5A	3.998	0.016
hsa-miR-99a			3.994	0.043
hsa-miR-551a			3.974	0.041
hsa-miR-1307			3.908	0.033
hsa-miR-29a*			3.904	0.016
hsa-miR-141	miR-141/miR-200a	**BAP1, CTNNB1, CP1B1, DLX5, ELMO2, MAP2K4	3.882	0.020
hsa-miR-629*			3.838	0.040
hsa-miR-22*			3.834	0.013
hsa-miR-30a			3.823	0.033
hsa-miR-210	miR-210 (human, mouse, rat)	ACVR1B, EFNA3, SDHD	3.819	0.013
hsa-miR-363*			3.809	0.028
hsa-miR-323-3p			3.757	0.016
hsa-miR-181d	miR-181a/miR-181b/miR-181d (includes others)	**BCL2, CD69, KRAS, NOTCH4, CDKN1B, GATA6	3.756	0.014
hsa-miR-301a			3.753	0.028

hsa-miR-15b	miR-16/miR-497/miR-195 (includes others)	**BCL2, CDK6, E2F3, EGFR, EIF4E, F2, HMGA1, IGF2R, JUN, MCL2, NOTCH2, PLK1	3.747	0.015
hsa-miR-550a			3.740	0.037
hsa-miR-551b*			3.724	0.016
hsa-miR-16-2*			3.672	0.033
hsa-miR-642b			3.659	0.036
hsa-miR-196a	miR-196a/miR-196b	ANXA1, IKBKB, S100A9	3.659	0.017
hsa-miR-150	miR-150/miR-5127	AICDA, BACH1, CEBPB, CSF1R, PDGFB, VEGFA	3.655	0.037
hsa-miR-423-5p			3.543	0.032
hsa-miR-1255a			3.496	0.045
hsa-miR-200c	miR-429/miR-200b/miR-200c	BAP1, ELMO2, ERBB21P, ERRF11, FN1, MARCKS, PTPN12	3.450	0.021
hsa-miR-3170			3.450	0.042
hsa-let-7f-2*			3.447	0.014
hsa-miR-25			3.440	0.028
hsa-miR-146b-3p			3.138	0.022
hsa-miR-30b*			3.437	0.013
hsa-miR-181a-2*			3.427	0.038
hsa-miR-15a			3.424	0.022

hsa-miR-222	miR-222/miR-221/miR-1928	**BCL2L11, CDKN1B, CDKN1C, FOS, KIT, MMP1, PIK3R1, PTEN	3.378	0.015
hsa-miR-27a*			3.300	0.043
hsa-let-7i			3.295	0.013
hsa-miR-1275			3.276	0.018
hsa-miR-193a-3p	miR-193/miR-193b/miR-193a-3p	CCNDA, E2F6, ESR1, ETS1, MCL1, PLAU, PTK2	3.274	0.025
hsa-miR-27b*			3.270	0.014
hsa-miR-34a	miR-449a/miR-34a/miR-34c (includes others)	**CCND1, DLL1, E2F3, E2F5, JAG1, NOTCH1, NOTCH2	3.265	0.014
hsa-miR-3148			3.249	0.016
hsa-miR-92a			3.245	0.037
hsa-miR-140-3p			3.245	0.023
hsa-miR-3622b-3p			3.221	0.028
hsa-miR-125b-1*	miR-125b-1-3p/miR-125b-1*/miR-125b-3p	IL13, IL1B, TNF	3.137	0.013
hsa-miR-148b	miR-152/miR-148b/miR-148a (includes others)	CCKBR, DNMT1, DNMT3B, NR1I2, RPS6KA5	3.132	0.028
hsa-miR-1298			3.116	0.033
hsa-miR-639			3.116	0.037
hsa-miR-4287			3.104	0.043
hsa-miR-431*	miR-431*	CD81, IRAK1	3.062	0.038

hsa-miR-196b			3.046	0.013
hsa-miR-574-3p			3.044	0.016
hsa-miR-135b	miR-135a/miR-135b	ALOX5AP, APC, JAK2, RUNX2, SMAD5	3.043	0.035
hsa-miR-26b*			3.022	0.022
hsa-miR-601			3.021	0.036
hsa-let-7i*			3.016	0.025
hsa-miR-191	miR-191	Ccl9, CRP, IL6, TLR3	3.014	0.045
hsa-miR-31	miR-31	**CASR, CDKN2A, FOXP3, HIF1A, MMP16, ROX, RHOA	3.006	0.043
hsa-miR-26a-2*			3.003	0.026
hsa-miR-4329			2.988	0.025
hsa-miR-622			2.978	0.016
hsa-miRPlus-I382*			2.977	0.033
hsa-miR-675	miR-675/miR-4466/miR-675-5p	RB1	2.698	0.036
hsa-miR-4306	miR-185/miR-3473/miR-4306 (includes others)	AKT1, CCNE1, CDC42, CDK6, RHOA	2.944	0.033
hsa-miR-197	miR-197	ACVR1, TSPAN3	2.924	0.042
hsa-miR-3175			2.895	0.0329
hsa-miR-93			2.880	0.020
hsa-miR-505*			2.869	0.042
hsa-miR-944			2.844	0.049

hsa-miR-125a-5p	miR-125b-5p/miR-125a-5p/miR-125b (includes others)	**BAK1, CASP6, CASP7, CDC25A, CDK6, E2F3,IGFBP3, JARID2, TP53	2.829	0.013
hsa-miR-509-3p	miR-509-3p (human)	NTRK3	2.795	0.042
hsa-miR-1273e			2.784	0.013
hsa-let-7g			2.745	0.042
hsa-miR-106b*			2.705	0.022
hsa-miR-33a	miR-33/miR-33a/miR-33b	ABCA1	2.698	0.049
hsa-miR-3690			2.676	0.021
hsa-miR-124*			2.675	0.037
hsa-let-7e			2.633	0.020
hsa-miR-196a*			2.618	0.021
hsa-miR-4320			2.607	0.037
hsa-miR-103			2.602	0.014
hsa-miR-193b			2.577	0.021
hsa-miR-3685			2.567	0.021
hsa-miR-519d			2.555	0.022
hsa-miR-3647-3p			2.528	0.014
hsa-miR-29b-1* hsa-miR-877			2.526	0.021
hsa-miR-542-3p			2.488	0.041
hsa-miR-130a			2.472	0.025
hsa-miR-337-3p			2.425	0.042

hsa-miR-361-5p			2.423	0.034
hsa-miR-223*			2.399	0.044
hsa-miR-20a			2.389	0.017
hsa-miR-320a	miR-320d/miR-320b/miR-320c (includes others)	HSPB6, MCL1, VIM	2.364	0.026
hsa-miR-340			2.331	0.022
hsa-miR-23a	miR-23b/miR-23a/miR-23c (includes others)	**CXCL12, HES1, IL6R, LMNB2, MDH2, MET, NOTCH1, SMAD3	2.308	0.016
hsa-miR-25*			2.302	0.020
hsa-miR-17			2.295	0.016
hsa-miR-16			2.289	0.043
hsa-miR-518d-5p			2.246	0.020
hsa-miR-302c*			2.229	0.013
hsa-miR-106a			2.200	0.012
hsa-miR-574-5p			2.199	0.033
hsa-miR-1908			2.178	0.014
hsa-miR-3667-5p			2.170	0.049
hsa-miR-1914			2.168	0.049
hsa-miR-1207-5p			2.168	0.047
hsa-miR-1469			2.142	2.136
hsa-miR-20b*			2.136	0.019

hsa-miR-24-1*			2.091	0.036
hsa-miR-485-3p	miR-485-3p	MLL3, NTRK3	2.030	0.014
hsa-miR-30d			1.989	0.027
hsa-miR-22	miR-22	BMP7, ESR1, MAX, PPARA	1.983	0.027
hsa-miR-3935			1.952	0.020
hsa-miR-320e			1.901	0.013
hsa-miR-101	miR-101/miR-101a/miR-101b	ICOS, MCL1, MYCN, PTGS2	1.855	0.033
hsa-miR-1184			1.835	0.033
hsa-miRPlus-C1057			1.716	0.025
hsa-miR-767-5p			1.713	0.042
hsa-miR-320b			1.658	0.036
hsa-miR-300			1.565	0.013
hsa-miR-609			1.544	0.045
hsa-miR-874			1.444	0.043
hsa-miR-3646			1.422	0.016
hsa-miR-4288			1.385	0.022
hsa-miR-518e*			1.374	0.019

III. MCF7 mock transfected versus MCF 10a mock transfected
   a. N/A: no significant results

IV. MCF7 siRNA depletion of hnRNP A1 versus MCF 10a siRNA depletion of hnRNP A1

miRNA ID	**Symbol**	**Validated Target**	**Fold**	**q-value**

		Genes	Change	
hsa-miR-342-3p			6.557	0.016
hsa-miR-200b	miR-429/miR-200b/miR-200c	**ERBB2IP, ERRFI1, FN1, PTPN13, LHFP, MARCKS	6.546	0.017
hsa-miR-200c			6.494	0.017
hsa-miR-141	miR-141/miR-200a	**ZFPM2, ZEB2, PTPRD, PRKACB, PPM1E	6.439	0.017
hsa-miR-98	let-7a/let-7f/let-7c (includes others)	**WNT1, TMEM2, IGF2BP1, CDC25A, APC1	6.151	0.021
hsa-miR-331-3p	miR-331-3p/miR-331	ERBB2	5.562	0.043
hsa-miR-1285	miR-1285/miR-612/miR-3187-5p	TP53	5.553	0.017
hsa-miR-301a	miR-130a/miR-130b/miR-301a (includes others)	ZFPM2, MEOX2, MAFB, HOXA5, CSF1	5.539	0.028
hsa-miR-182	miR-182	RARG, MITF, IGF1R, ADCY6	5.461	0.031
hsa-miR-96	miR-96/miR-1271	TYK, MYRIP, MITF, IRS1, FOXO1, CELSR2, ADCY6	5.449	0.016
hsa-miR-296-3p			5.351	0.015
hsa-miR-374c			5.133	0.028
hsa-miR-425			4.969	0.017
hsa-miR-130b			4.859	0.017

hsa-miR-374b			4.761	0.016
hsa-miR-99b	miR-100/miR-99a/miR-99b	MTOR, IFG1R, FGFR3	4.660	0.028
hsa-miR-659			4.557	0.024
hsa-miR-421			4.547	0.043
hsa-miR-708			4.405	0.020
hsa-miR-20a*			4.352	0.024
hsa-miR-32	miR-92a/miR-92b/miR-32 (includes others)	MYLIP, MAP2K4, ITGA5, HIPK3, CDKN1C, BMPR2, BCL2L11	4.318	0.032
hsa-miR-340*			4.167	0.029
hsa-miR-744			4.141	0.026
hsa-miR-106b	miR-20a/miR-106b/miR-17-5p (includes others)	**VEGFA, STAT3, RUNX1, RBL2, RB1, PTEN PKD2, E2F, CDKN1A, BCL2L11, ARID4B	4.131	0.016
hsa-let-7f-2*			4.094	0.017
hsa-miR-660			4.091	0.028
hsa-miR-500a			4.077	0.043
hsa-let-7d*			4.020	0.030
hsa-miR-140-5p	miR-140/miR-876-3p/miR-140-5p	VEGFA, IGFBP5, HDAC4	3.950	0.025
hsa-miR-629*			3.887	0.043
hsa-miR-877			3.867	0.029

hsa-miR-25			3.816	0.039
hsa-miR-16-2*			3.790	0.037
hsa-miR-1307			3.786	0.039
hsa-miR-30e*			3.764	0.017
hsa-miR-30b	miR-30c/miR-30a/miR-30d (includes others)	**UBE2I, TNRC6A, RUNX2, PTGFRN, BCL6, AP2A1, ACVR1	3.662	0.043
hsa-miR-1304			3.593	0.025
hsa-miR-196a	miR-196a/miR-196b	HOXC8, HOXB8, HOXA7	3.573	0.028
hsa-miR-675			3.563	0.040
hsa-miR-107	miR-103/miR-103a/miR-107	RAB1B, PLAG1, NF1A, EIF2C1, CDK6, CDK6, CCNE1	3.545	0.017
hsa-miR-210	miR-210 (human, mouse, rat)	SDHD, EFNA3, ACVR1B	3.517	0.020
hsa-miR-622			3.487	0.017
hsa-miR-193a-5p			3.453	0.021
hsa-miR-15b	miR-16/miR-497/miR-195 (includes others)	**NOTCH2, FGFR1, E2F3, BCL2, CDK6, CLDN12	3.408	0.013
hsa-let-7i			3.390	0.027
hsa-miR-193a-3p	miR-193/miR-193b/miR-193a-3p	PLAU, MCL1, ETS1, E2F6, CCND1	3.378	0.042

hsa-miR-224	miR-224	AP15	3.330	0.024
hsa-miR-551b*			3.240	0.037
hsa-miR-26b	miR-26a/miR-26b	SMAD1, MAP2, EZH2, EPHA3, BAK1	3.240	0.037
hsa-miR-363*			3.222	0.045
hsa-miR-106b*			3.173	0.021
hsa-miR-3170			3.173	0.027
hsa-miR-148b	miR-152/miR-148b/miR-148a (includes others)	RPS6KA5, NR1I2, DNMT1, CCKBR	3.140	0.028
hsa-miR-450a			3.018	0.027
hsa-miR-4299			2.979	0.024
hsa-miR-93			2.978	0.017
hsa-miR-550a			2.966	0.038
hsa-miR-15a			2.963	0.028
hsa-miR-1275			2.955	0.021
hsa-miR-146b-3p			2.889	0.029
hsa-miR-3148			2.885	0.021
hsa-miR-601			2.878	0.040
hsa-miR-1273e			2.836	0.022
hsa-let-7i*			2.834	0.017
hsa-miR-197	miR-197	TUSC2, ACVR1	2.818	0.043
hsa-miR-323-3p			2.797	0.022

hsa-miR-26b*			2.765	0.028
hsa-miR-3622b-3p			2.708	0.038
hsa-miR-193b			2.707	0.022
hsa-miR-1226 hsa-miR-26a-2*			2.686	0.024
hsa-miR-27b*			2.643	0.037
hsa-miR-22*			2.610	0.017
hsa-miR-4329			2.566	0.015
hsa-miRPlus-A1087			2.467	0.037
hsa-miR-519d			2.447	0.039
hsa-miR-181d	miR-181a/miR-181b/miR-181d (includes others)	**TIMP3, NOTCH4, GATA6, HOXA11, KRAS, BCL2	2.417	0.028
hsa-miR-103			2.404	0.022
hsa-miR-518d-5p			2.392	0.020
hsa-miR-3647-3p			2.368	0.022
hsa-let-7g			2.352	0.017
hsa-miR-140-3p			2.342	0.022
hsa-miR-4306	miR-185/miR-3473/miR-4306 (includes	RHOA, HMGA2M CORO2B, CDK6, CDC42, AKT1	2.260	0.031

	others)			
hsa-miR-125a-5p			2.183	0.048
hsa-miR-20a			2.157	0.017
hsa-miR-340			2.103	0.025
hsa-miR-3149			2.051	0.028
hsa-miR-300			1.991	0.025
hsa-miR-4320			1.969	0.028
hsa-miR-431*			1.969	0.021
hsa-let-7e			1.960	0.028
hsa-miR-485-3p	miR-485-3p	NTRK3, MLL3, HCN1	1.918	0.022
hsa-miR-574-5p			1.904	0.037
hsa-miR-302c*			1.901	0.022
hsa-miR-3690			1.898	0.037
hsa-miR-22	miR-22	PPARA, MAX, ESR1	1.874	0.031
hsa-miR-320a	miR-320d/miR-320b/miR-320c (includes others)	VIM, MCL1	1.809	0.039
hsa-miR-34a	hsa-miR-34a	**SIRT1, NOTCH2, JAG1, E2F5, E2F3, DLL1, AXIN2	1.796	0.017
hsa-miR-3667-5p			1.787	0.037
hsa-miR-3685			1.768	0.045
hsa-miR-520d-3p	miR-302a/miR-	**VEGFA, TUSC2, TRPS1, TP63,	1.716	0.031

	302b/miR-291a-3p (includes others)	TNFAIP1, LEFTY2, LEFTY1		
hsa-miR-542-3p			1.704	0.017
hsa-miR-23a	miR-23b/miR-23a/miR-23c (includes others)	**TRIM63, SMAD5, SEPT3, POU4F2	1.696	0.022
hsa-miR-196b			1.689	0.017
hsa-miR-3646			1.569	0.038
hsa-miR-3935			1.557	0.024
hsa-miR-1908			1.507	0.045
hsa-miR-30d			1.504	0.040
hsa-miR-17			1.477	0.017
hsa-miR-25*			1.420	0.021
hsa-miR-20b*			1.293	0.028
hsa-miR-3907			1.288	0.037
hsa-miR-574-3p			1.269	0.020
hsa-miR-320e			1.074	0.017
hsa-miR-130a			-5.177	0.034
hsa-miR-125b	miR-125b-5p/miR-125a-5p/miR-125b (includes others)	**tp53, E2F3, ERBB2, ERBB3, BAK1, DICER1	-3.325	0.022
hsa-miR-4288			-2.445	0.017
hsa-miR-874			-1.816	0.039

hsa-miR-205	miR-205	ZEB2, BEGFA, PTEN, MED1, INPPL1, ERBB3, DOK4	-1.671	0.029
hsa-miR-29a	miR-29b/miR-29c/miR-29a	**TPM1, TDG, PPM1D, PIK3R1, MCL1	-1.497	0.016
hsa-let-7b			-1.076	0.040

APPENDIX III

List of Abbreviations

(listed in alphabetical order)

Symbols

α	Alpha
β	Beta
ɣ	Gamma
µ	Micro

Abbreviations

3-D	3-Dimensional
A-bomb	Atomic bomb
ABCC	Atomic Bomb Casualty Commission
ALT	Alternative Lengthening of Telomeres
AML	Acute Myeloid Leukemia
ARG	Arginine
ATM	Ataxia Telangiectasia Mutated
ATP	Adenosine Triphosphate
ATR	Ataxia Telangiectasia and Rad3 Related
BAC	Bacterial Artificial Chromosome
BER	Base Excision Repair
BFB	Breakage-Fusion-Bridge
Bp	Base pairs
BRCA1	Breast Cancer 1

BRCA2	Breast Cancer 2
BrdC	Bromodeoxycytidine
BrdU	Bromodeoxyuridine
BSA	Bovine Serum Albumin
CCD	Charged-Coupled Device camera
cDNA	complementary DNA
Ci	Curie
CIN	Chromosomal Instability
CIP	Calf Intestinal Phosphatase
CFU-A	Colony Forming Unit Assay
CFU-S	Spleen Colony Forming Unit
CO_2	Carbon Dioxide
CO-FISH	Chromosome-Orientation Fluorescence *In Situ* Hybridization
Cs	Cesium
CSK	Cytoskeleton
CTD	Carboxyl Terminal Domain
D-loop	Displacement loop
DAPI	4',6-diamidino-2-phenylindole, dihydrochloride
ddH_20	Deionized distilled water
DKC	Dyskeratosis Congenita
DMEM	Dulbecco's Modified Eagle's Medium
DMSO	Dimethyl Sulfoxide
DNA	Deoxyribonucleic Acid
DNA-PK	DNA Dependent Protein Kinase

DNA-PKcs	DNA Dependent Protein Kinase catalytic subunit
DSB	Double-Strand Break
dsDNA	double-stranded DNA
E	Energy
EBSS	Earle's Balanced Salt Solution
EDTA	Ethylenediaminetetraacetic Acid
EGF	Epidermal Growth Factor
EGTA	Ethylene Glycol Tetraacetic Acid
ES	Embryonic Stem
ETS	E-Twenty-Six
FBS	Fetal Bovine Serum
Fe	Iron
FISH	Fluorescence *In Situ* Hybridization
g	gram
GCR	Galatic Cosmic Rays
GeV	Giga electron Volt
GeV/n	Giga electron Volt/nucleon
GM-CSF	Granulocyte-Macrophage Colony-Stimulating Factor
GSR	Galatic Space Radiation
Gy	Gray
H3K4me3	Histone H3 trimethyl
HEPES	4-(2-hydroxyethyl)-1-piperazineethanesulfonic Acid
hnRNP A1	Heterogeneous nuclear Ribonucleoprotein A1
HP1	Heterochromatin Protein 1
HR	Homologous Recombination

hTR	Human telomerase RNA component
HZE	Highly ionizing, High Energy radiation
ICC	Immunocytochemistry
IMDM	Iscove's Modified Dulbecco's Media
IP	Immunoprecipitation
IR	Ionizing Radiation
ITS	Interstitial Telomere Sequence
Kbp	Kilo base pairs
KCL	Potassium Chloride
LET	Linear Energy Transfer
LSM	Lymphocyte Separation Media
LSS	Life Span Study
M-CSF	Macrophage-Colony Stimulating Factor
MACs	Magnetic Sorting Buffer
MDS	Myelodysplastic Syndrome
MEM	Minimum Essential Media
miRNA	microRNA
mL	milli Liter
mM	milli Molar
MMR	Mismatch Repair
MNCs	Mononuclear Cells
MNK	Map kinase signaling-integrated kinases
MRN	Mre11, Rad50 and Nbs1
mRNA	messenger Ribonucleic Acid
NER	Nucleotide Excision Repair

NHEJ	Non-Homologous End Joining
nM	nano Molar
NMD	Nonsense-Mediated Decay
NSRL	NASA Space Radiation Laboratory
NT	Non-target
NU7026	2-(Morpholin-4-yl)-benzo[h]chromen-4-one
O_2	Oxygen
ORC	Origin of Recognition Complex
^{32}P	Phosphorus-32
PAGE	Polyacrylamide Gel Electrophoresis
PBS	Phosphate Buffered Saline
PCR	Polymerase Chain Reaction
PI-3-K	Phospatidylinositol 3-kinase
PIKK	Phosphoinositide 3-kinase like
PMSF	Phenylmethylsulfonyl Fluoride
PNA	Peptide Nucleic Acid
POT 1	Protection Of Telomeres 1
PVDF	Polyvinylidene Fluoride
RBE	Relative Biologic Effectiveness
Rbl2	Retinoblastoma-like 2 protein
RNA	Ribonucleic Acid
ROS	Radical Oxygen Species
RPA	Replication Protein A
RPMI	Roswell Park Memorial Institute
SCID	Severe Combined Immunodefiency

SDS	Sodium Dodecyl Sulfate
SDS-PAGE	Sodium Dodecyl Sulfate –Polyacrylamide Gel Electrophoresis
SER	Serine
SFE	Signal Free Ends
siRNA	small interfering Ribonucleic Acid
SMG	Suppressors with Morphogenetic defects in Genetalia
SPE	Solar Proton Events
SSC	Saline Sodium Citrate
Sv	Sieverts
t-AML	Therapy-related Acute Myeloid Leukemia
T-loop	Telomere loop
T-SCE	Telomere Sister Chromatid Exchange
TBST	Tris-Buffered Saline with 0.1% Tween 20
TelRNA	Telomeric RNA
TERC	Telomerase RNA Component
TERRA	Telomeric repeat-containing RNA
TERT	Telomerase Reverse Transcriptase
TFRC	Transferrin Receptor
THR	Threonine
TIF	Telomere Induced Foci
TNFα	Tumor Necrosis Factor Alpha
TRF1	Telomere Repeat Factor 1
TRF2	Telomere Repeat Factor 2
Trp53	Transformation related protein 53

UV	Ultraviolet
V	Volt
WRN	Werner
Z	Charge